UNIVERSITY OF ZIMBABWE

FACULTY OF ENGINEERING

DEPARTMENT OF CIVIL ENGINEERING

THE SPATIO-TEMPORAL SOIL MOISTURE VARIATION ALONG THE MAJOR TRIBUTARIES OF ZAMBEZI RIVER IN THE MBIRE DISTRICT, ZIMBABWE

FARAYI BLESSING JAHURE

M.Sc. THESIS IN IWRM

HARARE, OCTOBER 2013

UNIVERSITY OF ZIMBABWE

FACULTY OF ENGINEERING

DEPARTMENT OF CIVIL ENGINEERING

In collaboration with

THE SPATIO-TEMPORAL SOIL MOISTURE VARIATION ALONG THE MAJOR TRIBUTARIES OF ZAMBEZI RIVER IN THE MBIRE DISTRICT, ZIMBABWE

by

FARAYI BLESSING JAHURE

Supervisors

Mr. Webster Gumindoga

Prof. Dr. Amon Murwira

A thesis submitted in partial fulfilment of the requirements for the degree of Master of Science in Integrated Water Resources Management of the University of Zimbabwe

October 2013

DECLARATION

I, Farayi Blessing Jahure, declare that this research report is my own work. It is being submitted for the degree of Master of Science in Integrated Water Resources Management (IWRM) of the University of Zimbabwe. It has not been submitted before for examination for any degree in any other University.

Date: _____

Signature: _____

The findings, interpretations and conclusions expressed in this study do neither reflect the views of the University of Zimbabwe, Department of Civil Engineering nor those of the individual members of the MSc Examination Committee, nor of their respective employers.

TABLE OF CONTENTS

LIST OF TABLES

LIST OF FIGURES

LIST OF APPENDICES

LIST OF SYMBOLS AND ABBREVIATIONS

%VWC	Percent Volumetric Water Content
AWF	African Wildlife Foundation
ASTER	Advanced Spaceborne Thermal Emission and Reflection Radiometer
AVC	Available Water Capacity
CIRAD	International Cooperation Centre in Agronomic Research for Development
DEM	Digital Elevation Model
DTM	Digital Terrain Model
ETa	Actual Evapotranspiration
ETp	Potential Evapotranspiration
FAO	Food and Agriculture Organization (United Nations)
FD	Frequency Domain
GIS	Geographic Information System
GPS	Global Positioning System
GWP	Global Water Partnership
HM	Hydrological Modelling
IDW	Inverse Distance Weighting
ILWIS	Integrated Land and Water Information System
IWRM	Integrated Water Resources Management
K	Kelvin
Km	Kilometres
Km^2	Squared Kilometres
Landsat	Land Satellite
LGDA	Lower Guruve Development Association
m^3/s	cubic meters per second
masl	meters above sea level
MODIS	Moderate Resolution Imaging Spectroradiometer
MSc.	Master of Science
n	Manning's coefficient
NASA	National Aeronautics and Space Administration
NGOs	non-governmental organizations
NSE	Nash-Sutcliffe's coefficient of efficiency
^oC	degree Celsius
PAW	Plant Available Water
PBIAS	percent bias
PDQ	percentage difference of runoff
PMW	Potential maximum wetness
RS	Remote sensing

SEBS	surface energy balance system
SM	soil moisture
TDR	Time Domain Reflectometry
TM	Thematic Mapper
TOPMODEL	Topographic Model
USDA	United States Department of Agriculture
USGS	United States Geological Survey
WMO	World Meteorological Organisation
ZINWA	Zimbabwe National Water Authority

DEDICATION

This work is dedicated to Mufaro Jahure.

ACKNOWLEDGEMENTS

This work would not have been possible without funding from my sponsors, WaterNet; I gratefully appreciate them.

I also gratefully acknowledge my supervisors Professor Amon Murwira and Mr. Webster Gumindoga for their generous help and contribution to my ability to complete the work.

My sincere thanks go to the Department of Civil Engineering (DCE) for their technical support offered during the laboratory sessions of this study. Many thanks go to the rest of the Lecturers at DCE, University of Zimbabwe for their support.

I also wish to extend my gratitude to my colleagues, 2012-2013 MSc IWRM class, I appreciate your support.

My special appreciations go to my family for their support.

ABSTRACT

The livelihoods and subsistence of the largest number of people in Mbire communal areas depends on soil moisture evolving from seasonal floods that is tapped for agriculture. The communities have not realised the full potential of floodplains soil moisture in increasing crop yields, vital for hunger and poverty alleviation. Proper quantification of soil moisture levels is very vital for improvement and management of agricultural activities in these floodplains. Soil moisture is typically measured in the field at point scale, which is expensive, tedious, time consuming and does not account for regional spatial variability. Methods based on Remote sensing (RS) and hydrological modelling provide alternative tools to obtain estimates of spatial and temporal variation of soil moisture which is vital in water resources management in ungauged and remote areas. In this study integration of the Surface Energy Balance System (SEBS) and the Topographic driven MODEL (TOPMODEL) was carried out in estimating soil moisture for Mbire district in Zimbabwe and comparing them against ground measurements. Five atmospherically corrected MODIS images were processed and compared from ground data collected once a month on fifty-four soil moisture sampling sites. The proportional relation of the relative soil moisture with the relative evapotranspiration was used for the estimation of soil moisture from remote sensing as SEBS was primarily developed for the estimation of surface turbulent fluxes. The rainfall runoff model (TOPMODEL) whose land surface inputs were obtained from Remote Sensing was calibrated with runoff data was used to simulate soil moisture and compared from ground information collected on fifty-two soil moisture sampling sites. An upscaling procedure to improve the comparison between point measurements, remote sensing and TOPMODEL outputs was accomplished by the use of geostatistical tools. Land suitability analysis for flood recession farming was done using distance from stream network, vertical channel distance, and land use/cover datasets. The performance indicators for TOPMODEL simulations showed an acceptable match with measured discharge, indicating a satisfactory Nash Sutcliffe model efficiency (NSE= 0.77 and 0.81) and good percent bias (PBIAS= -6.04% and -10.5%) for Manyame and Angwa sub catchments respectively. The study revealed that there is a strong relationship (R^2= 0.80) between upscaled ground soil moisture measurements and remote sensing methods (SEBS) for the period of March to July 2013. This allowed this methodology for modelling initialisation to be adopted. The study revealed that there is a fair relationship (R^2= 0.60) between upscaled ground soil moisture measurements and hydrological modelling (TOPMODEL) for the period of March to July 2013. Results also show that 22800 hectares of Mbire district is suitable to moderately suitable for flood recession farming. The study concludes that use of remote sensing and hydrologic models coupled with Geographic Information System (GIS) are effective in soil moisture monitoring which is vital for planning and management of available water resources for sustainable development Mbire community.

KEYWORDS: MODIS, Soil moisture variation, SEBS, TOPMODEL

CHAPTER ONE

1. Introduction

1.1. General introduction

Mbire District, is prone to low rainfall, seasonal floods, and agricultural droughts but with four major tributaries of the mighty Zambezi River passing through the District and the Zambezi River bordering it to the north. Despite this 'richness' in water resources, the inhabitants are facing a challenge in securing enough water for agricultural production resulting in increased hunger and poverty since their livelihoods and subsistence depends on agriculture (AWF, 2010). The community have not realised the full potential of floodplains soil moisture in increasing agricultural production. Understanding soil moisture variation has become a global concern especially in view of climate change and variability. The spatial and temporal distribution of soil moisture has enormous implications in hydrological, agricultural, economic and social planning and development (Vicent *et al.*, 2004; Western *et al*., 2002). Soil moisture is a key hydrologic parameter since it has close relationship with the infiltration, evapotranspiration, surface runoff, and groundwater recharge (Mekonmen, 2009). Understanding soil moisture trend is critical in drought and flood prediction, water resources management and agricultural production (Liu *et al*., 2008).

Soil moisture is typically measured in the field at point scale, which is expensive, tedious, time consuming and does not account for regional spatial variability. Methods based on remote sensing and hydrological modeling provide alternative tool to obtain estimates of spatial and temporal variation of soil moisture (Mattikalli *et al.,* 1998). Soil moisture affects the partitioning of latent and sensible heat fluxes and hence evapotranspiration (Su *et al.,* 2003). The commonly used Heat Flux Balance method is based on the partitioning of energy into latent and sensible heat fluxes to infer soil moisture content (Scott *et al*., 2003). Surface energy balance system (SEBS) and surface energy balance algorithm for land (SEBAL) algorithms are the techniques used in this theory to compute relative evaporation that is related to relative soil moisture hence computation of soil moisture (Oku *et al.,* 2007; Ma *et al.*, 2007; Jia *et al*., 2007; Wang *et al.,* 2007; Su, 2002)

Nowadays many hydrological models are available to simulate rainfall-runoff processes and to predict soil moisture. These include Soil and Water Assessment Tool (SWAT), the TOPographic driven MODEL (TOPMODEL) and Hydrologysca Byrans Vattenbalnavdelning (HBV). In different model versions, TOPMODEL has been applied in more than 40 countries all over the world. It has been applied to countries with such different climatic conditions as for example Sweden, Zimbabwe, Ethiopia, India, Colombia and United Kingdom. (Beven, 1983; Hornberger *et al.*, 1985; Beven, 1993; Robson *et al.*, 1993; Albek *et al.*, 2004; Gumindoga, 2010; Gumindoga, 2010; Muhammed, 2012). However few studies have applied the model in floodplains such as the Zambezi basin. Therefore in this study, the ability of SEBS and TOPMODEL to estimate spatio-temporal soil moisture variation was assessed

1.2. Research background

Water and environmental management in the Middle Zambezi Valley presents a unique challenge to proponents of IWRM and integrated natural resources management (INRM). Mbire District, experience low rainfall and high temperatures but with four major tributaries of the mighty Zambezi River passing through the District and the Zambezi River bordering it to the north. Despite this 'richness' in water resources, the inhabitants are very poor and prone to seasonal floods and droughts, besides wild animals they have to co-exist with. Previous research by Dube (2011), Phiri (2011) and Shumba (2012), showed that available water and land resources management is lagging behind, the acquisition of spatio-temporal soil moisture variation remains a gap which is vital for sustainable utilisation of water and water resources in Mbire district. This research is closely related to these aforementioned studies but tries to deepen the understanding of how the management of reservoirs upstream and downstream of the Middle Zambezi Basin has affected the livelihoods of riparian communities of the Mbire District. Since one of the major challenges in the District is poverty alleviation, especially food insecurity, this research seeks to enhance better utilisation of critical ecosystem resources (recession farming in fragile floodplains) by using scientific knowledge in understanding and prediction of soil moisture fluctuations.

1.3. Research problem

The communities in Mbire district face water challenges and increased hunger and poverty due prevailing climatic variation and change. They have not realised the full potential of

floodplains soil moisture in increasing crop yields, thereby eradicating hunger and poverty, resulting in improved livelihoods. There is little understanding of the soil moisture dynamics resulting from flooding in the floodplains of the Mbire District, and the impacts of these floods on spatial and temporal variation of soil moisture (LGDA, 2009, Shumba, 2012). For the purposes of water resources planning and poverty eradication, there is a need to improve the understanding of the temporal and spatial variation of soil moisture which is relevant to maximise crop production and equipping the floodplain communities with the necessary knowledge and skills to sustainably utilise the soil and water resources during flooding events. However soil moisture monitoring at point scale is expensive, tedious, time consuming and does not account for regional spatial variability. Data acquisition through remote sensing in near time and hydrological modeling therefore could be an alternative and reliable resource to alleviate this problem.

1.4. Research objectives

1.4.1. General objective

The main objective of this research is to integrate Earth observation techniques, ground observations and hydrological modeling to assess the spatial and temporal variation soil moisture along major tributaries of Zambezi River in the Mbire District.

1.4.2. Specific objectives

i. To estimate the spatial temporal variation of soil moisture in the Mbire District as inferred from the SEBS driven relative evaporation
ii. To calibrate the rainfall runoff model (TOPMODEL) with hydrometeorological data for soil moisture prediction in the Mbire District's hydrological catchments
iii. To analyse and apply geo-statistical tools to interpolate point based measurements of soil moisture along the major tributaries of the Zambezi basin in the Mbire district and compare outputs with SEBS and TOPMODEL based simulations
iv. To evaluate suitable land for flood recession crop farming in the district

1.5. Research questions

i. To what extent can the SEBS algorithm be used to retrieve soil moisture levels in the Mbire district?
ii. What is the best method for computing soil moisture content from relative soil moisture in the district?

iii. To what extent can TOPMODEL be used to simulate soil moisture in the Mbire district?

iv. Is there any significant difference between upscaled point based soil moisture measurements and soil moisture outputs from SEBS and TOPMODEL?

v. Where are the most suitable areas to practise flood recession crop cultivation in the district?

1.6. Research justification

The spatio-temporal soil moisture variation influences a number of environmental systems and water resources management (Western *et al*., 2002). Soil moisture is an important bio-physical parameter that is used as an interface for the land surface and for the atmosphere and is also a key hydrologic variable linked to water availability and is also used as a control volume for storing water for plant growth (Mekonmen, 2009). This study seeks to analyse the spatio-temporal variation of soil moisture in the floodplains. This is important in, maximising the use of available soil moisture for agricultural purposes and in drought and flood monitoring.

Floodplain utilisation, conservation and protection decisions can be made after carrying out this study by quantifying the levels of available soil moisture both spatially and temporarilly moreover by delineating suitable areas for flood recession farming. The study results can assist decision makers in selecting appropriate locations to establish permanent soil moisture monitoring sites for drought and flood monitoring. The results will also assist all stakeholders in selecting appropriate agricultural area as to maximise production for alleviation of hunger and poverty and to sustainably utilise the floodplains in Mbire district. The overall goal of the study is to provide information to decision makers and all stakeholders that are needed in improving utilisation and monitoring of soil moisture thereby improving economic, environmental and social benefits to the people in the Mbire floodplains.

1.7. Hypotheses

We test the null hypothesis that there is no significant difference between upscaled point based soil moisture measurements and soil moisture outputs from SEBS and TOPMODEL at p=0.05.

1.8. Scope and limitations of the study

The study focused on the assessment of spatial and temporal variation of soil moisture along the major tributaries (Manyame River, Musengezi River and Angwa River) of Zambezi River in Mbire District by integrating earth observation techniques, hydrological modeling techniques and ground observations. It comprises of modeling (rainfall-runoff and soil moisture mapping) tools to assist on decision-making process and feasible measures to enhance maximum utilisation of available water resources in the district. The limitations of the study area includes: a vast study area (4,600 km^2), the high complexity of ungauged river network and the 'fixed' time available for data collection, difficulties in accessing all the critical sites in the district; limited meteorological and hydrological data in the district; the neglected effects of the Kariba and Cabora Bassa dam operations and unavailability of historical data on soil moisture and soil physical properties.

1.9. Presentation of the thesis

This thesis is presented in five (4) chapters, namely: Chapter 1, introduction that deals with a general background, problem statement, justification of the study, objectives (general and specific), research questions and scope and limitations of the study; Chapter 2, reviews different literature flooding patterns in the study area, flood recession farming , soil moisture (in general and measurement), relation of soil moisture and evapotranspiration, estimation of evapotranspiration (in general and the use of surface energy balance system (SEBS) top model (theory and assumptions); Chapter 3, materials and methods refers to the study area (location, population, flora and fauna, soils, climate, drainage, and hydro-meteorological instrumentation) and methods used on the research in (estimating soil moisture from SEBS, soil moisture simulating from TOPMODEL, upscaling of ground based soil moisture and comparisons and flood recession farming land suitability analysis). Within the methods section, the field work (existing data and information and 'in-situ' measurements and readings) and desk study (satellite images, rainfall-runoff model, and maps) are presented and Chapter 4, results and discussions are presented by specific objectives. In the same chapter, the conclusions and recommendations are also presented by objectives.

CHAPTER TWO

2. Literature review

2.1. Flooding patterns in the Mbire District

Madamombe (2004) defines a flood as an overflow of water, an expanse of water that submerges land, a deluge. A flood is usually due to the volume of water within a body of water, such as a river or lake, exceeding the total capacity of the body, and as a result some of the water flows or sits outside of the normal perimeter of the body. It can also occur in rivers, when the strength of the river is so high it flows right out of the river channel, usually at corners or meanders.

Mbire district affected by seasonal flash floods, this occurs in most years normally in January and February. This is at the peak of the rainfall season(LGDA, 2009). The study area affected by floods because of its location; it is located downstream of Kariba dam but upstream of Cabora Bassa and near the confluence of Manyame and Musengezi (Madamombe, 2004). As from December to February the Kariba dam rises to a certain level, water is released from the dams to avoid dam failure. This causes substantial increase in discharge in the Zambezi River. Subsequently Manyame, Mwanzamutanda, Kadzi and Musengezi rivers will thus not be able to discharge in the Zambezi as result water begins to accumulate at the confluence of these rivers to Zambezi River leading to flooding in the Mbire district area (Shumba, 2011). Also Cabora Bassa dam levels continue to rise as releases from the dam are exceeded by inflows due to releases from Kariba and Zambezi tributaries. The swelling of the Cabora Bassa dam leads to flooding in the area under study. This has led to loss of livestock and human life, crops and infrastructure have been destroyed leaving the rural folk in general poorer (Madamombe, 2004). The actual costs of the flood damages are not available as most of the assessments done so far are of a qualitative nature. Women are the most affected since they are responsible for the day-today management of the families such as looking after the health of the child and securing food for the family. Diseases outbreaks such as malaria and cholera have been quite common during this period (Madamombe, 2004).

2.2. Flood recession crop cultivation

Riparian areas along streams and rivers are distinct environments usually with greater soil moisture and soil fertility than the surrounding land (Mlowoka, 2008). The floodplain is the area covered by the water when it flows beyond the river channel, including the riparian zone (Fritz *et al*., 2003). The WMO (2006) defines a floodplain as a flat or nearly flat land adjacent to a stream or river that stretches from the banks of its channel to the base of the enclosing valley walls and experiences flooding during periods of high discharge. The growing of crops in floodplain after flood occurrence is termed flood recession farming. The Zimbabwean law prohibits the growing of crops in 30 metres from (CIRAD, 2001). The impact of streambank and floodplain cultivation is that it loosens the soil hence prone to erosion resulting in siltation of water bodies and crops are sometimes washed away or waterlogged during flooding thereby compromising food security. Flood recession farming has become an act of improving food security in most parts of the world especially in those areas that experience low rainfall and high stream flows and poor soil fertility(Armah, 2013).

2.3. Soil moisture

2.3.1. General

Near surface soil moisture influences the partitioning of precipitation into infiltration and runoff and is important in evapotranspiration because it controls water availability to plants and thus affects the partitioning of latent and sensible heat (Grayson, 1998). Soil moisture is affected by land use and land cover change and different hydrological components like interception, infiltration and evaporation (Gumindoga, 2010). Moisture content or water content can be expressed in two ways that is gravimetric water content which is the mass of water per unit mass of dry soil and volumetric water content which is the volume of water per unit volume of soil. Rowell (1997) defines the saturated water content as the maximum amount of water a soil can hold, typically 40 % to 60 % of the total volume. The water is important for supplying the water requirements for the plants, containing dissolved ions and molecules including nutrients and as the medium in which chemical reactions occur. Evans *et al*. (1996), Rowell (1997) and Sandor (2008) analysed the soil moisture as an integral quantity that represents the average conditions in a finite volume of soil.

Three types of soil water are given by Sandor (2008) and these are gravitational, capillary

water and hygroscopic. The gravitational water is not available to plants as it drains to the zone of saturation. After the redistribution process is complete, the soil is at field capacity and contains the greatest amount of water that is potentially available to plants. Plants get most of their water from capillary water which is water retained in soil pores after gravitational water has drained. Surface tension or suction holds capillary water around the soil particles. When the surface tension becomes high, the plant is unable to take up any of the remaining water (hygroscopic water) and permanent wilting results and the plant has removed all the available water (Evans *et al*., 1996). The plant available water (PAW) is the volume of water stored in the soil reservoir that can be used by plants and is the difference between the field capacity and the permanent wilting point. Soil texture is the sole determinant of water holding capacity and movement. Available water increases with increasing fine textured soil, from sands to loams. Coarse textured soils have lower field capacity because of large pores subject to free drainage. Fine textured soils have a greater occurrence of small pores that hold water against free drainage resulting in higher field capacity. Soils with a high salt concentration tend to have a reduced available water capacity because more water is retained at the permanent wilting point (USDA, 2008; Zoratelli *et al*., 2010). The plant available water is given by:

$$PAW = (\theta f - \theta w) \times D \quad [1]$$

Where;
D = the depth of soil exploited by plant roots in m,
PAW = the plant available water in m of water,
θw = the moisture content at the wilting point in $m^3\ m^{-3}$ or % and
θf = the moisture content at field capacity in $m^3\ m^{-3}$ or %.

From studies by Western *et al*. (2002), the soil moisture store is primarily replenished by infiltration depleted by soil evaporation and plant transpiration. The amount of soil moisture and its dynamics change with time. Provided a soil is free to drain, wet soils drain to the point where gravity can no longer remove water from the pores. The soil moisture at this point is the field capacity *θf*. When the water content falls below the field capacity creating a soil moisture deficit, irrigation must be applied to return the soil to field capacity (Fullen, 2004).

Field capacity is a parameter with important uses in hydrology and water resources management. Soil is a major reservoir for water. In areas where there is excessive rainfall available water is of little importance to plants but in arid and semi-arid regions where plants remove more water than is supplied by precipitation, the amount of water held by plants is

critical. By holding water for future use the soil buffers the plant-root environment during periods of water deficit (Ohio, 2005). According to Bashour (2007) water is held in the soil by adhesive and cohesive forces. Adhesion is the force of attraction between the solid soil particles and water molecules. Western *et al*. (2002) showed the water content can also be calculated using equation [2]:

$$\theta v = \rho b \; x \; \theta g \qquad [2]$$

Where;

ρb *=the bulk density of the soil in kg/* m^3,

θg *=the gravimetric moisture content in kg* kg^{-1} *or%, the ratio of the mass of water (Mw) to the mass of solid soil particles or dry soil and*

θv *=the ratio of the volume of water to the volume of the soil in* m^3 m^{-3} *or %.*

2.3.2. Soil moisture measurements

Soil moisture content measurement at a point in general can be categorized into two; direct and indirect. According to studies by Dorigo *et al.* (2010) and Robock *et al.* (2000), gravimetric method is a direct and absolute technique for estimating the water content of soils. Soil moisture is indirectly measured in a number of ways such as the time domain reflectometry (TDR) method, the frequency domain measurement (FD) method (using capacitance probes) (Fullen, 2004), electric resistance blocks and radiological methods (Munoz *et al*., 2007). These methods have advantage in giving continuous soil moisture reading if used with data loggers. However there are few standard stations or networks with high resolution that observe and measure soil moisture apart from research sites.

Indirect spatial soil moisture measurement is accomplished by integrating remote sensing (RS) and hydrological modeling (Engman, 1991). According to Chen *et al.* (2008) soil moisture retrieval from RS is attempted from optical (including reflective near-infrared), thermal and microwave systems. Wang *et al.* (2007) have developed an algorithm to retrieve soil moisture from the optical/infrared region while the microwave regions of the electromagnetic spectrum have been used by Wagner *et al.* (1999b) and Wegner *et al.* (2003). The basic principle that is used in microwave is the relation between surface emissivity and the apparent dielectric constant of soil/water mix as described.

Thermal infrared remote sensing of soil moisture is based on the thermal emission ability of earth surface and soil moisture retrieval is based on Thermal Inertia, Heat Flux Balance, Universal Triangle and the Presumed TIR-SM Conversion Model methods (Monteith 1981;

Ben-Asher *et al*., 1983, Carlson *et al.*, 1994). Heat Flux Balance method as applied in this research is based on the partitioning of energy into latent and sensible heat fluxes to infer soil moisture content, (Scott *et al*., 2003). SEBS and SEBAL algorithms are the techniques used in this theory to compute relative evaporation that is related to relative soil moisture hence computation of soil moisture (Oku *et al.*, 2007; Ma *et al.*, 2007; Jia *et al*., 2007; Wang *et al.*, 2007; Su, 2002).

2.4. Interpolation of point measurements of soil moisture

Hydrological modeling (HM) and Remote Sensing has the potential to provide information on spatial soil moisture variation. Ground instruments however give only a point scale measurement. To compare the values of these parameters and variables obtained from the RS and HM models against the point scale ground measurements there is need of averaging, interpolating and up scaling or downscaling.

For interpolation purposes nearest point, moving average and geostatistical methods (like ordinary kriging, inverse distance weighting and anisotropic kriging) are now some of the routine functions in a number of GIS software. Different types of approaches are found in literature in scaling up soil moisture values from point scale to field average scale. Antonio *et al.* (2005) used arithmetic average to obtain field average plant available water content from point measurements. De Lannoy *et al.* (2007) explored some statistical methods including a time-mean bias correction, a linear transformation and cumulative density function to convert point measurement of soil moisture to field averaged soil moisture. Their analysis was based on the temporal stability analysis which was also used by Cosh *et al.* (2004) to establish the validity of this method to provide water shed scale soil moisture estimates. However Grayson and Western (1998) argue that geostatistical methods require samples that are closely spaced relative to the correlation length of the spatial soil moisture. In this research Inverse Distance Weighting was applied to closely spaced relative to the correlation length of the spatial soil moisture

2.4.1. Inverse Distance Weighting

Inverse distance weighted (IDW) interpolation determines cell values using a linearly weighted combination of a set of sample points. The weight is a function of inverse distance. The surface being interpolated should be that of a locationally dependent variable. The

{power} option of IDW lets one control the significance of known points on the interpolated values, based on their distance from the output point (Watson and Phillip, 1985). It is a positive, real number. The default value is 2. By defining the higher {power} option, more emphasis can be put on the nearest points. Thus, nearby data will have the most influence, and the surface will have more detail (be less smooth). As the power increases, the interpolated values begin to approach the value of the nearest sample point. Specifying a lower value for power will provide a bit more influence to surrounding points a little farther away.

Since the IDW formula is not linked to any real physical process, there is no way to determine that a particular power value is too large. As a general guideline, a power of 30 would be considered extremely large, and thus of questionable use. An optimal value for the power can be considered to be where the minimum mean absolute error is at its lowest. ArcGIS Geostatistical Analyst provides a way to investigate this. IDW relies mainly on the inverse of the distance raised to the power. If the distances are large, or the power value is large, the results may be incorrect (Philip and Watson, 1982). The characteristics of the interpolated surface can also be controlled by limiting the input points for calculating each interpolated point. The input can be limited by the number of sample points to be used or by a radius within which there is points to be used in the calculation of the interpolated points.

2.4.2. Soil moisture and evapotranspiration

Soil moisture affects the partitioning of latent and sensible heat fluxes and hence evapotranspiration. In estimating actual evapotranspiration commonly used methods is to linearly relate the PET with the relative soil moisture as shown below.

$$\frac{ETact}{ETp} \propto \theta rel \qquad [3]$$

Where;
ET_{act} *=the actual evapotranspiration (m)*
ET_p *=the potential evapotranspiration (PET)(m)*
θ_{rel} *=the relative soil moisture.*

PET is estimated from meteorological data and by the combination of meteorological data and energy balance considerations. For relative soil moisture various definitions are found in literature. Dingman (2002) defines relative water content as:

$$\theta rel = \frac{\theta - \theta pwp}{\theta fc - \theta pwp} \qquad [4]$$

Where;
θ *=the current water content (m),*
θ_{fc} *=the field capacity (m) and*
θ_{pwp} *=the permanent wilting point of the root zone soil (m).*

Van der Lee and Gehrels (1990) define it as:

$$\theta rel = \frac{\theta - \theta r}{\emptyset - \theta r} \quad [5]$$

Where;
θr *=the residual soil moisture (m) and*
$\emptyset$ *=the porosity of the soil (m^3).*

SEBS algorithm make the use of energy balance consideration at the limiting cases and the concept of relative evaporation was developed as in the following equation.

$$\Lambda r = \frac{\lambda E}{\lambda E wet} \quad [6]$$

Where;
Λr *=the relative evaporation,*
λE *=the evaporation (m),*
λE_{wet} *=the potential evaporation (m).*

This was further developed into soil moisture by Su *et al.,* (2003) considering water balance of a soil layer in the vertical direction at the limiting cases similar to the relative evaporation. It is shown that the relative soil water content is directly related to the relative evapotranspiration.

$$\theta rel = \frac{\theta}{\theta wet} = \frac{\lambda E}{\lambda E wet} \quad [7]$$

Where;
θ_{wet} *= the water content at limiting case taken as porosity of the soil.*

This potential maximum wetness (limiting) value has also been shown to be approximated to a midpoint between the field capacity and the total water capacity (porosity) by Wagner *et al.,* (1999a), after a histogram analysis of gravimetric soil moisture data. This can be expressed as:

$$\theta wet = \frac{\theta fc + \emptyset}{2} \quad [8]$$

These relations could were used in computing soil water content after computing the relative evaporation from energy balance methods.

2.5. Evapotranspiration

Allen *et al.* (1998) defines potential evapotranspiration (PET) as the maximum possible

evapotranspiration according to prevailing atmospheric conditions and vegetative properties. Vegetated surface requires water such that soil moisture forms no limitation to stomata aperture. The reference crop evapotranspiration defined in FAO paper no 56 (Allen *et al*., 1998) is a special case of PET with fixed properties and without variability while potentially evaporating or transpiring surfaces have temporal and spatial variability.

2.5.1. Estimation of evapotranspiration

Methods for estimating potential and actual evapotranspiration (AET) are classified basing on data requirement (Dingman, 2002)**.** They are grouped as temperature based, radiation based, combination and pan methods. For the AET the widely used methods are the water balance approaches, the potential evaporation approach and the energy balance approach. In water balance approaches lysimeters are used to measure evapotranspiration by measuring the components of the water balance. The potential evaporation approach is based on the complementary relationship approach, as discussed in Brutsaert (2005). The energy balance approach deals with conservation of energy, the Penman-Monteith, the Bowen ratio and the Eddy correlation approaches are classified into this group.

2.5.2. Remote Sensing approaches in estimating evapotranspiration

RS quantification is based from measurements of the reflected and emitted electromagnetic radiation of the Earth's surface. In estimation of atmospheric turbulent fluxes two basic physical principles, the conservation of energy and turbulent transport is considered (Su, 2002a). Conservation of energy is the basis of the surface energy balance approaches and latter also called the aerodynamic approach, recognizes the importance of wind in transporting vapour away from the evaporating surface. Energy available in the energy balance approach needs to be distributed between sensible and latent heat fluxes which include the principle of turbulent transport. Surface energy balance equation for an evaporating surface can be written in its simplest form as:

$$Rn = G + H + \lambda E \qquad [9]$$

Where;
Rn =the net radiation (Wm^{-2}),
G =the soil heat flux; the energy utilized in heating the soil (Wm^{-2}),
H =the energy conducted as sensible heat (Wm^{-2}) and
λE =the latent heat flux; the energy utilized for evaporation(Wm^{-2}).

The net radiation is the sum of all incoming and outgoing radiation of both short and long wavelengths (Allen, 1998).

A number of algorithms that employ RS imageries have been developed to compute evapotranspiration. These algorithms are Disaggregated Atmosphere Land Exchange Inverse model (DisALEXI) by Norman *et al.* (2003), SEBAL by Bastiaanssen et al (1998), Simplified Surface Energy Balance Index(S-SEBI) by Roerink et al (2000), and SEBS by Su (2002b) (used in this research). It is also possible to estimate actual evapotranspiration for days without satellite imagery using these algorithms (Immerzeel *et al.*, 2006) in combination with daily meteorological data.

2.5.3. The Surface Energy Balance System (SEBS)

The Surface Energy Balance System (SEBS) was developed to estimate atmospheric turbulent fluxes and surface evaporative fraction using satellite data in the visible, near infrared, and thermal infrared range in combination with meteorological data. The algorithm requires inputs that consist of land surface albedo, temperature, fractional vegetation coverage and leaf area index, roughness height, meteorological data such as air temperature and pressure, humidity and wind speed at a reference height and downward solar radiation and downward long wave radiation (Su, 2002b). The following Energy balance components extracts are based on the SEBS article (Su, 2002b) and related ancillary papers.

Net radiation

The net radiation is the difference between the incoming short wave radiation and the outgoing long wave radiation, described as:

$$R_N = R_{snet} + L_{net} \quad [10]$$

Net short wave radiation net radiation is calculated by:

$$R_{snet} = (1 - \alpha) R_{swd} \quad [11]$$

Net long wave radiation component of the net radiation is expressed as:

$$L_{net} = \varepsilon L_{in} - \varepsilon \sigma T_s^4 \quad [12]$$

Where;

R_{snet} *=the net shortwave radiation (Wm^{-2}),*
R_{swd} *=the incoming shortwave solar radiation (Wm^{-2}),*
L_{net} *=the net long wave radiation (Wm^{-2}),*
L_{in} *=the incoming long wave radiation (Wm^{-2}),*
α *=the surface albedo, ε is the surface emissivity,*

σ =*the Stefan-Boltzmann constant which is equal to 5.67 x 10^{-8} $Wm^{-2}K^{-4}$ and*
T_s =*the surface temperature in Kelvin.*

The incoming long wave radiation, L_{in} is computed from the following formula.

$$L_{in} = \varepsilon_a \sigma T_a^4 \quad [13]$$

Where;
ε_a =*the atmospheric emissivity and*
T_a =*the air temperature in K at the reference height*.

The atmospheric emissivity can be estimated as given in (Su, 2002a):

$$\varepsilon_a = 9.2 \times 10^{-6}(T_a + 273.15)^2 \quad [14]$$

In SEBS α, ε and T_s are calculated in the algorithm using the following formula as given in Iqbal (1983).

$$R_{swd} = I_{sc} e_o cos\theta_z e^{-mt} \quad [15]$$

Where;
I_{sc} =*1367 Wm^{-2} is the solar constant,*
e_o =*the eccentricity factor,*
θ_z =*the solar zenith angle,*
m =*the air mass and*
τ =*the optical thickness.*

Soil Heat flux

The soil heat flux is related with the net radiation and the type of the surface whether it is bare soil or fully vegetated or mixed. In SEBS it is given as:

$$G_o = R_n(T_c + (1 - P_v) * (T_s - T_c)) \quad [16]$$

Where;
T_c =*the ratio of soil heat flux to net radiation for full vegetation canopy, is equal to 0.05,*
T_s =*the ratio of soil heat flux to net radiation for bare soil, equal to 0.315 and*
P_v =*is the fractional vegetation coverage*

Sensible heat flux

Sensible heat flux is the flow of energy due to the temperature gradient of the air upwards or downwards depending on the time of the day. In SEBS the derivation requires wind speed and temperature at the reference height and the surface temperature. It is calculated by solving the system of three equations (equations 17-19) involving the friction velocity and the Obukhov stability length.

$$u = \frac{u.}{k}[In\left(\frac{z-d_o}{z_{om}}\right) - \Psi_h\left(\frac{z-d_o}{L}\right) + \Psi_h\left(\frac{z_{om}}{L}\right)] \quad [17]$$

$$\theta_o - \theta_a = \frac{H}{ku.\rho Cp}\left[In\left(\frac{z-d_o}{z_{oh}}\right) - \Psi_h\left(\frac{z-d_o}{L}\right) + \Psi_h\left(\frac{z_{oh}}{L}\right)\right] \quad [18]$$

$$L = \frac{-\rho C_p u_*^3 \theta_v}{kgH} \quad [19]$$

Where;

U =*the mean wind speed in* ms^{-1},
θ_o =*the potential temperature at the surface in K,*
θ_a =*the potential air temperature in K at height z,*
H =*the sensible heat flux in* Wm^{-2},
U =*equal to* $(\tau_o/\rho)^{1/2}$ *is the friction velocity in* ms^{-1},
τ_o =*the surface shear stress in* Nm^{-2},
ρ =*the density of air in* kgm^{-3},
k =*0.4 is the von Karman's constant,*
z =*the height above the surface in m,*
d_o =*the zero plane displacement height in m,*
Z_{om} =*the roughness height for momentum transfer in m,*
Z_{oh} =*the scalar roughness height for heat transfer in m,*
Ψ_m =*the stability correction function for momentum*
Ψ_h =*the stability correction function for sensible heat transfer respectively, and*
L =*the Obukhov stability length in m defined as the ratio between the kinetic energy produced by convective and mechanical forces,*
G =*the acceleration due to gravity in* ms^{-2}*and*
θ_v =*the potential virtual temperature in K near the surface.*

Sensible heat flux at the dry limit (**H_{dry}**)-Under the dry-limit, the latent heat (**λE_{dry}**) becomes zero due to the limitation of soil moisture and the sensible heat flux is at its maximum value it follows that:

$$H_{dry} = R_n - G_o \quad [20]$$

Sensible heat flux at the wet limit *(H_{wet})* – Under the wet limit where the evaporation takes place at the potential rate *(λE_{wet})*, the sensible heat takes its minimum value *(H_{wet})*,

$$H_{wet} = R_n - G_o - \lambda E_{wet} \quad [21]$$

The sensible heat at the wet limit can be derived by combining equation 21 with the PenmanMonteith combination equation

Relative evaporation

The relative evaporation Λ_r is evaluated as:

$$\Lambda_r = \frac{\lambda E}{\lambda E_{wet}} = 1 - \frac{\lambda E_{wet} - \lambda E}{\lambda E} \quad [22]$$

Substitution of equations 9 and 20 into equation 21 and after some algebra:

$$\Lambda_r = 1 - \frac{H - H_{wet}}{H_{dry} - H_{wet}} \quad [23]$$

Evaporative fraction

The evaporative fraction is defined as the ratio of the latent energy to the available energy.

$$\Lambda = \frac{\lambda E}{(R_n - G_o)} = \frac{\Lambda, \lambda E_{wet}}{(R_n - G_o)} \quad [24]$$

Latent heat flux

Finally by inverting equation 24 the instantaneous latent heat flux can be calculated.

$$\lambda E = \Lambda(R_n - G_o) \quad [25]$$

Daily actual evapotranspiration

Assuming that the net daily soil heat flux is close to zero and that the daily evaporative fraction is the same as the instantaneous evaporative fraction given by equation 24 and also, the actual daily latent heat of evapotranspiration from the average daily net radiation can be calculated as:

$$\lambda E_{daily} = \Lambda R_{n\ daily} \quad [26]$$

Daily net radiation is calculated by averaging the incoming and outgoing short and long wave radiations to 24 hour period and the evaporation in mm day^{-1} is given as:

$$E_{daily} = 0.0353 \Lambda R_{ndaily} \quad [27]$$

2.6. Hydrological models

Nowadays many hydrological models are available to simulate rainfall-runoff and soil dynamics processes and these include Soil and Water Assessment Tool (SWAT), TOPMODEL, Hydrologysca Byrans Vattenbalnavdelning (HBV) and the Hydrologic Engineering Centre-Hydrologic Modeling System (HEC-HMS) (Beven, 1979; Robson *et al.*, 1993; HEC-HMS User Manual, 2010; Muhammed, 2012). In selecting a model for this research the ability of the model to simulate soil moisture, availability of the model, the availability of the data and information with regards to the input to the model were considered. In line with this, the TOPMODEL rainfall runoff model that uses the IDL source code was used. The model predicts the catchment responses following a series of rainfall events and maintains a continuous accounting of the storage deficit, which identifies the saturated source areas within a catchment and does not require as much data as required by other hydrological model (Beven, 1997a).

2.6.1. Background of TOPMODEL

TOPMODEL was originally developed to simulate small upland catchments in the United Kingdom (Beven, 1979). It is a semi-distributed model which is based on a simple theory of hydrological similarity of points in the catchment (Kirkby, 1997). The model it simulates runoff from a watershed based on the concept of saturation excess overland flow, subsurface using topographic (topographic index) data and meteorological data (Gumindoga, 2010). The model has been used to study a range of topics, including spatial scale effects on hydrological process, topographic effects on stream flow, the identification of hydrological flow path, landcover land use effects on streamflow and soil moisture estimation different catchments around the world including Zimbabwe (Beven, 1983; Hornberger *et al*., 1985; Beven, 1993; Robson *et al.*, 1993; Albek, *et al.*, 2004; Gumindoga, 2010; Gumindoga, 2011; Muhammed, 2012). However to the best of our knowledge, few or no studies have applied the model in floodplains such as the Zambezi basin.

2.6.2. The topographic index

The index approximates the distribution of the variables source areas within catchment. It is given by ln (a/tan β) index of each grid square, the contributing area (a) for that grid square need to be calculated and then divided by the tangent of the slope (tan β) relevant to that grid

(Quinn, *et al*,. 1995; Rientjes 2007). As stated by Quinn (1993) the topographic index has direct relation with soil moisture, higher topographic index relate to lowest soil moisture deficit. The TI provides the area draining through a point from upslope and the local slope angle and helps to predict local variations in soil moisture and water table (Kirkby, 1975; Wolock, 1995; Quinn *et al.*, 1995).

2.6.3. TOPMODEL assumptions and theories

Catchment topography of a catchment is analysed using a Digital Elevation Model (DEM) which represent elevation distribution of the catchment. Topographic characteristic such as slope, specific catchment area and topographic convergence are directly related to surface saturation and soil moisture deficits across the sub surface model domain (Rientjes, 2010). According to Beven *et al*,. (1995), Gumindoga (2010), and Muhammed (2012) there four basic simplifications and assumptions that are considered to reproduce the hydrological behaviour of catchment in semi-distributed way are:

i. The dynamic of the saturated zone can be approximated by successive steady state representations;
ii. The hydraulic gradient of the saturated zone can be approximated by local surface topographic slope, tan β;
iii. The distribution of down slope transmissivity with depth is an exponential function of storage deficit or depth of water table and
iv. Saturation of a soil column occurs from the below and such runoff is generated by saturation excess overland flow.

Flow through unsaturated zone

The drainage is assumed to essentially vertical and drainage flux per unit area q_v is calculated for each topographic index class. It was shown that in terms of storage deficit, Beven and Wood (1983) suggested that a suitable functional form for the vertical flux q_v at any point *i* is

$$q_v = \frac{S_{uz}}{D_i t_d} \quad [28]$$

Where;

S_{uz} *=storage in the unsaturated (gravity drainage) zone (m),*

D_i *=the local saturated zone deficit due to gravity drainage and dependent on the depth of the local water table (m).*

t_d *=time constant, expressed as a mean residence time for vertical flow per unit of deficit*.

q_v =*the flux of water entering the water table locally at any time.*

Actual evapotranspiration is calculated as a function of potential evaporation, and root zone moisture storage for cases where E_a cannot be specified directly. When the gravity drainage zone is exhausted, evapotranspiration may continue to deplete the root zone store at the rate E_a, given by

$$Ea = Ep(1 - \frac{S_{rz}}{S_{r\,max}}) \quad [29]$$

Where;
S_{rz} =*root zone storage (m)*
$S_{r\,max}$ =*maximum available root zone storage (m)*
E_a =*Actual evapotranspiration (m)*
E_p =*potential evaporation (m)*

To account for the catchment average water balance, all the local recharges have to be summed. If Q_v is the total recharge to the water table in any time step, then

$$Q_v = \sum_j q_{v.i}\, A_i \quad [30]$$

Where;
A_i *= the area associated with topographic index class I (*m^2*).*

Overland Flow and Channel Routing

For overland flow, the travel time to the outlet from any point in the watershed can be calculated by:

$$t = \sum_{i-1}^{N}[x_i/(v * \tan\beta_i)] \quad [31]$$

Where:
t =*Travel time or time delay (hr)*
x_i =*length of the flow path containing N segments (m)*
tanβ =*slope of the ith segment (%)*
v =*velocity parameter (m/hr)*

If the velocity parameter is assumed constant then this equation allows a unique time delay histogram to be derived on the basis of basin topography for any runoff contributing area extent. Detailed equation and descriptions of TOPMODEL theories can be found in Beven and Kirkby (1979); Rientjes (2007); Gumindoga (2010); and Muhammed (2012).

2.6.4. TOPMODEL parameter values

The version of TOPMODEL has a total of 12 parameters and only 11 of these parameters were used in this study in exception of CHV, and are described in the Table 2.5 below

Table 2.1: TOPMODEL parameters (Gumindoga, 2010).

Parameter	**Description**
SZM	Controls rate of decline of T (z).This is the parameter of the exponential transmissivity function or recession curve (units of depth, m), acceptable range of 0.001 to 0.050m.
LN_T0	The natural logarithm of the effective transmissivity of the soil when just saturated. A homogeneous soil throughout the catchment is assumed {units of ln(m^2/h)}.Published values for ln(To) include 35 or a 60 m grid cell (Franchini et al.,1996) &42 for a 20 m grid cell size (Saulnier et al.1997).
TD	Time delay constant for routing unsaturated flow[h] Range of values used for the dynamic TOPMODEL 0.1 - 120 (Peters et al., 2003. Should always be >0.0.
CHV	Channel flow outside of the catchment. This parameter is only used if the gauging location is further downstream than the catchment outlet (m/h).
RV	The internal subcatchment routing velocity. Or channel flow inside catchment [m/hr]
SRmax	Soil profile storage available for transpiration, i.e.an available water capacity (units of depth, m). Is also the Maximum root zone storage.
Q0	Initial stream discharge, where by default Q0 is set to the first observed discharge but may be changed by user [m/time step]
SR0	SRinit. Initial value of root zone deficit [m].
INFEX	An infiltration flag. Set to 1 to include infiltration excess calculations, otherwise 0) [-]
XK0	Hydraulic conductivity at surface, XKO declines exponentially with depth) [m/hr]
HF	(d_psi) Effective suction head [m]
DTH	(d_theta) moisture deficit [-] water content change across the wetting front

CHAPTER THREE

3. Methodology

3.1. Description study area

3.1.1. Location of study area

The Mbire District is located between 30.60° and 31.20° East and 15.60° and 16.40° South. The area covers an area of approximately 4,700 km^2. The Mbire District is characterized mainly by the former floodplains of the Zambezi River basin, at an average altitude of 400 meters above mean sea level, and drained by the rivers Mwanzamutanda, Angwa, Manyame, Musengezi and Kadzi rivers (LGDA, 2009). The District is surrounded on most sides by wildlife management areas. The western boundary is in the Chewore Safari Area while a significant part of the southern boundary is adjacent to the Doma Safari Area. Both of these areas are hunting concessions and settlements are not permitted (Chenje, 2000). In the east, part of the District is adjacent to the Mavuradonha Wilderness Area in the Muzarabani District. Along the Mozambican border, the District is adjacent to the Magoe District. Fig: 3.1 show the study area

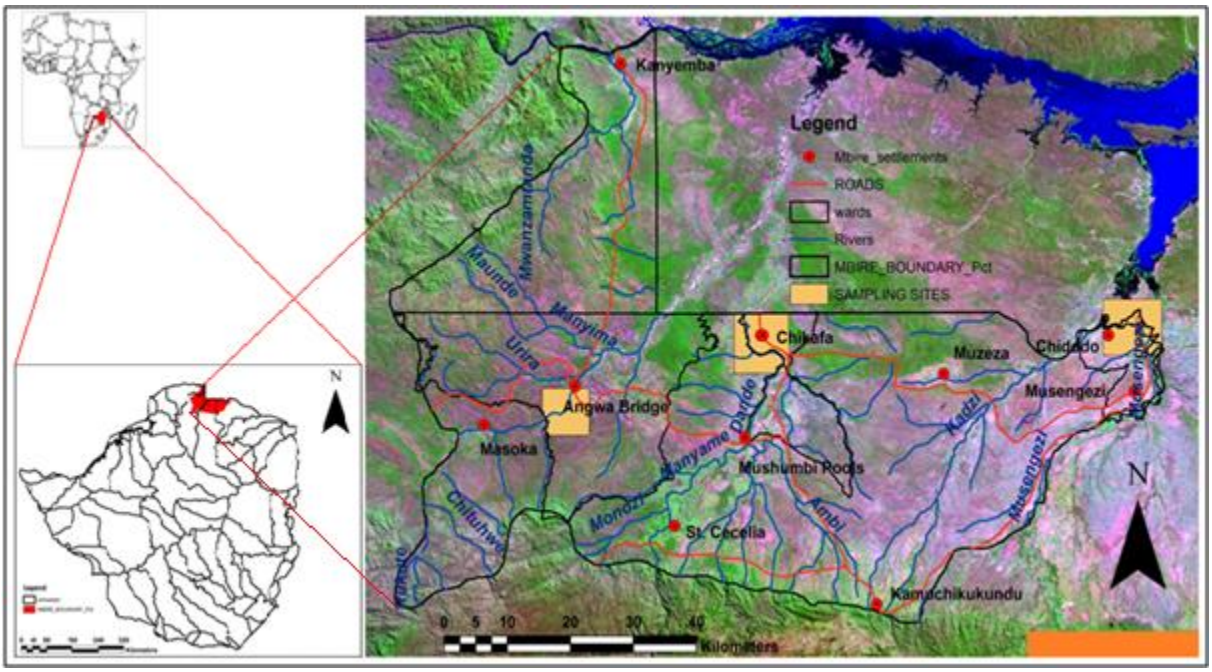

Figure 3.1: Location of Mbire District in relation to Zimbabwe and Africa

3.1.2. Climate

Mbire District is in Zimbabwe's Natural Agro-ecological region IV The climate is dry tropical, with low and very variable annual rainfall of approximately 650-700 mm but it is highly variable with one year in four being below 550 mm and one in four being above 800 mm (Phiri, 2011). The rainy season lasts a little over 100 days per annum between November and March. The rainfall is characterized by high intensities with around 40 days on which rain will fall this leads to high soil erosion rates. The district has a mean annual temperature of 25 ºC. The months; October and November, which precede the arrival of the rains, are the hottest months with maximum temperatures of over 40 ºC, whereas June and July have a minimal temperature around 10 ºC (Fritz *et al.*, 2003; AWF, 2010). Fig: 3.2 shows daily rainfall and temperatures for the district.

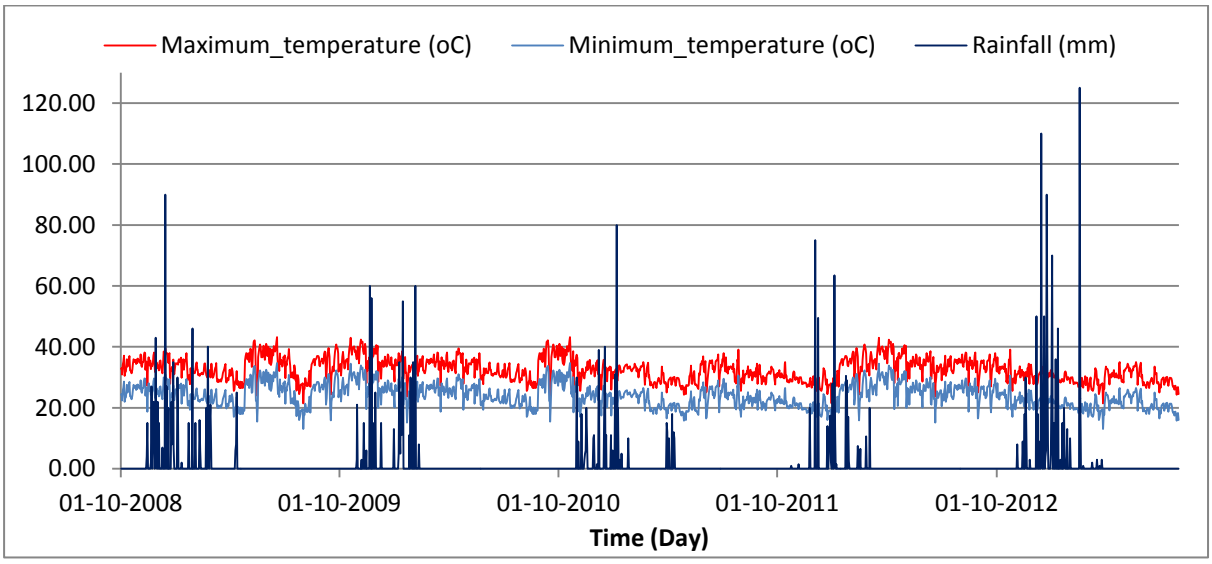

Figure 3.2: Daily average rainfall and temperatures for Mbire District;(Karoi, Centenary, Kanyemba, Mushumbi Pools and Guruve Rain Guaging stations)

3.1.3. Soils

Mbire District has a diversity of soils, however a significant part of the district is characterized by calcic solonetz soils, and these soils are sodic (FAO, 1996). Mbire District has diverse of soils with a significant part being characterised by calcic solonetz soils which are sodic ((FAO 1996); (LGDA 2009); Dube, 2011). The main soil types in the basin are the acid, leached out tropical soils of low fertility commonly known as red soils which are easily degradable and erodible promoting the occurrence of gullies. However, black soils which are of high fertility are also found in this cotton growing area. The following soil types are also dominant: calcic luvisols, eutric cambisols, eutric leptosols and ferrall-hypoluvic arenosols.

The Mbire District lies on sedimentary geological formations on sandstone and lime foundations (CIRAD, 2001) and these have led to the formation of varied soils often rich in sodium and lacking in organic matter. Fig: 3.4 shows the soil types in Mbire district

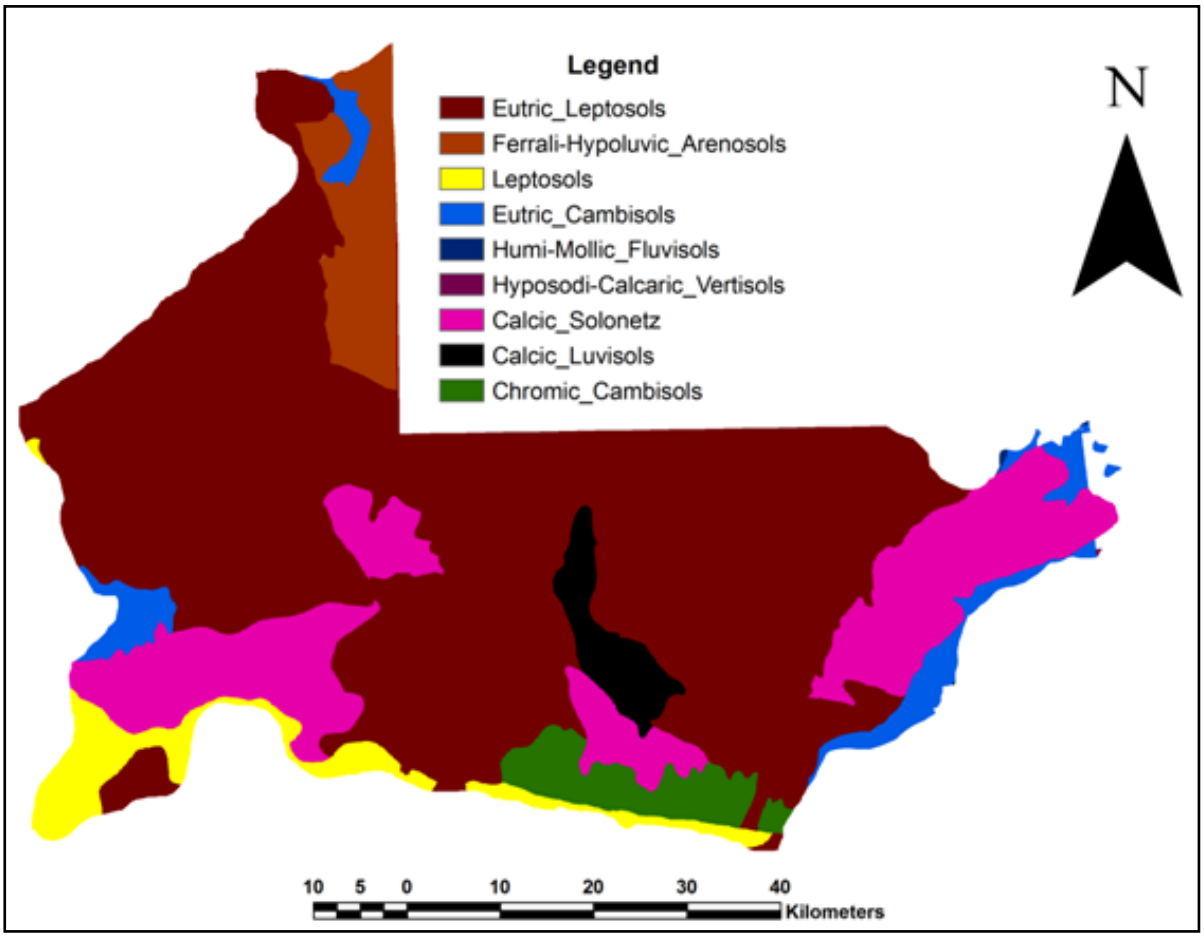

Figure 3.3: Soil types in Mbire district

3.1.4. Drainage and Flooding

Mbire District experience occasional localised flooding, the floods result from reservoir operation related floods from Kariba Dam and Cahora Bassa Dam which create a throwback effect (Phiri, 2011). This is in addition to floods generated in the area upslope of the escarpment and brought to the valley by the tributaries of the Zambezi River which are Manyame, Mwanzamutanda, Angwa, Kadzi, Musengezi and Dande Rivers as shown in Figure 3.1 the location map.

3.1.5. Socio-economic and livelihoods

The District has a predominantly agricultural economy, where the communities selected alluvial soils along watercourses (Pwiti, 1996). Historically, human population was very low

in the district due to high tsetse fly (*Glossina sp*.) infestations that causes trypanosomiasis to humans and livestock. However in the late 1970s to early 1980s a regional tsetse fly control programme managed to substantially reduce the tsetse fly infestation thereby making the area habitable (Kusena, 2009). According to a ZimStat (2012) the District had a total of about 116,000 inhabitants and about 21,500 households. These people are mainly settled along main rivers where farming is their dominant activity growing mainly cotton, small grains and maize (Biodiversity Project, 2001; (AWF, 2010). Livestock populations are relatively low and grazing around settlements, although cattle numbers have been increasing recently. Cash crop production is more significance even more demand for agriculture land and demand for fuel wood and timber has promoted deforestation (LGDA, 2009). Such developments are incompatible with the natural ecosystem (Murombedzi, 1999) particularly the soils of the area because deforestation makes the soil vulnerable to erosion by water.

3.1.6. Flora and fauna

Deciduous dry savannas of mopane *(Colophospermum mopane*), mukwa/bloodwood (*Pterocarpus angolensis*), silver terminalia (*Terminalia sericea*), splendid acacia (*Acacia robusta*), buffalo-thorn (*Ziziphus mauritiana*) and knob-thorn (*Acacia nigrescens*), marula (*Sclerocarya*) and baobab (*Andansonia digitata*) cover most of the district (CIRAD, 2001). The grass cover is mainly represented by *Andropogon gayanus* and *Loudetia flavida* (CIRAD, 2001). A total of more than 729 species have been identified in the Mbire District comprising 545 dicotyledons, 181 monocotyledons and 3 Pteridophytes (CIRAD 2001). The district has an important diversity of mammals with more than 37 species of large mammals. The animals include common duiker (*Sylvicapra*), Impala (*Aepyceros melampus*), lion (*Panthera leo*) Cape buffalo (*Syncerus caffer*), leopard (*Panthera pardus*), birds, reptiles, amphibians and fish (CIRAD, 2001).

3.1.7. Hydro-meteorological gauging and instrumentation

The Mbire district is partially gauged. There is one weather station (Kanyemba) within the district and three are close outside the district which is Guruve, Muzarabani and Karoi. There are also three water levels monitoring sites and two discharge stations though they are located at the edge of the district. There is no soil moisture monitoring station in the district. Fig: 3.5 the gauging instrumentation used in this study.

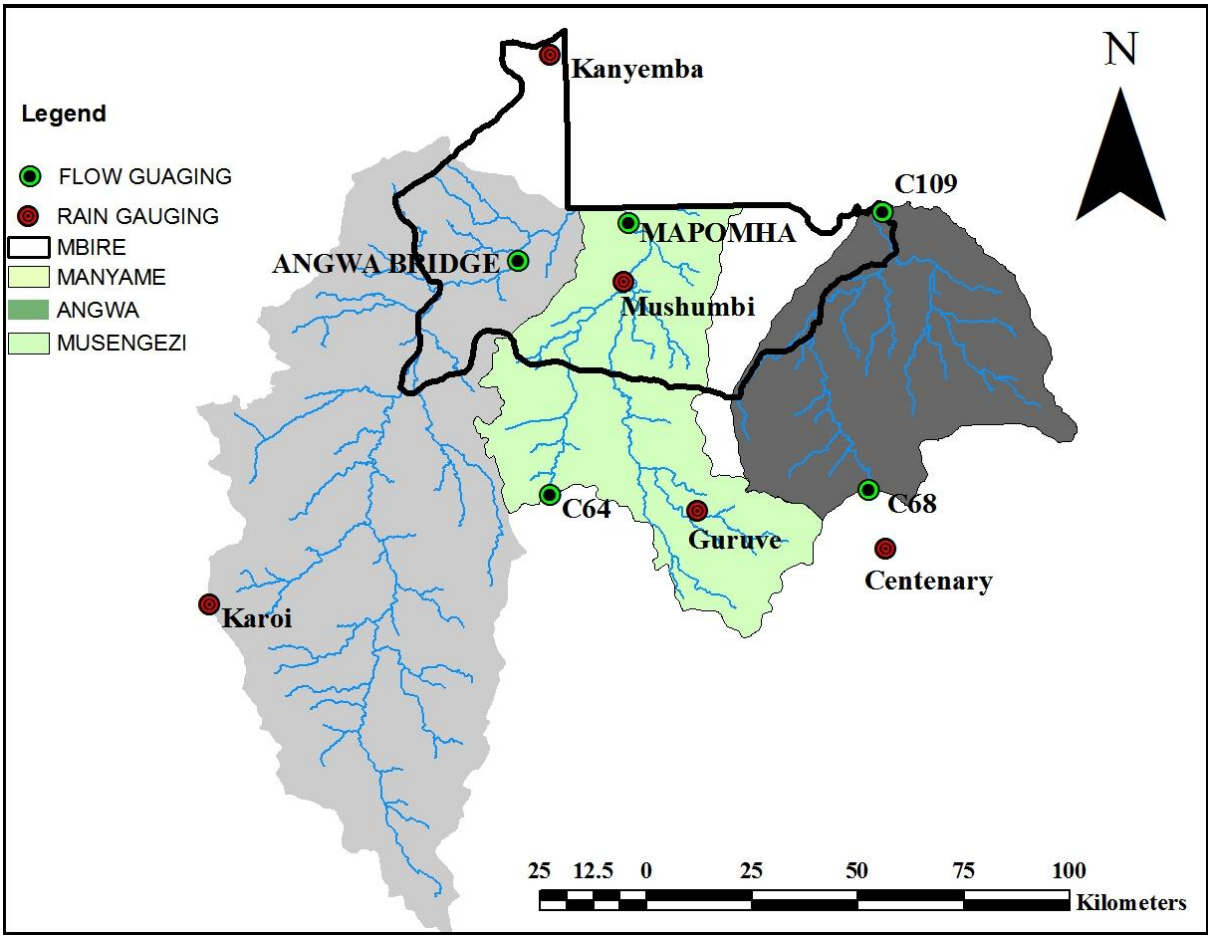

Figure 3.4: Flows and rainfall gauging stations

3.2. Research design

SEBS and TOPMODEL were used to determine spatio-temporal soil moisture variation and the outputs were compared to ground based measurements. Suitable land for flood recession farming was delineated for Mbire district Fig: 3.6 show the research process.

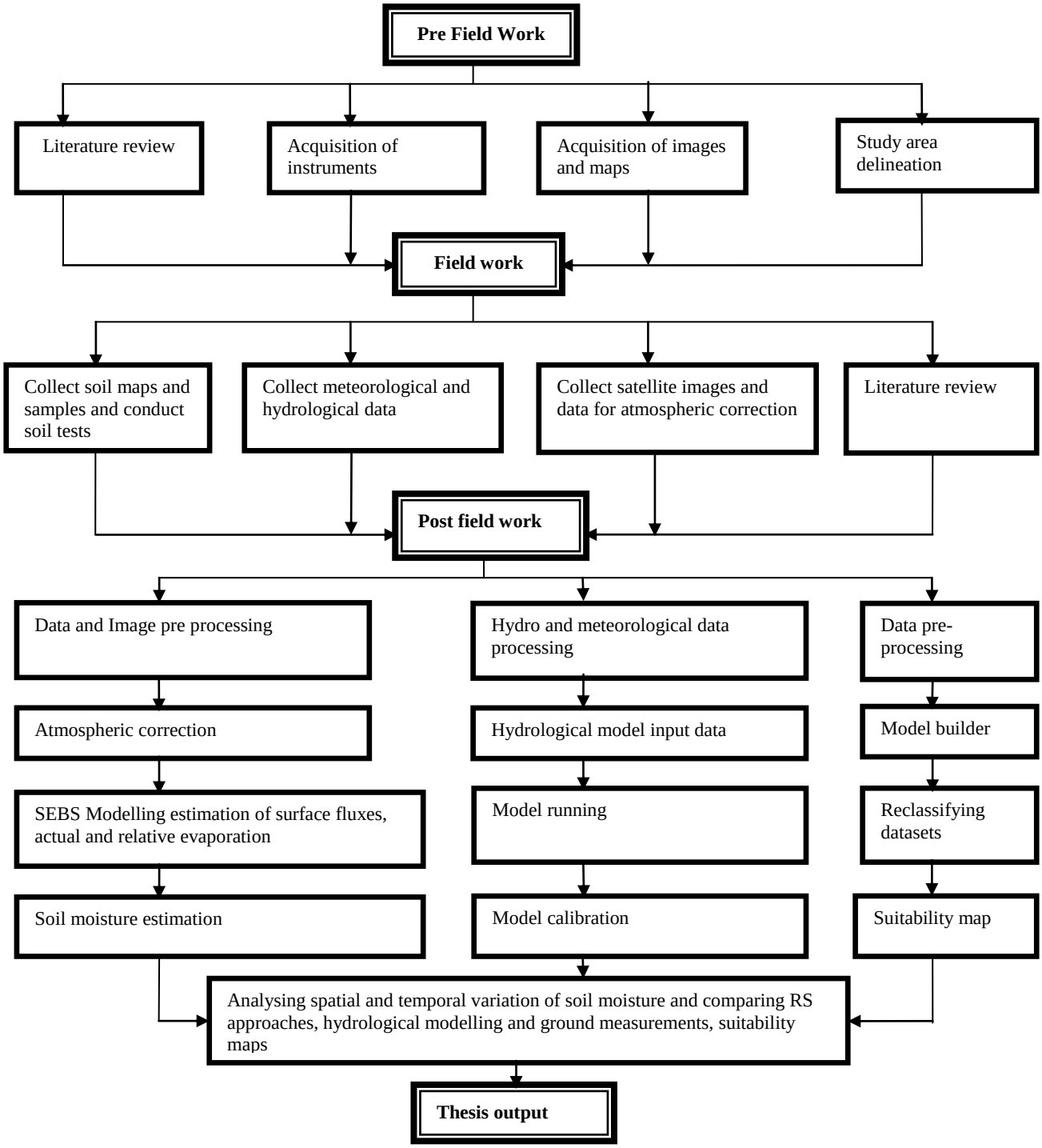

Figure 3.5: Schematic diagram showing the research process

3.3. Data collection and availability of ground data

Different data sets were required for assessing spatial and temporal variation of soil moisture by integrating remote sensing techniques, ground observations and hydrological models and also for suitability analysis. For this research the following datasets were required and were collected from the study area, web sites, previous studies and laboratory analysis. Table 3.1 below shows data sets requirements and research methodology

Table 3.1: Summary of datasets that were used and their sources

Specific objective	**Datasets used**	**Dataset source**
(i)	➢ MODIS images(1km*1km) dated 28/04/13, 16/04/13, 10/05/13, 12/06/13 and 13/07/13 ➢ Data on soil physical properties ➢ Hydrometeorological (28/04/13, 16/04/13, 10/05/13, 12/06/13 and 13/07/13)	➢ http://ladsweb.nascom.nasa.gov/browse_images ➢ Field observations ➢ Met Department and www.wunderground.com
(ii)	➢ Hydrometeorological data (temperature, humidity, sunshine hours, wind speed and rain fall) ➢ Topographic and GIS data, ASTER DEM 30m*30m ➢ Hydrological data (Daily water levels and discharge (01/10/2008-07/07/2013)	➢ Met Department and www.wunderground.com ➢ http://weather online.com ➢ NASA ➢ ZINWA and field observations
(iii)	➢ Ground based point soil moisture observations 28/04/13, 16/04/13, 10/05/13, 12/06/13 and 13/07/13 ➢ Soil moisture retrieved from remote sensing ➢ Soil moisture simulated by TOPMODEL	➢ Field and lab analysis ➢ Objective one ➢ Objective two
(iv)	➢ DEM, ➢ Landuse/ cover maps ➢ Soils shape files ➢ River shape files	➢ NASA ➢ LANDSAT Images (02/07/2012) ➢ Zimbabwe soils map ➢ DEM

3.3.1. Meteorological data

Meteorological data was collected from four weather stations two within the catchment namely Kanyemba, Mushumbi (rainfall only) and three stations outside the catchment, Guruve, Muzarabani and Karoi. The stations are monitored by the Zimbabwe Meteorological department except Mushumbi which is being monitored by AGRITEX. Data on precipitation, wind speed, relative humidity and temperature at two meters height was collected from the stations, www.wunderground.com, http://weather online.com and NASA covering the period of 2008-2013.

3.3.2. Data on physical properties of soils

54 soil sampling sites in transects were located at a 5km stretch along the major tributaries of Zambezi River in Mbire District that are Manyame, Angwa, and Musengezi. Euclidean distances from the river channels (at most 1000 m), elevation and site accessibility were the main factors that were considered in locating these sampling sites. Both systematic and stratified sampling was implemented. Fig 3.7 shows how the sampling points were located

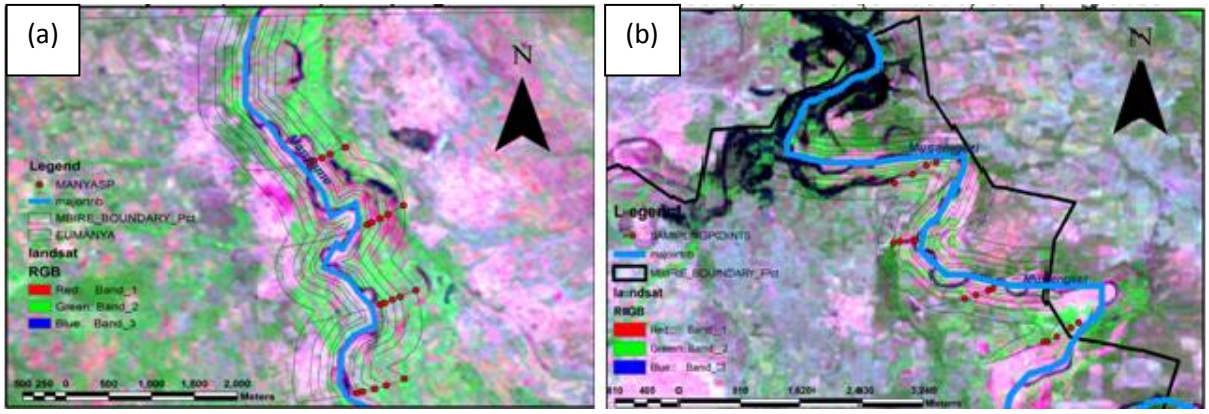

Figure 3.6: Sampling stations along the major tributaries of (a)Manyame and)b) Musengezi of Zambezi in Mbire District

Soil moisture data was obtained through sampling and laboratory analysis. To determine the field capacity values, soil water characteristic software (Soil Water Characteristics, Version 6.02.74 by Keith E. Saxton (2004) was used together with soil particle size distribution. Particle density which is the mass of the soil particles (mineral grains) in a given volume given as the mass of the soil divided by the volume of the mineral grains only was used with bulk density data to calculate the porosity of a soil. A value of 2.65 g cm^{-3} was assumed for most soils. Bulk density was determined by dividing the mass of a sample dried for 24 hours or more at 105 °C by the volume. Porosity is given by subtracting the ratio of the bulk density to the particle density from one.

3.3.3. Discharge data

Daily discharge data for C64, and C68 flow gauging station on Manyame and Musengezi River respectively and levels data at C109 on Musengezi River for the period August 2008 to July 2013 was provided by the Zimbabwe National Water Authority (ZINWA). Daily levels at Angwa Bridge on Angwa River and at Mapomha on Manyame River were converted to daily discharge data using Manning's equation and respective river cross section area.

3.4. Determination of spatial and temporal soil moisture variation using SEBS

3.4.1. Acquisition of MODIS images and coefficients

Five cloud free TERRA MODIS (Moderate resolution spectroradiometer sensor**)** Level 1b images covering the Mbire district dated 28 March 2013, 16 April 2013, 10 May 2013, 12 June 2013 and 13 July 2013 and their Geolocation were downloaded from http://ladsweb.nascom.nasa.gov/browse_images.MODIS coefficients for each band are ASCII file containing the description of the sensor calibration curve and responses for a particular sensor and band. The coefficients are incorporated in SMAC for ILWIS for each sensor and its specific bands and were downloaded from. http://ladsweb.nascom.nasa.gov/

3.4.2. Reprojecting and converting MODIS level-1B data with ModisSwathTool

The MODIS L1B data are in swath (orbit based) format, therefore the data was reprojected to standard projection and format compatible with GIS software. Both the MODIS Level-1B and geolocation data products were converted to GeoTIFF format, and reprojected to Geographic projection ready for ILWIS importing. In ModisSwathTool desired bands and coordinates for each image were selected. Table 3.2 shows bands that were selected, converted to TIFF file format and used for this research:

Table 3.2: MODIS bands that were used in this research

Band	**Band**	**Bandwidth**	**Primary Use**
EV_250_Aggr1km_RefSB_b0	channel 1	620-670 nm	Land Boundaries
EV_250_Aggr1km_RefSB_b1	channel 2	841-876 nm	Land Boundaries
EV_500_Aggr1km_RefSB_b0	channel 3	459-479 nm	Land Properties
EV_500_Aggr1km_RefSB_b1	channel 4	545-565 nm	Land Properties
EV_500_Aggr1km_RefSB_b2	channel 5	1230-1250 nm	Land Properties
EV_500_Aggr1km_RefSB_b3	channel 6	1628-1652 nm	Land Properties
EV_500_Aggr1km_RefSB_b4	channel 7	2105-2155 nm	Land Properties
EV_1KM_Emissive_b10	channel 31	10.780-11.280 µm	Surface Temperature
EV_1KM_Emissive_b11	channel 32	11.770-12.270 µm	Surface Temperature

The same steps as above were applied to the Geolocation file, in this case, SolarZenith, SolarAzimuth, SensorAzimuth, SensorZenith and Height bands were selected and converted to GeoTIFF files (Sobrino, 2003).

3.4.3. MODIS image pre-processing for SEBS

All the selected and reprojected bands were imported to ILWIS for further processing, on which ILWIS script was used to import all the files.

Converting Raw to radiances/reflectance (MODIS)

The MODIS Level 1b data are given in SI (simplified integer number); therefore, the data were converted to reflectances and radiances. MODIS channels 1 to 7 were converted to reflectances, and channels 31 and 32 were converted to radiances. The SEBS in ILWIS provided the tools to convert the imported MODIS channels in digital number /simplified integer into radiances or reflectance, which is done by applying the proper calibration coefficients. The calibration coefficients consist of a scale and offset and are provided in the HDF header file. The calibration coefficients were extracted using the HDF view. The conversion from SI (simplified integer)/raw data to reflectance was conducted using the equation below:

$$Reflectance = reflectance\_scale\ (SI - reflectance\_offset) \quad [32]$$

The conversion from SI/raw data into radiance was conducted using this equation:

$$Radiance = radiance\_scale\ (SI - radiance\_offset) \quad [33]$$

Solar and satellite zenith and azimuth angles needed were corrected by scale factor 0.01; this was done using the ILWIS map calculator, applying the following formulas in the command line:

$$Solarzenith\ angle = solarzenith\_dn * 0.01. \quad [34]$$

$$Solaraazimuth\ angle = solaazimuth\_dn * 0.01 \quad [35]$$

$$Sensorzenith\ angle = sensor\ zenith\_dn * 0.01 \quad [36]$$

$$Sensorazimuth\ angle = sennsorazimuth\_dn * 0.01 \quad [37]$$

Brightness temperature computation

The SEBS in ILWIS provided the tools to convert the bands 31 and 32 of MODIS from radiances to blackbody temperatures this is done applying the well-known Planck equation

Atmospheric Correction (SMAC)

SMAC is a tool for the atmospheric effect correction of the visible and near visible bands MODIS band 1 to 7 algorithm by Rahman, (1994) was used. Values in Table 3.3 were used

for the atmospheric correction together with Coefficient file for the sensor with the SEBS in ILWIS providing tools for this process.

Table 3.3: values for atmospheric correction of MODIS bands 1-7

0verpass date and time UTC	AOT at 550 nm	Ozone (grams.atm.cm)	Water vapor (cm)
28/03/2013 11:05	0.224	0.301	1.850
16/04/2013 11:35	0.176	0.294	1.770
10/05/2013 11:10	0.031	0.269	0.650
12/06/2013 11:10	0.097	0.288	0.513
13/07/2013 11:05	0.082	0.256	0.432

Optical thickness, water vapour and ozone content data which were used for atmospheric correction were downloaded from http://aeronet.gsfc.nasa.gov and http://jwocky.gsfc.nasa.gov

Land surface albedo computation

Using MODIS atmospheric corrected reflectance bands 1, 2, 3, 4, 5 and7, the surface albedo was computed as follows the formula by Liang et al., 2001, 2003 is used:

*albedo = 0.160*r1+0.291*r2+0.243*r3+0.116*r4+0.112*r5+0.018*r7–0.0015* [38]

Where, *r1, r2, r3, r4, r5, r7* are the surface reflectance derived from MODIS's bands 1, 2, 3, 4, 5, and 7

Land surface emissivity computation

The Land surface emissivity computation operation was used to produce the surface emissivity using the visible and near infrared bands Bred and Bnir (Sobrino, 2003,) which considers three different types of pixels depending on the NDVI thar are bare soil pixels, NDVI < 0.2, mixed pixels 0.2 =< NDVI < = 0.5 and for vegetation pixels NDVI > 0.5

Land surface temperature computation

The formula by Sobrino, (2003) was used in this operation to compute the land surface temperature using a split window method.

$$LST = btm31 + 1.02 + 1.79 * (btm31 - btm32) + 1.2 * (btm31 - btm32)2 + (34.83 - 0.68 * \mathrm{W}) * (1 - \mathrm{e}) + (-73.27 - 5.19 * \mathrm{W}) * \mathrm{de} \quad [39]$$

Where;
LST =Land surface temperature (K)
btm3 =brightness temperature obtained from MODIS band 31 (K)
btm32 =brightness temperature obtained from MODIS band 32 (K)
W =Water vapour content (g.cm^{-2})
e *=Surface emissivity*
de =Surface emissivity difference

3.4.4. Determination of daily relative evapotranspiration in SEBS Model

The SEBS algorithm in ILWIS was used to estimates the radiation balance components, atmospheric turbulent fluxes, surface evaporative fraction, and daily relative evapotranspiration and daily using data in the Table 3.4

Table 3.4: Instantaneous used for SEBS algorithm

Overpass date and time UTC	**Wind speed at 2m (m/s)**	**Vapour pressure (kpa)**	**Temperature (°C)**	**Specific humidity (kg/kg)**	**Visibility estimated (km)**
28/03/2013 11:05	4.62	1.199	16.28	0.0081	27
16/04/2013 11:35	3.02	1.115	25.04	0.0076	39
10/05/2013 11:10	0.99	0.679	17.43	0.0046	244
12/06/2013 11:10	2.15	0.411	20.90	0.0028	98
13/07/201311:05	4.15	0.511	25.30	0.0030	45

3.4.5. Validation SEBS determined evapotranspiration

Estimated evapotranspiration from SEBS was validated using E pan evaporation data from the study area.

3.4.6. Deriving potential maximum wetness (PMW) for the sampling sites

Physical properties of the top soil in the study area were analyzed in the laboratory. To determine the field capacity values, soil particle size distribution for the 54 sampling stations were determined and used to retrieve field capacity using soil water characteristic software Soil Water Characteristics, Version 6.02.74 by Saxton (2004). For Particle density value of 2.65 g cm^{-3} was assumed for most soils. Core method was used to determine the bulk density of the soil for the 54 sampling stations. The bulk density value was determined by dividing the mass of a sample dried for 24 hours or more at 105 °C by the volume. To determine soil Porosity for each of the 54 sampling sites the following formula was used

$$\emptyset = 1 - \frac{Bd}{Pd} \quad [40]$$

Where;
Ø =porosity,

Bd =bulk density and
Pd =the particle density

Potential soil wetness map for the study area was derived from field capacity and porosity using the following relationship

$$\theta wet = \frac{\theta fc + \emptyset}{2} \quad [41]$$

Where;
θfc *=field capacity and*
Θwet =the water content at limiting case taken as porosity of the soil.

This potential maximum wetness (limiting) value has also been shown to be approximated to a midpoint between the field capacity and the total water capacity (porosity) by Wagner *et al.* (1999a). Point based potential maximum wetness was upscaled by interpolation using the Inverse Distance Weighting. Finally the PMW was used to down scale SEBS outputs to 30m*30m pixel resolution and infer soil moisture from relative evapotranspiration as a product of PMW and relative evapotranspiration.

3.5. Determining spatial and temporal soil moisture variation using TOPMODEL

3.5.1. DEM hydroprocessing

An ASTER DEM (30m resolution) covering the study area has been retrieved free of charge from the website of the Global Aster Gdem, http://www.gdem.aster.ersdac.or.jp/.

Removal/filling of sinks

The fill sinks operation removes local depressions. According to Maathuis (2006) the height value of a single pixel depression is raised to the smallest value of the neighbours of a single-pixel depression and height values of a local depression consisting of multiple pixels are raised to the lowest value of a pixel that is adjacent to the outlet for the depression and that would discharge into the initial depression (Hengl *et al*., 2007). This will ensure that flow direction will be found for every pixel in the map.

Flow determination

Flow direction was computed using the D8 algorithm in Integrated Land and Water Information System (ILWIS) software which can take eight different directional values

expressed as degrees or as numeric codes. The D8 method is more applicable to delineation of the drainage network for drainage areas with well-developed channels (Garbrecht,1999).

Network and catchment extraction

The algorithm in ILWIS was used extract drainage network from the filled DEM, flow direction and flow accumulation; order the drainage network and to extract desired catchments on which three desired catchments for Mbire district were extracted basing on the location of upstream flow gauging stations.

3.5.2. Preparation of TOPMODEL inputs

The Topographic Index Map Data File (TI file)

In this study the Topographic index for each subcatchment was calculated from 30m*30m ASTER DEM using the following formulae in ILWIS 3.3 Academic.

$$SLOPEPCT = 100 * HYP(DX, DY)/30 \quad [42]$$

$$SLOPEDEG = RADDEG(ATAN(SLOPEPCT/100)) \quad [43]$$

$$TANB = TAN(DEGRAD\ (SLOPEDEG)) \quad [44]$$

$$A = Flow\ accumulation * 900 \quad [45]$$

$$TI = ln(A/tanB) \quad [47]$$

Where;
SLOPEPCT =slope in percentage,
SLOPEDEG =slope in degrees,
A =the contributing area

After generation of slope (percentage) map in ILWIS 3.3 Academic the slope map was converted to slope in degrees and radian by giving command because TOPMODEL required slope in radian. The contributing area (*A*) was computed by multiplying the flow accumulation (derived through the DEM hydroprocessing algorithm). Topographic index map was generated using equations 47 in ILWIS 3.3 Academic. The maximum and minimum value of these topographic index distribution values were reclassified in to different classes to fit in the limitation of less than or equal to 30 classes of the TOPMODEL program available. Tabular distribution of topographic index was converted to a text file ready for TOPMODEL input file.

Catchment Data File (The Area distance file)

Area distance maps were computed from the ILWIS 3.3 Academic for routing of overland flow by the use of a distance-related delay. Using a point outlet maps, distance calculation was produced and to each pixel the shortest distance to the catchment outlet was computed. The distance map was reclassified into segments for simplicity for the routing of surface flows to the outlet. Tabular distribution of distance was converted to a text file ready for TOPMODEL input file.

Meteorological data quality checking

The data quality check was done to all the collected and recorded data of rainfall, temperature, relative humidity, wind speed, sunshine hours and discharge. Several techniques described by were used which include replacing outliers with mean, for missing data moving averages, deleting missing periods, simple proportions and double mass analysis was used to fill in missing gaps (Dahmen, 1989). Data was analysed for trends, relationships and differences.

Potential evapotranspiration calculation

For daily estimate of potential evapotranspiration the (Food and Agricultural Organization (FAO) Penman-Monteith method was used (Allen *et al*., 1998).

$$ET_o = \frac{0.408\Delta(R_n - G) + \gamma \frac{900}{(T+273)} u(e_s - e_a)}{\Delta + \gamma(1 + 0.34u} \quad [48]$$

Where:

ET_0 =*daily reference crop evapotranspiration [mm day^{-1}]*

R_n =*net radiation flux [MJ m^{-2} day^{-1}]*

G =*heat flux density into the soil, it is very small and can be neglected, [MJ m^{-2} day^{-1}]*

T =*mean daily air temperature [^{o}C]*

γ =*psychometric constant [kPa ^{o}C^{-1}]*

U =*wind speed measured at 2m height [ms^{-1}]*

e_s =*saturation vapour pressure,* $e_s = 0.611exp\left(\frac{17.27T}{T+273.3}\right)$ *(kPa)*

e_a =*actual vapour pressure* $e_a = e_s \times \frac{RH}{100}$

RH =*relative humidity [%]*

$e_a - e_s$ =*saturation vapour pressure deficit [kPa]*

Δ =*slope of saturation vapour pressure curve [kPa °C^{-1}*

Discharge calculation

Discharge data was computed using from observed water levels data at ZINWA gauging stations C109, Mapomha and Angwa Bridge using the Manning's Equation and the different respective river cross sectional area and rating curves by (Phiri, 2011). The Manning's Equation uses estimate velocities and flow rates given a measure of the physical characteristics of a stream

$$V = \frac{1.486}{n} R^{2/3} S^{1/2} \quad [49]$$

Where;
V =*velocity (m/s)*
N =*Manning's coefficient,*
R =*Hydraulic radius (m),*
S =*Slope of river channel (m/m)*

Fig: 3.8 shows information on the cross sectional area and a rating curve that were used with respect to the Manyame river at Mapomha Village

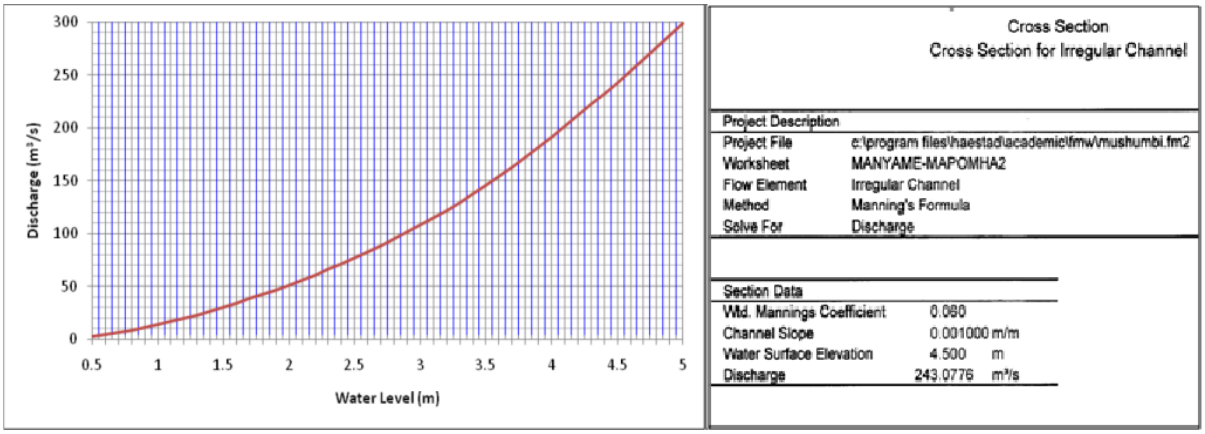

Figure 3.7: Cross section area accompanied by a Ratinng curve for Manyame River at Mapomha and section data ((Phiri, 2011)

For Manyame river and Musengezi river sub catchments the resultant discharge was obtained by subtracting discharge from ZINWA gauging stations C64 and C68 from computed discharge from levels from Mapomha and C109 respectively.

Areal precipitation calculation

Areal precipitation was calculated using the Thiessen method. The rainfall measurements at five individual Karoi, Centenary, Kanyemba, Guruve and Mushumbi pools gauges were first weighted by the fractions of the catchment area represented by the gauges, and then summed up as in equation 3.5.8.

$$\bar{P} = \sum_{i=n}^{n} W_i P_i \quad [50]$$

Where;

P = *average precipitation in mm*

P_i =*gauge precipitation for polygon i*

W_i =*weighted area* (A_p/A)

A_p =*area of the polygon within the topographic basin in* km^2

A =*total area in* km^2

n =*total number of polygons*

Fig: 3.9 shows the Thiessen polygon for all the sub catchments and Thiessen weights for Angwa River sub catchment

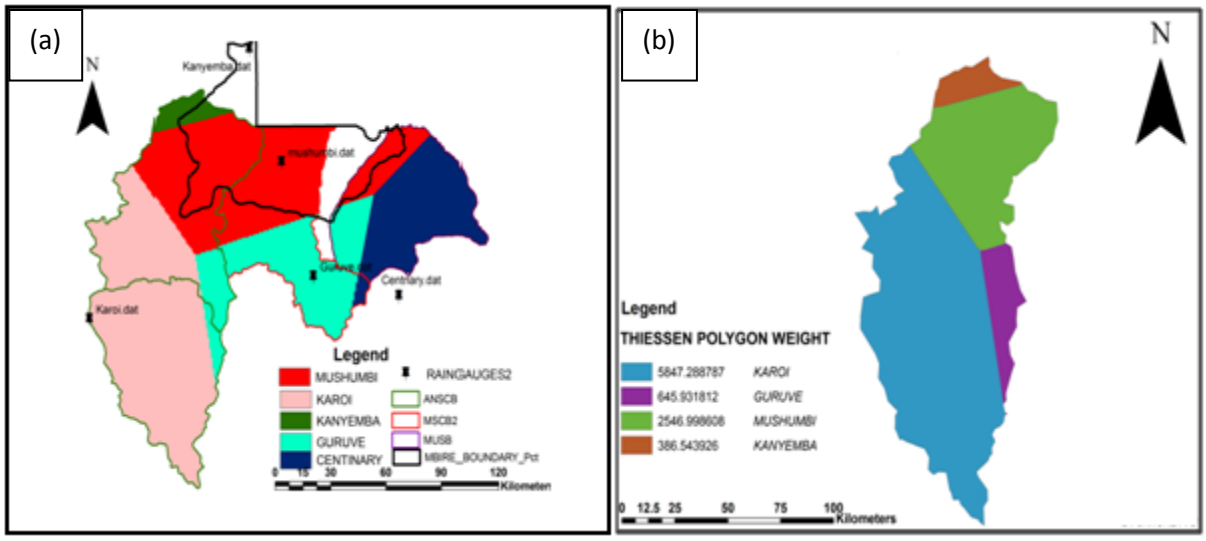

Figure 3.8: Thiessen polygons catchments(a) and Thiessen weights for Angwa River subcatchment(b)

Precipitation, discharge and potential evapotranspiration for each sub catchment were converted to required units and format for TOPMODEL as a Meteorogical Data file.

3.5.3. Estimating TOPMODEL parameters

The soil hydraulic conductivity decay parameter (m) was estimated by recession curve analysis from historical river discharge data. The parameter (m) is simply the reciprocal of the slope of the curve of base flows against time (Ambroise *et al.*, 1996; Beven, 1997). The fractional area and its distance from the outlet as well as channel velocity were used as inputs as to estimate flow travel time used in the flow routing procedure of the model class (Gumindoga, 2011). To estimate most critical parameter in root zone soil moisture prediction, the maximum root zone storage (SRrmax) weighted average catchment soil available water capacity were used (FAO/IIASA/ISRIC/ISSCAS/JRC, 2008).

3.5.4. TOPMODEL calibration

The model was calibrated basing on three parameters using knowledge obtained from the following literature (Beven and Kirkby, 1979; Beven et al., 1995; Beven, 1997, 2001; Beven and Freer, 2000; Gumindoga, 2010; Muhammed, 2012)) of which parameters is most sensitive. These are the soil hydraulic conductivity decay parameter (m) and the soil transmissivity at saturation (T_0). An average root zone available water capacity (SRmax) was used for each sub-catchment. A time step of 24 hour was selected for computations to calibrate the model. The value of parameter 'm' was varied, holding values of remaining four parameters at initial value and value of parameter 'm' was determined which yield the highest efficiency. This method was repeated for remaining parameters to arrive at a set of parameters, which gave highest value of efficiency. The final calibration for the years 2008–2010 was done by changing TOPMODEL parameters manually to optimize model performance for each model run. After each run two objective indices of goodness of fit were used for model performance evaluation. These are Nash-Sutcliffe's coefficient of efficiency (NSE) and percent bias (PBIAS)

$$NSE = 1 - \frac{\sum_{i=1}^{n}(S_i - O_i)^2}{\sum_{i=1}^{n}(O_i - \bar{O})^2} \quad [51]$$

$$PBIAS = \frac{\sum_{i=1}^{n}(S_i - O_i) * 100}{\sum_{i=1}^{n} O_i} \quad [52]$$

Where;
S_i =*Simulated value,*
O_i =*Observed value and*
$\bar{O}$ =*Average observed value.*

3.5.5. TOPMODEL validation

The model was validated using the 2011 October–2013 July dataset. Simulated streamflow was then compared to observed streamflow, graphically (visual comparison) and numerically using performance indicators. The performance indicators used in this study are the Nash-Sutcliffe Efficiency (NS) (Nash and Sutcliffe, 1970) and percent bias (PBIAS). The percentage difference of runoff (PDQ) and lead-time (L_t) were used to evaluate model performance during the peak flows.

$$PDQ = \frac{(S_i - O_i) * 100}{O_i} \quad [53]$$

$$L_t = t_i^S - t_i^O \quad [54]$$

Where;
S_i *=Simulated value,*
O_i *=Observed value,*
t_i^S *=Date of occurrence of simulated value and*
t_i^O *=Date of occurrence of simulated value.*

Predicted root zone soil moisture in depth for desired days was then converted to spatially distributed root zone volumetric soil moisture content in ILWIS 3.3 Academic for comparison purposes.

3.6. Point based soil measurement (Gravimetric method) and interpolation

A hand auger was used to collect samples at a depth of 0.25-0.5m from 54 sampling sites. The depth for sampling were chosen based on the rooting depths of the various crops grown in the flood plain which range from 0.2m for maize to 0.5m for leguminous plants since these are the most common crops grown in the study area. At each sampling site four subsamples were collected and mixed to form a composite sample. Composite sample of approximately 200 g was collected at each site in a sealed container to preserve the moisture. The procedure was repeated once per month for the months March 2013, April 2013 May 2013, June 2013, and July 2013.The moisture content was determined in the laboratory using the gravimetric method as described by Western *et al*. (2002) and Sandor (2008).

The resultant gravimetric soil moisture content was converted to volumetric water content by multiplying it by bulk density. Point based soil moisture measurements were up scaled using Inverse Distance and compared to SEBS and TOPMODEL derived soil moisture. The cross tool in ILWIS was used to allow pixel to pixel comparison. Regression analysis and two paired T-test was used to test for difference between spatial soil moisture outputs in SPSS software at $p<0.05$.

3.7. Land evaluation for flood recession crop cultivation for Mbire district

The essence of land evaluation is to compare or match the requirements of each potential land use with the characteristics of each land unit. The result of Land Evaluation is a measure of the suitability of each land unit for a given land use. These suitability assessments are then examined in the light of economic, social and environmental considerations in order to develop an actual land use plan. Generally flood recession farming land is situated in flood plain, at very low vertical height from river channel, at flat slope (less than 2%) and on soils with high water holding capacity and high plant available capacity (Oku *et al.*, 2007; Ma *et al.*, 2007; Jia *et al*., 2007) In Mbire district flooding is mainly influenced by high stream flows and back throws from the Zambezi River due to its geographical location and Kariba dam and Cabora Bassa dam operations. Crop cultivation in flood plain must be situated as far as possible from sensitive areas such as water bodies and river bed channel because of environmental implications and from protected areas and parks. As a result there are minimum requirements used to identify the most suitable land and exclude certain land. Table 3.5 shows criteria that were used in this research

Table 3.5 Criteria for land suitability mapping

Criteria	**Justification**	**Dataset used**
At least 50m away from river bed channel	As stipulated by legislation (Environmental Management Act of Zimbabwe)	Elevation and Stream network shape file
At least 200m from water bodies	As to void siltation of water bodies	Land use/cover shape file
Clay-rich soils	Have high water holding capacity and are rich in nutrients	Soils shape file
At least 3 km from protected areas	Avoid encroachment of protected areas	Land use/cover shape files from Surveyor General
In flood plain	Available soil moisture for plant growth after flooding	Land use/cover shape files from Surveyor General
Suitable vertical height above channel less than 5m	As soil moisture flow is governed by elevation and water table an	30m ASTER DEM from GLOVIS website
slope	Vital in controlling water surface flow and soil moisture accumulation	ASTER DEM from GLOVIS website
High effective soil depth	Vital for plant roots development	Soils shape files from Surveyor General
Closeness to Zambezi river less than 30 km	Influence flooding due to throw back	Elevation and Stream network shape file
Closeness to river channels less than 1.5 km	Influence flooding due to high stream flows	Elevation and Stream network shape file

Different land use, soils, vertical height from river bed channel and distance from stream network may be more suitable than others hence three suitability classes were used as shown in Table 3.6.

Table 3.6. Suitability classes and criteria

Suitability Classes and criteria			
	Suitable (code 2)	**Moderately suitable (code 1)**	**Not suitable (code 0)**
Vertical height above channel	Less than 1m	1-5m	5m and above
Water bodies	More than 200m	-	-
Distance from river banks	More than 50m but less than 500m	500-1500m	Less than 50m
soils	Eutric cambisols	Calcic lavisols, Calcic solonetz, Eutric leptosols	-
Landuse/cover	Grassland, cropland, regular flood land	Open forest land	Closed forest, protected land
Slope	Less than 1 %	1- 2 %	Greater than 2 %

3.7.1. Derivation and preparation of datasets

Distance map

Distance allocation tool in ArcGIS spatial analyst tools was used to allocate euclidean distance of each pixel from stream network derived from DEM hydroprocessing. The distance operation assigns to each pixel the smallest distance to the nearest channel. The output is called a distance map.

Height above channel

Flow accumulation, drainage network and filled ASTER DEM 30m resolution was used to derive the channel base elevations in ILWIS 3.3 Academic. The channel base elevations were then interpolated to form a channel height layer that, if subtracted from the DEM produces the vertical distance to the closest channel of each location in the study area (Murwira *et al.*, 2005a). The vertical height above the nearest channel was then determined by subtracting the channel base height interpolation from the original DEM:

$$k = v - r \quad [55]$$

Where
K =height above channel (m),
V =elevation (DEM) (m) and
R =channel height (m).

Landcover classes

A Landsat TM satellite image of the 02/07/2012 was used to determine landcover within the Mbire District. Landsat TM image was used because of their relatively high spatial resolution (30m) and their wide application for landcover classification across the world (Lillesand, 2000; Chen *et al.*, 2004; Masek *et al.*, 2006). Landsat has the optimal ground resolution and spectral bands to efficiently. Maximum Likelihood Supervised Classification Method was used because it dichotomizes the area into the following main classes: forest (woodland, mixed shrub and grassland, grassland, water bodies and cropland and open ground. Maximum likelihood classification assumes that the statistics for each class in each band are normally distributed and calculates the probability that a given pixel belongs to a specific class (Lucas *et al.*, 2002).

For land classification validation ground control points using Global Positioning System (GPS) were taken from different landuse/cover classes include grassland, agricultural fields, water and forest. The error matrix was used to quantify the level of error from the correct or actual measurements on the ground. To assess the accuracy of an image classification, error matrix (Confusion matrix) was calculated to determine the accuracy of the classification and to identify where misclassification occurs. The overall average accuracy of the classified landuse/ land cover map for 2012 was 88.11% which is excellent.

Slope

The Digital Elevation Model (fill) was used to calculate height differences in X and Y-direction: using linear filter operation in ILWIS. To calculate a slope map in percentages from height differences equation 56 was used

$$SLOPE = 100 * HYP(DX, DY)/30 \quad [56]$$

Where;
HYP =an internal Mapcalc/Tabcalc function,
30 =pixel size (m),
DX =height difference in X direction,
DY =height difference in Y direction

3.7.2. Deriving Suitability Map

Model builder in ArcGIS spatial analyst was used to reclassify all the derived datasets into desired three suitability classes using the criteria in Table (3.6) using my own discretion and knowledge of the area and literature from similar studies. Reclassifying was done to combine

the four layers in their present form. A weighted overlay tool was used to combine the five coded layers. All classes of zeros were assigned to restricted scale values which are areas that are not suitable for flood recession farming. Each reclassified layer was assigned to a percentage of influence (weight) as in Table 3.7.

Table 3.7: Weight for overlay analysis

Reclassified layer	**Weight in percentage**
Soil type	40
slope	15
Distance from Zambezi river	10
Landcover	5
Vertical height above channel	20
Distance from river channel network	10

Suitability map was obtained after running the model. Figure 3.10 shows the model builder setup as it was used in ArcGIS 9.3 Software

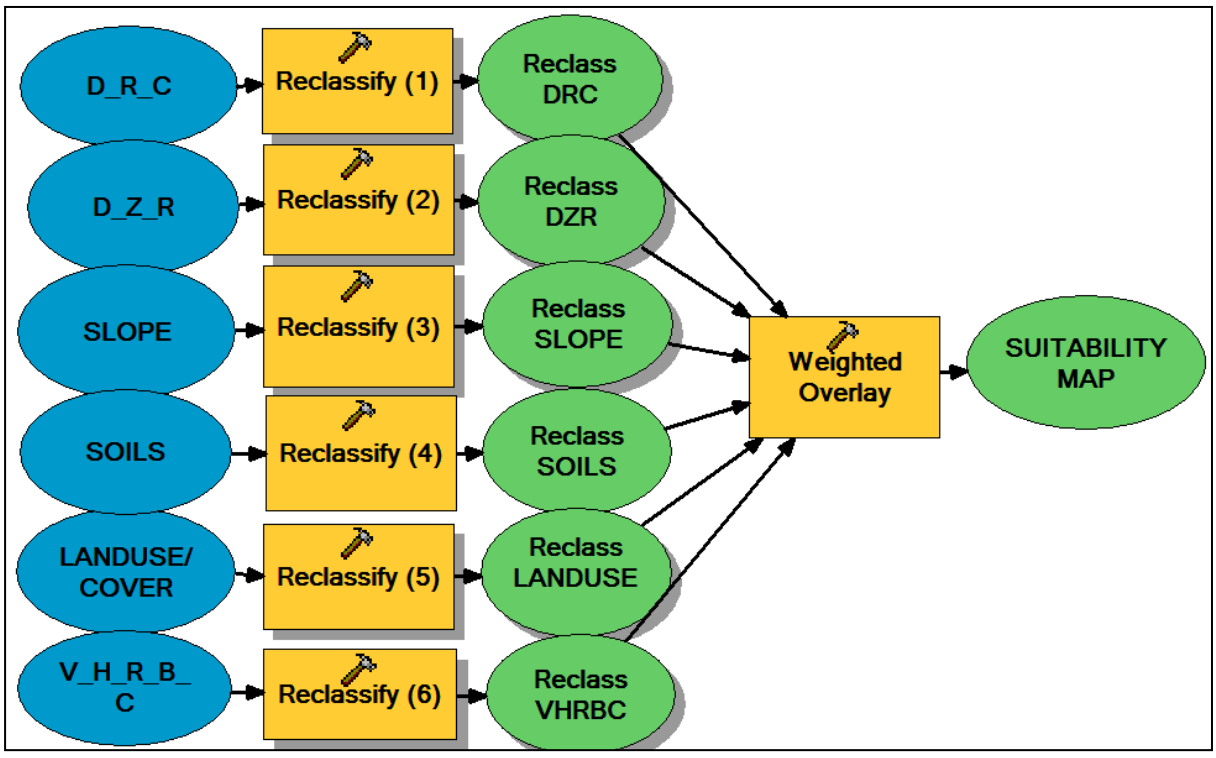

Figure 3.9: Model for land evaluation

CHAPTER FOUR

4. Analysis of results and discussion

In this chapter the results and findings of the outputs of this thesis will be discussed. The soil moisture results obtained from the RS methods are analysed and later compared with the upscaled ground stations. Secondly the soil moisture results obtained from the TOPMODEL methods are analysed and later compared with the upscaled ground stations soil moisture. Thirdly the soil moisture results obtained from the point based ground observations are analysed and compared with the TOPMODEL and RS soil moisture and the land suitability results are analysed.

4.1. Determination spatio-temporal soil moisture variation using SEBS

Using TERRA MODIS images coupled with respective instantaneous meteorological data SEBS algorithm successfully managed to retrieve evapotranspiration and relative evapotranspiration Fig 4.1 and Fig.4.3 shows relative evapotranspiration for the whole district.

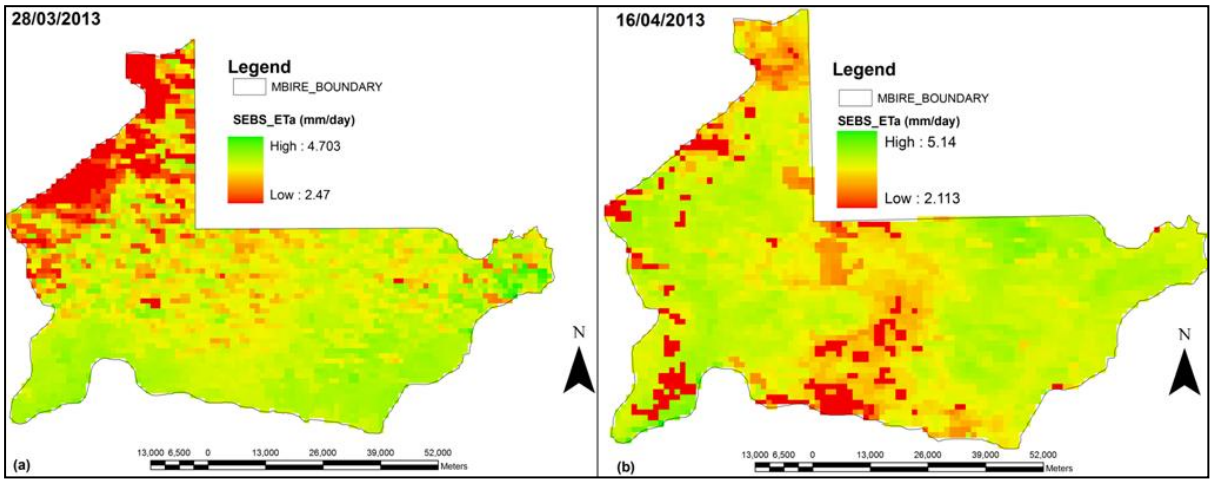

Figure 4.1: Spatial variation of actual evapotranspiration as retrieved by SEBS from (a)28 March (b) 12 June 2013 MODIS

Validation of SEBS evapotranspiration was done using pan evaporation data from Cabora Bassa on which SEBS evapotranspiration pixel was compared to pan evaporation from the same pixel. Fig 4.2 shows that there is very good relation between pan evaporation and SEBS retrieved evapotranspiration.

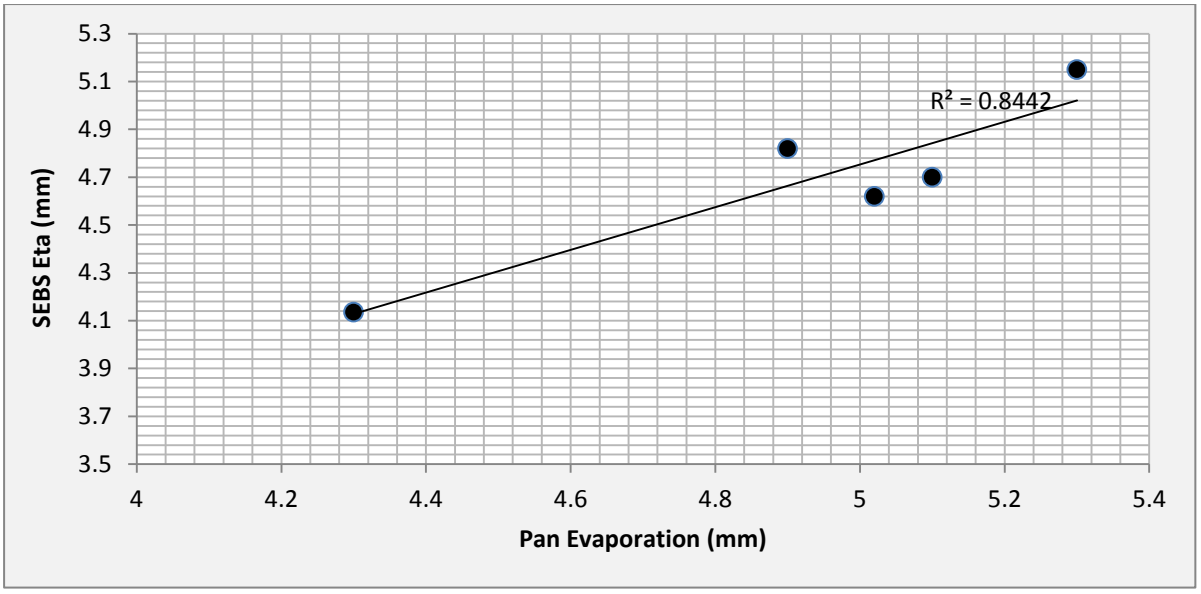

Figure 4.2:Comparison of pan evaporation and SEBS retrieved evapotranspiration for all the images

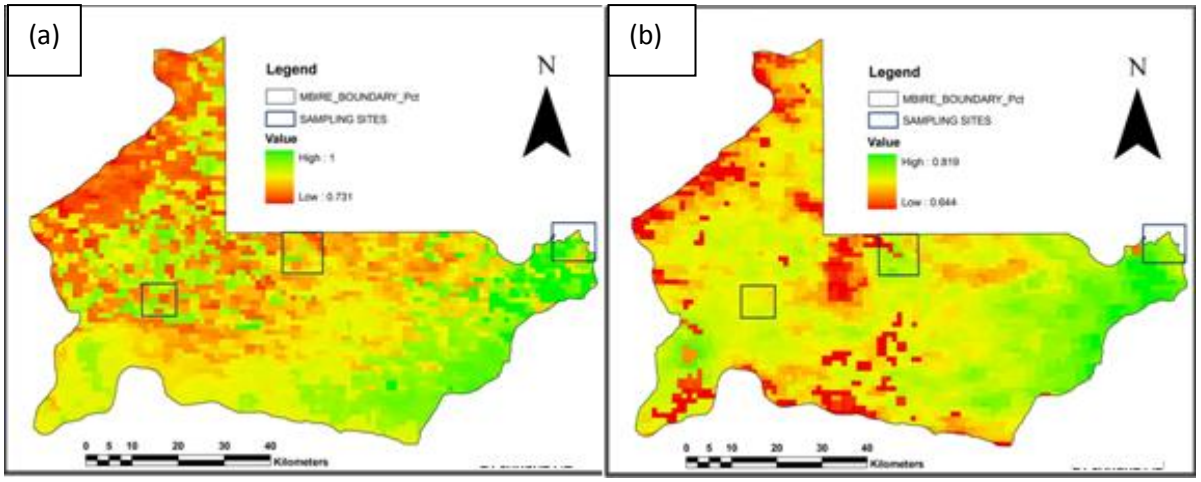

Figure 4.3: Spatial variation of relative evaporation as retrieved by SEBS from (a) 28 March 2013 (b)12 June 2013 MODIS images

Low values of relative evapotranspiration were observed in densely forested area compared to grassland. This may be due to that available energy is partitioned into the sensible heat flux and the latent heat dense forest covered areas which have high values of displacement heights and roughness heights for heat transfer, the aerodynamic resistance becomes low (Su, 1999). This in combination with higher difference in the surface air temperature leads to high values of the instantaneous heat flux only to be limited by the dry sensible heat limit (Rwasoka, 2010). This in turn leads to low relative evaporation values and the daily evaporation and the evaporative fraction values will become low. As a result the soil moisture will also below.

High potential maximum wetness was observed for Manyame sampling site compared to the other two sites. The potential maximum wetness is mainly affected by soil texture; soils with

high proportion of clay particles have high water holding capacity due to high volume of microspores. Fractional soil particle distribution analysis that was conducted during the research showed that Manyame sampling site have high clay particle fraction compared to the other two sampling site hence high potential maximum wetness. For all sampling sites high potential maximum wetness were observed close to the river channel due to clay deposition by flooding. Fig: 4.4 shows the spatial potential maximum wetness variation of two sampling sites.

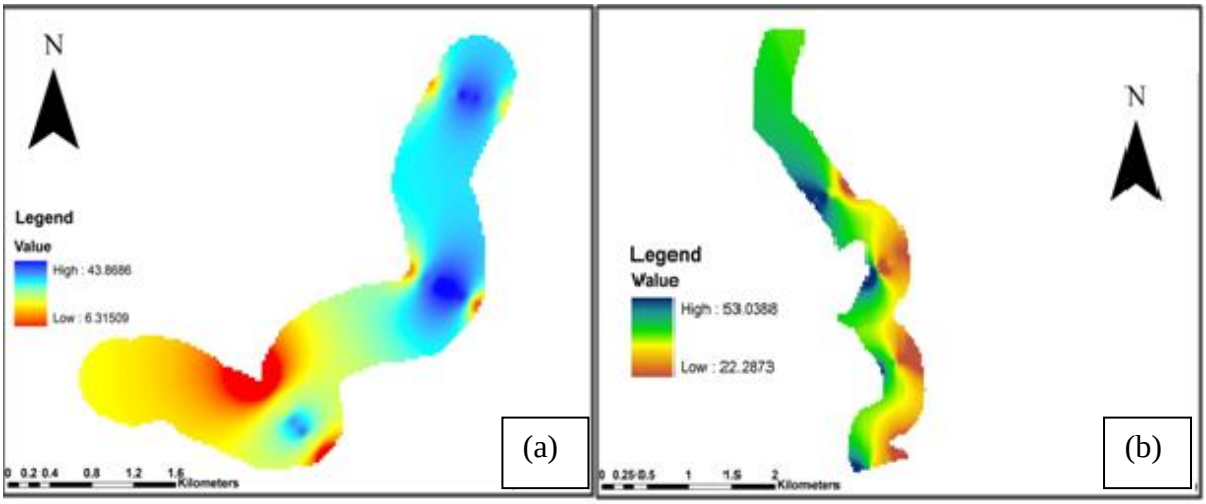

Figure 4.4: Spatial variation of potential maximum wetness expressed as percent volumetric water content for (a) Angwa and (b) Manyame river study sites

In this research top soil moisture retrieval was attempted from RS methods developed for estimation of surface turbulent fluxes. SEBS model has been explored to retrieve soil moisture using the relation between evapotranspiration and soil moisture. The average of the porosity and the field capacity was considered for the potential wetness capacity of the top soil. The result of the relative evaporation from the SEBS algorithm was multiplied by the average of the porosity and the field capacity to get the soil moisture. Figure 4.5 and 4.6 shows soil moisture obtained from objective one.

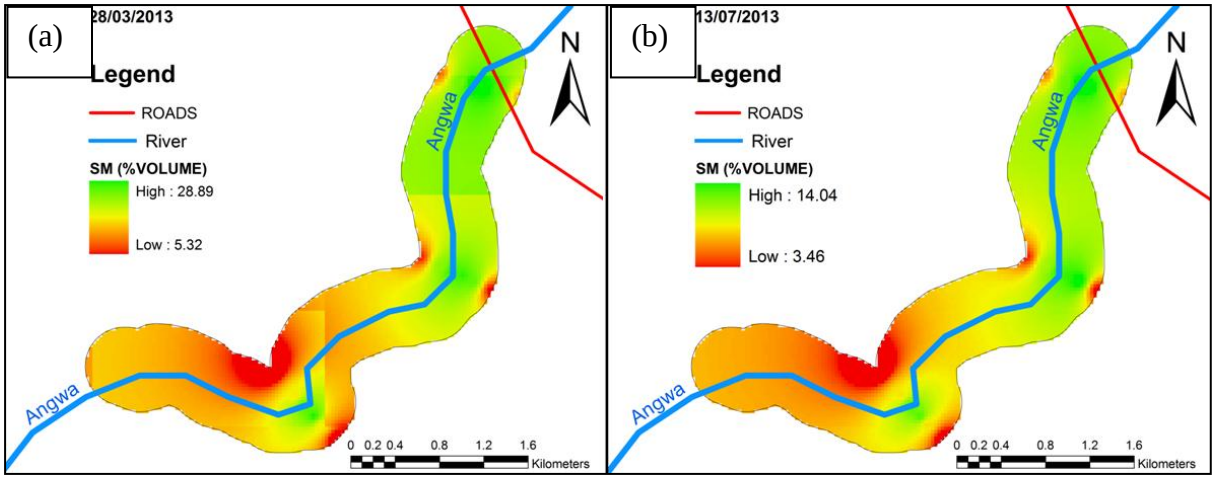

Figure 4.5: The spatial and temporal variation of soil moistureT inferred from SEBS for Angwa sampling site for (a)28/03/2013 (b)13/07/2013

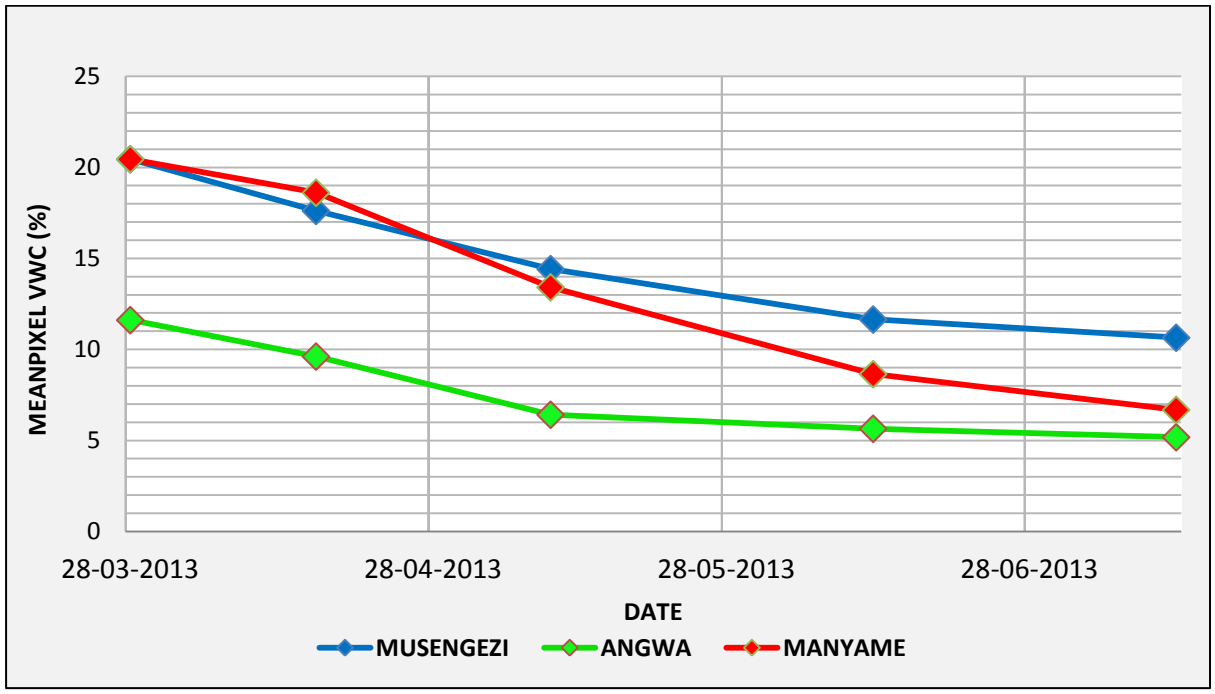

Figure 4.6: Mean pixel volumetric water content for all the sampling sites as retrieved from SEBS for the days 28/03/2013, 16/04/2013, 10/05/2013, 12/06/2013 and 13/7/2013

From (Figure 4.6) there is temporal variability in soil moisture as there is an overall decrease in soil moisture from March 2013 to July 2013. There is a uniform decrease in average soil moisture for all sampling sites except for Musengezi sampling site for the period 10/05/2013-13/7/2013 were there is a slight decrease in soil moisture. This is explained by the effect of Cabora Bassa back throw as observed from the ZINWA gauging station (C109) levels and from point based soil measurements close to the river channel.

4.2. Soil moisture simulation using TOPMODEL

4.2.1. DEM hydroprocessing

Fig: 4.7 Show delineated sub catchments, and the inputs into the topographic index such as filled DEM, flow direction and flow accumulation are shown for Musengezi River subcatchment as computed from DEM hydroprocessing.

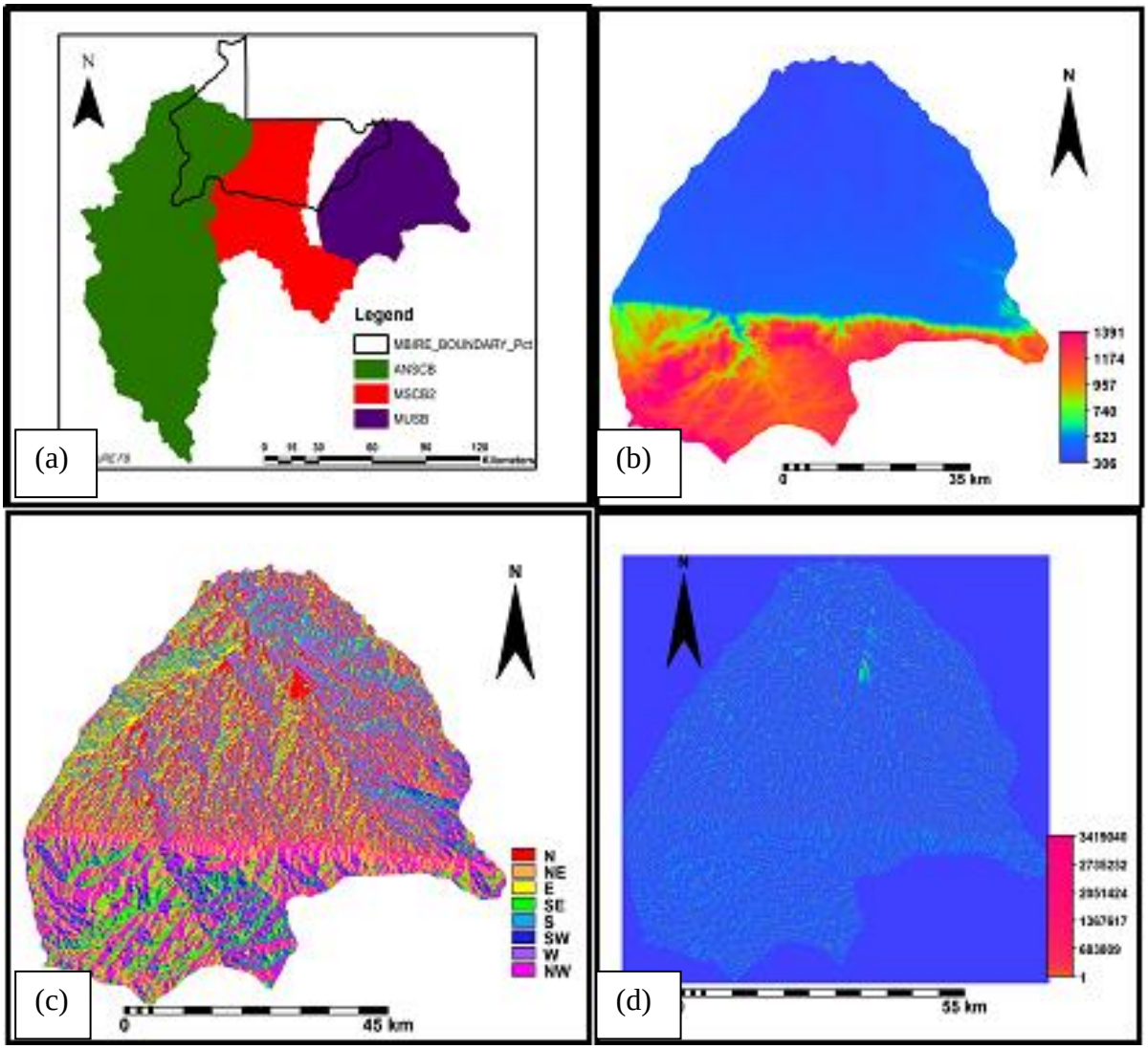

Figure 4.7: Outputs of DEM hydroprocessing (a)delineated subcatcments, (b) filled DEM, (c) flow direction and (d) flow accumulation)

4.2.2. The spatial variation of the Topographic Index

The topographic index map and the histogram for the topographic index, *Ln(a/tanβ)* of the Musengezi River subcatchment derived from ASTER DEM is shown in Fig: 4.8.

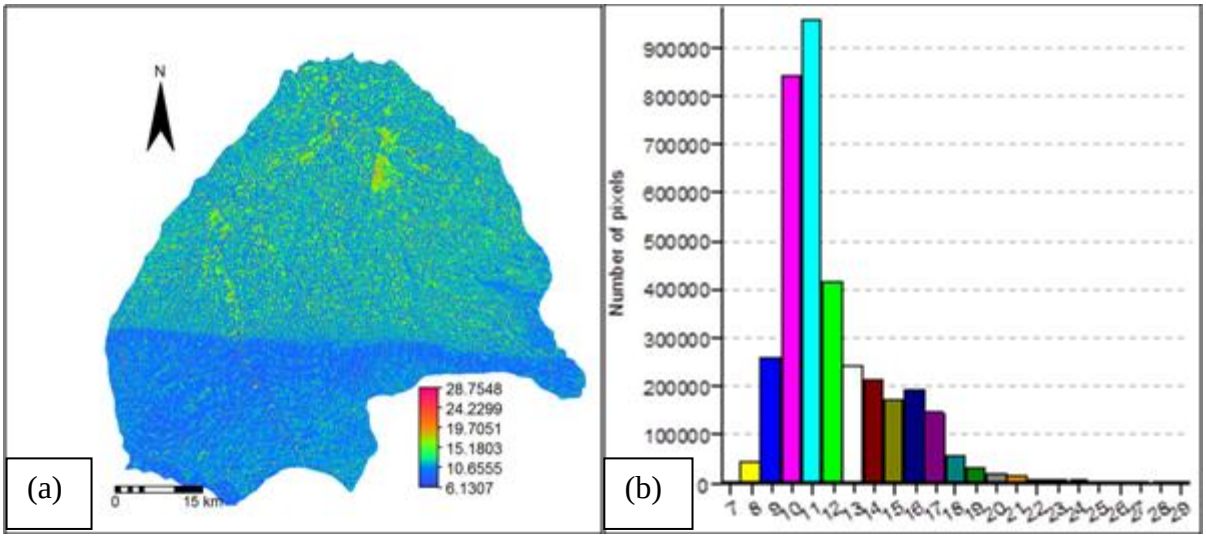

Figure 4.8: TI histogram and map for Musengezi River sub catchment

Higher topographic indices are found in the central and northern part of the basin especially in and around the streams. The highest number of pixels is found in the topographic index of 11. Lower *Tanβ* values indicate lower hydraulic gradient and more accumulation of water. The areas with higher *ln(a/tanβ)* imply a higher degree of wetness thus more soil moisture contents by higher upslope contributing areas. This is consistent with TOPMODEL's demonstrated principles of hillslope hydrology in which locations with large upslope contributing areas and low surface gradients maintain higher soil moisture levels than locations that are steep or have a small upslope contributing areas (Band *et al.,* 1991).

4.2.3. Runoff calibration results for Manyame and Angwa River subcatchments

The available data for the calibration and validation was 4 years long starting from 01 October 2008 and ending 31 July 2013. The first run and calibration of the simulation for all sub catchments was done for the period starting 0ctober 01, 2008 and ending September 30, 2010. Final calibration was only done for Manyame and Angwa River sub catchments. Validation and root zone soil moisture simulation using the optimised parameters was done for the period 0ctober 01, 2011 - July 31, 2013. The optimised model parameter obtained from final calibration for the parameters specified in section (3.5.5) and their corresponding Nash-Sutcliffe's coefficient of efficiency (NSE) value and percent bias (PBIAS) for Manyame and Angwa River sub catchments are shown in Table 4.1.

*Table 4.**1**: The accepted best parameter values and model efficiency after calibration*

Subcatchment	Parameter	Optimized	NSE	PBIAS (%)
Manyame River subcatchment	m (m)	0.046	0.76	-10.45
	T0 (m^2/s)	3		
	Srmax (m)	0.075		
Angwa River subcatchment	m (m)	0.031	0.80	-5.56
	T0 (m^2/s)	3.5		
	Srmax (m)	0.05		

Fig: 4.9 and 4.10 show the comparison between simulated and observed flows for Manyame River sub catchment.

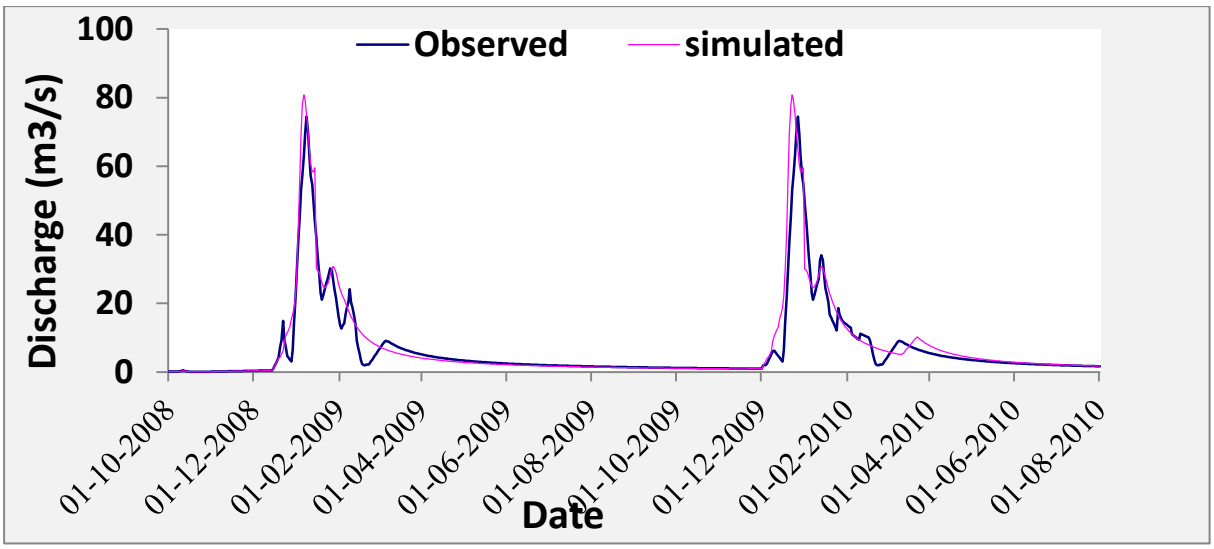

Figure 4.9:Comparison between simulated and observed runoff for Angwa River subcatchment for (1-Oct-2008 – 30 July-2010)

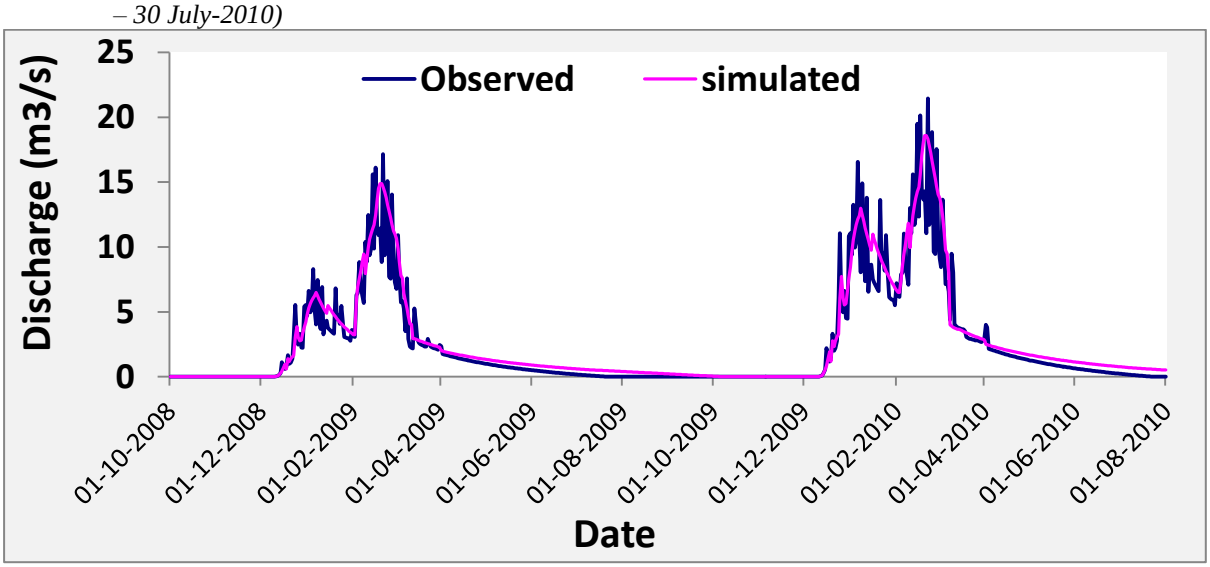

Figure 4.10:Comparison between simulated and observed runoff for Manyame River subcatchment for (1-Oct-2008 – 30 July-2010)

The simulated runoff curve performed well particularly for the low flows. The Nash-Sutcliffe coefficient of efficiency (NSE) indicates an acceptable good match (NSE= 0.757 and 0.801 for Manyame river and Angwa river subcatchments respectively) (Krause *et al.*, 2005;

Willmott *et al.*, 2011) while the percent bias (PBIAS) (PBIAS= -10.45 % and -5.56 % for Manyame river and Angwa river subcatchments respectively) shows an acceptable performance. This combination of performance indicators were the best found during the calibration exercise and the model was used to simulate flows. This allowed the transfer of model parameters for soil simulation

4.2.4. Runoff validation results for Manyame and Angwa River subcatchments

Figures 4.11 and 4.12 show the comparison between simulated and observed flows for Manyame River and Angwa River subcatchments from 1-Oct-2011 – 31-July-2013. The three (3) higher flows observed varies from 16.59m³/s, 21.46m³/s and 23.40m³/s and were recorded on 05-Jan-2012, 21-Feb-2012 and 22-Feb-2013. For the validation period, the simulated runoff curve follows the same trend as the observed curve. Table 4.1 shows the difference in magnitude and lead-time of the five simulated flows. High flows are under-estimated (-19.8%), -24.5% being the global average (under-estimation). The lead-time (the time between when a forecast is made and the forecasted event occurs) vary from -2 to 2 days with an overall average of -0.2 days which is good for forecasting soil moisture.

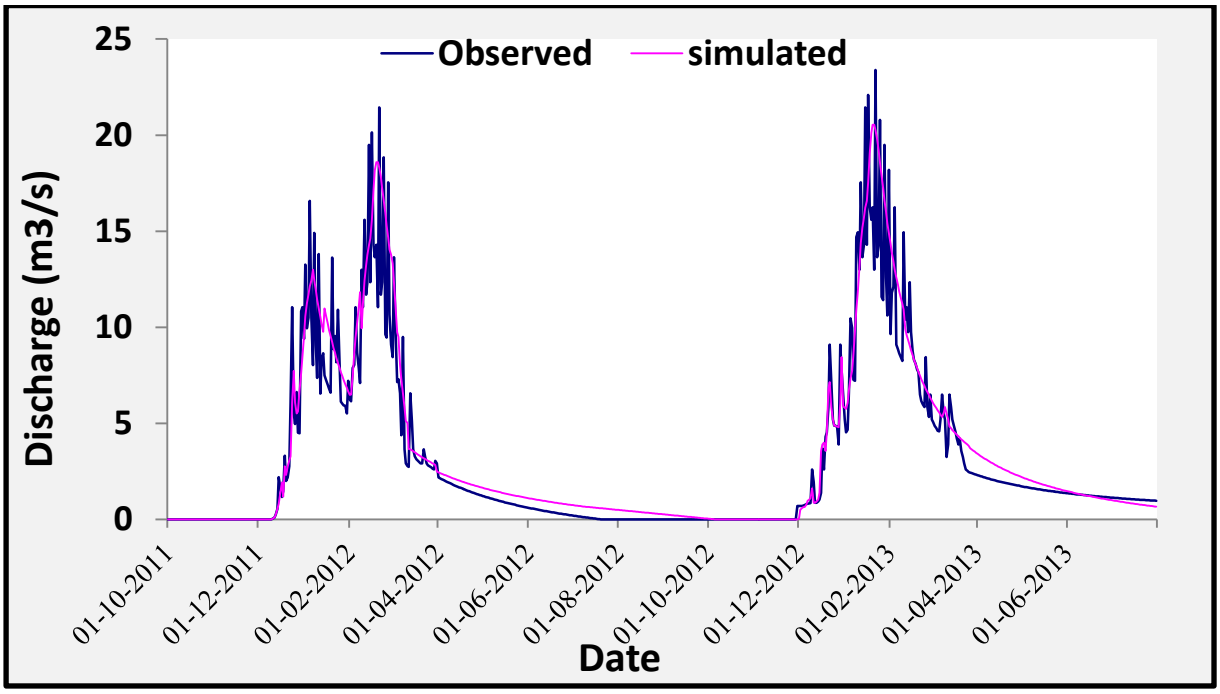

Figure 4.11:Comparison between simulated and observed runoff for Manyame River subcatchment (1-Oct-2011 – 31-July-2013)

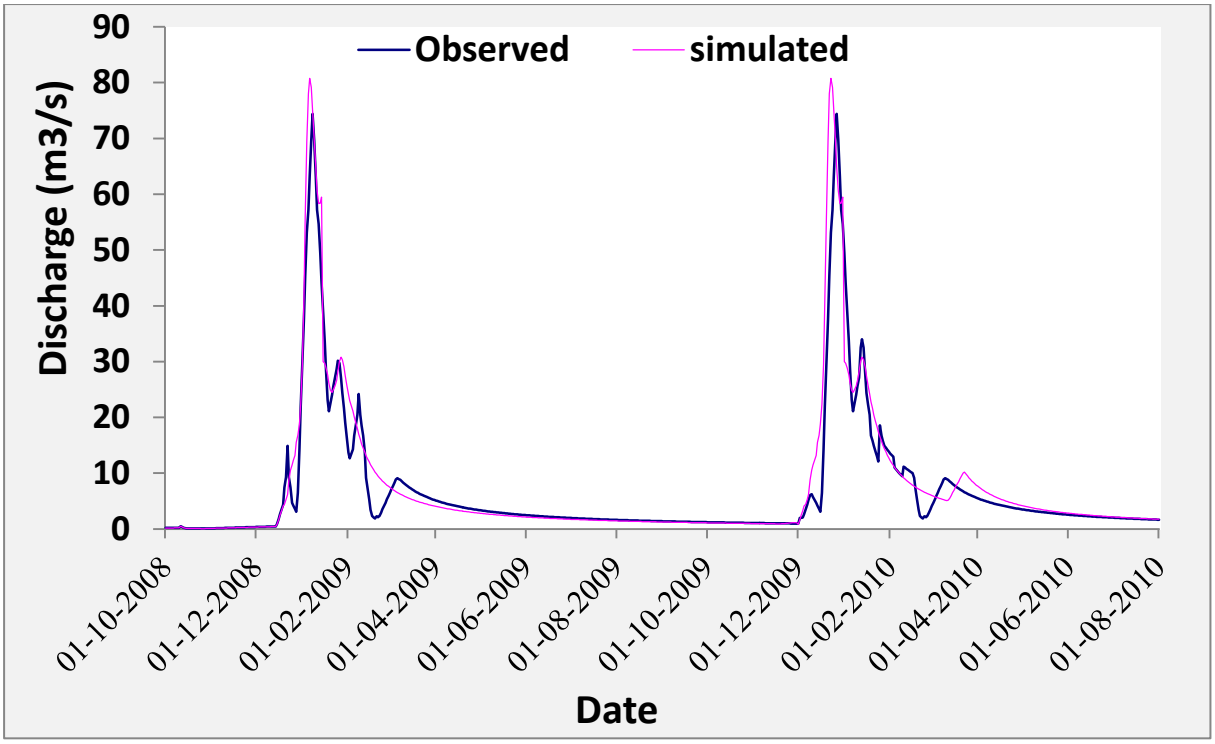

Figure 4.12:Comparison between simulated and observed runoff for Angwa River subcatchment (1-Oct-2011 – 31-July-2013)

The under and overestimation of the peaks, baseflow and recession limbs in both the final calibration and validation process are not entirely due to the modeling errors but could be due to data errors and the spatial distribution of rainfall. This is because four of the five weather stations used in the Thiessen polygon rainfall estimation method was outside the study area thus could have an impact on the simulated discharge or the observed runoff which was converted from water levels using unreliable rating curves.

Table 4.2: Difference and lead-time of the five highest simulated and observed discharges for Manyame River subcatchment

Simulated		Observed		% Difference	Lead-time (days)
Date	Q (m^3/s)	Date	Q (m^3/s)		
25-12-2011	7.74	24-12-2011	9.0000	-16.279	1
07-01-2012	13	05-01-2012	16.5932	-27.64	2
19-02-2012	18.6	21-02-2012	21.4563	-15.356	-2
22-12-2012	7.15	22-12-2012	9.0000	-25.874	0
20-01-2013	20.55	22-01-2013	23.4040	-13.888	-2
Average				-19.808	-0.2

The Nash-Sutcliffe coefficient of efficiency (NSE) indicates an acceptable with very good match (NSE= 0.765 and 0.81 for Manyame river and Angwa river subcatchments respectively) while the percent bias (PBIAS) (PBIAS= -9.54 and -6.03% for Manyame river

and Angwa river subcatchments respectively) shows an acceptable performance after validation as in Table 4.3.

Table 4.3: The accepted best parameter values and model efficiency after validation

Subcatchment	Parameter	Optimized	NSE	PBIAS (%)
Manyame River subcatchment	m (m)	0.046	0.77	-9.54
	T0 (m^2/s)	3		
	Srmax (m)	0.075		
Angwa River subcatchment	m (m)	0.031	0.81	-6.03
	T0 (m^2/s)	3.5		
	Srmax (m)	0.051		

4.2.5. The spatial variation of soil moisture using TOPMODEL

The aim of running and calibrating the hydrological modeling was to compare the outputs of the soil moisture from this model with the results found in the RS method and the measured values from the point based observations (gravimetric measurements) on catchment level. Only for Musengezi River subcatchment for the whole period the simulated discharge is not in good agreement with the observed discharge for Musengezi River subcatchment and hence no comparison could be made for the subcatchment. This is due to the fact that levels from ZINWA gauging station C109 overestimate discharge due to Cabora Bassa water back throw.

Simulated spatial soil moisture varies temporarily and spatially with high values near the river channel. Low soil moisture values were simulated for Angwa sampling site compared to Manyame sampling site this is mainly because of high topographic index in the later samplings site. Simulated soil moisture is decreasing with time. Fig: 4.13 and 4.14 shows soil moisture simulated by the TOPMODEL.

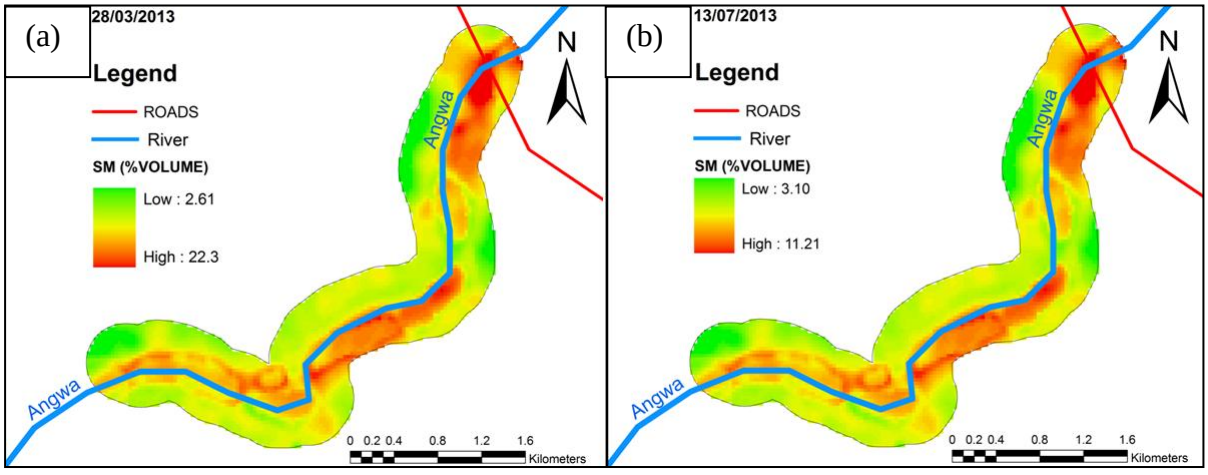

Figure 4.13: The spatial and temporal variation of soilmoisture as simulated by TOPMODEL for Angwa sampling site for (a)28/03/2013 (b) 13/07/2013

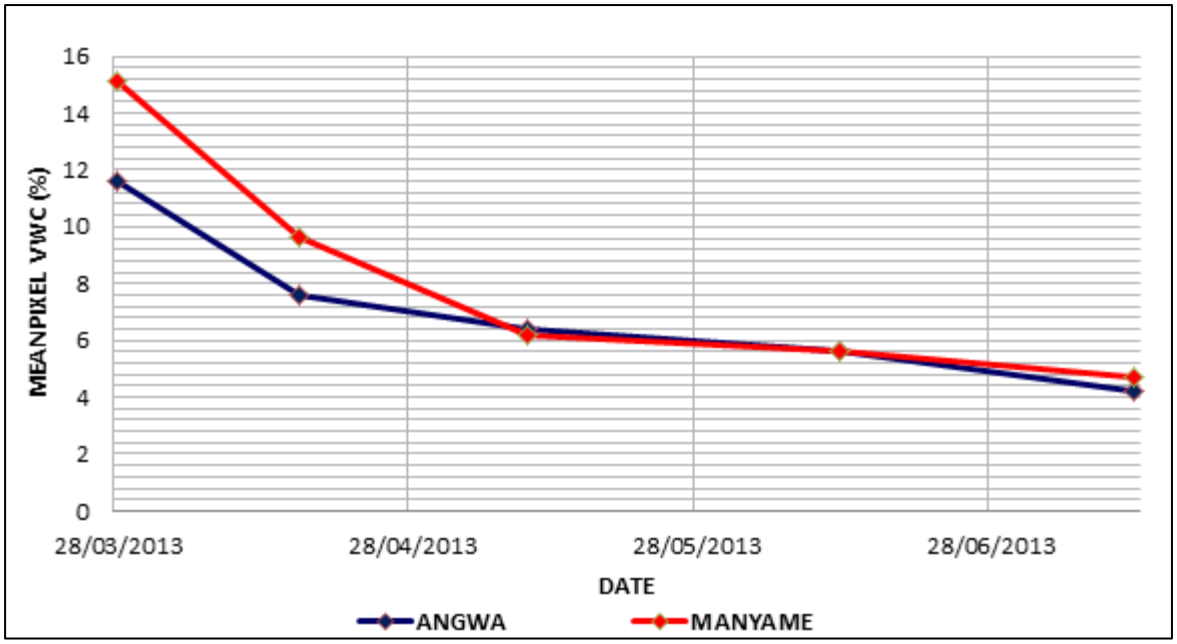

Figure 4.14: Mean pixel volumetric water content for all the sampling sites as simulated from TOPMODEL for the days 28/03/2013, 16/04/2013, 10/05/2013, 12/06/2013 and 13/7/2013

4.3. Upscaled point based soil measurements

4.3.1. Analysis of point based soil measurements

Figures 4.15 and 4.16 show the moisture content variation with distance from the Musengezi River sampling site at Chidodo and Manyame river sampling site at Chikafa for selected transect. The results show that the moisture content decreased with distance from the flood plain. At Musengezi high moisture content values were obtained during the month of March 2013 for all sampling stations across the flood plain with station 1 having the highest due to its closeness to the river channel. A peak in soil in soil moisture content was observed in June 2013 at sampling station 1 for all transect at Musengezi river sampling site due to Cabora Bassa back flows explained by high water levels for that months at ZINWA C109 gauging station. Residual soil moisture at Musengezi is mainly due to combination of high stream flow floods and back flows from Zambezi River. Figure 4.15 and 4.16 clearly shows that soil moisture in the flood plain decrease with increase in distance from the river channel.

At Manyame for transect three sampling station one near the river channel recorded the highest soil moisture content throughout the study period and low values were from station four furthest from the river channel. The soil moisture at Manyame decreased gradually for all the stations compared to Musengezi this site is because this site is not affected by back flows from Cabora Bassa as the later site. High soil residual soil moisture at Manyame

sampling site is mainly influence high stream flow and soil type which are rich in clay content and the effect of back throw which are experienced during peak discharge in Manyame river.

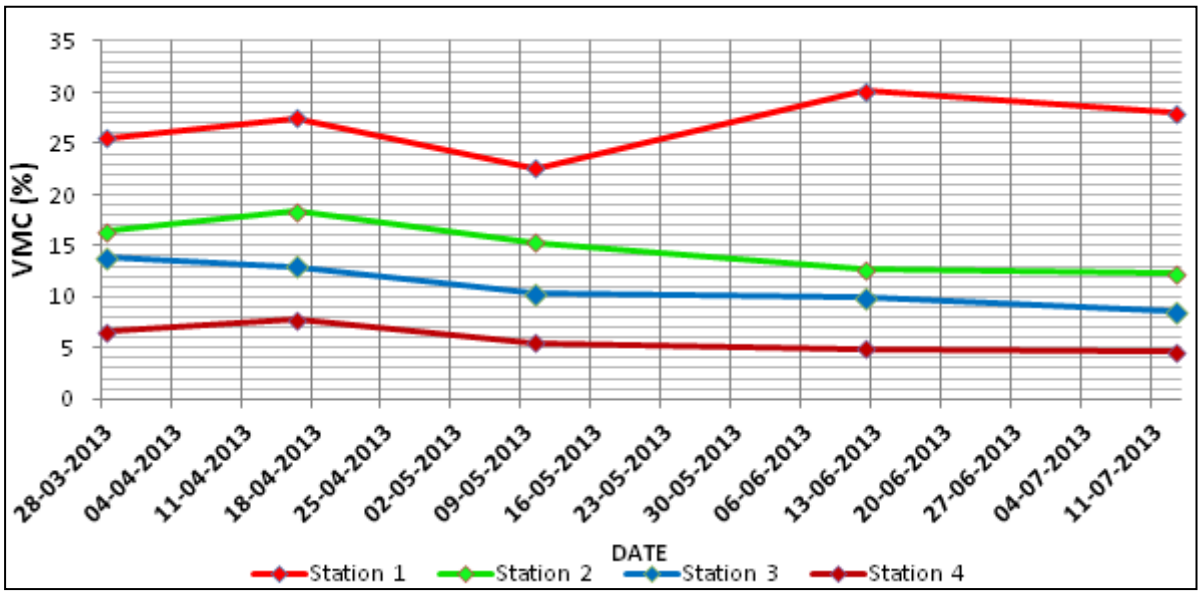

Figure 4.15: Point based soil moisture measurements for Musengezi sampling site transect three for the days 28/03/2013, 16/04/2013, 10/05/2013, 12/06/2013 and 13/7/2013

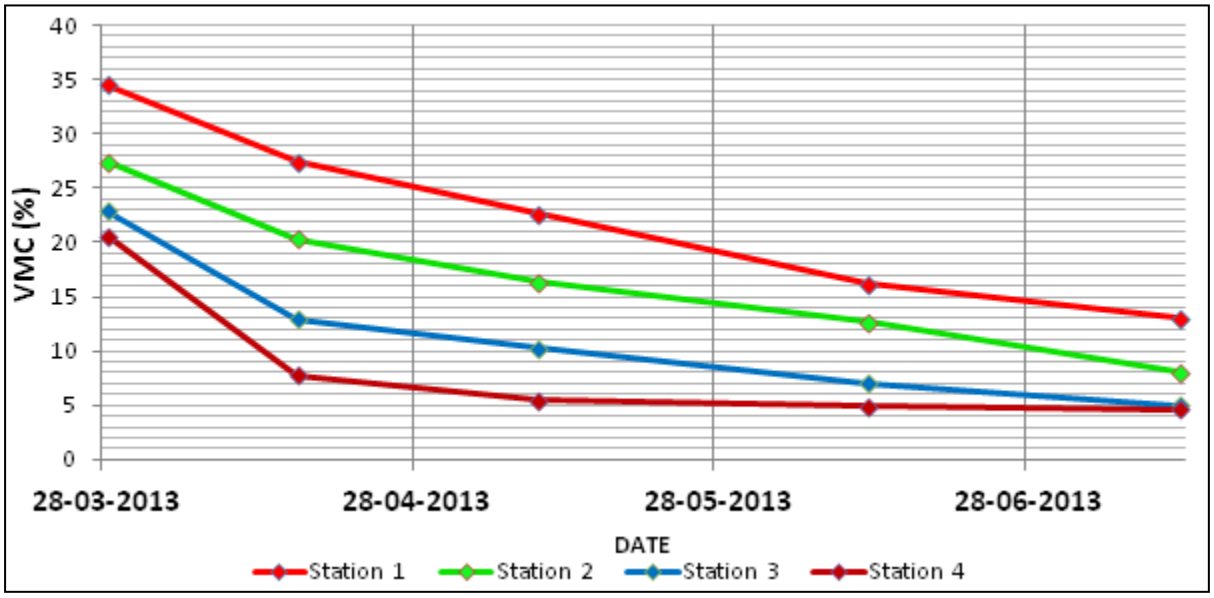

Figure 4.16: Point based soil moisture measurements for Manyame sampling site transect three for the days 28/03/2013, 16/04/2013, 10/05/2013, 12/06/2013 and 13/7/2013

Angwa sampling site recorded the least soil moisture values. This is due to that the sampling site does not experience back throw and the soils have poor water holding capacity compared to Manyame sampling site where the effect of back throw is less. Residual soil moisture at this site is mainly influenced by high stream Figs 4.17 shows upscaled ground based

measurements and their mean pixel soil moisture for all sampling sites, and soil moisture outputs of SEBS and TOPMODEL

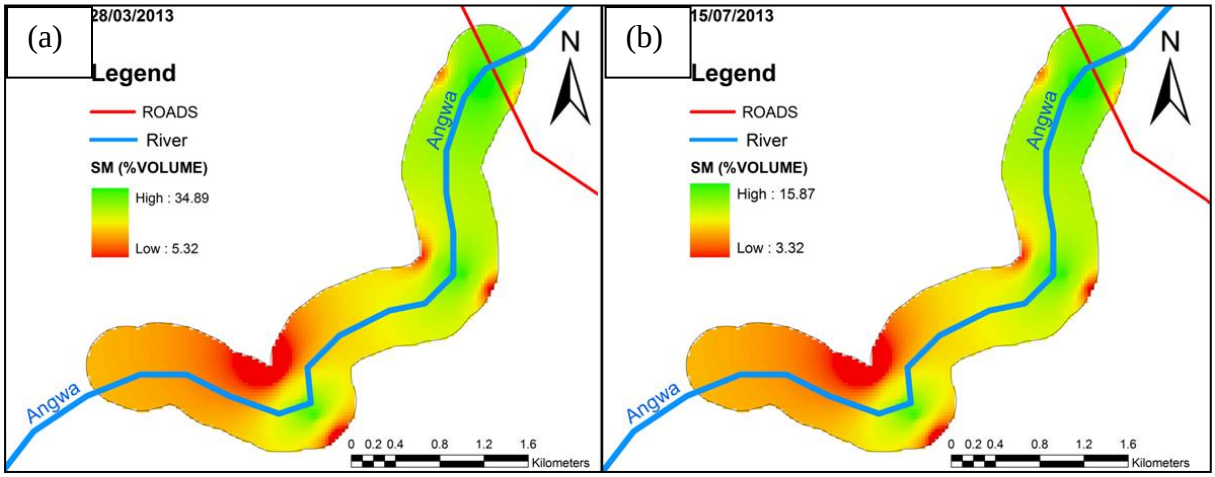

Figure 4.17: The spatial and temporal variation of soilmoisture as interpolated from point based measurements for Angwa sampling site for (a)28/03/2013 (b) 13/07/2013

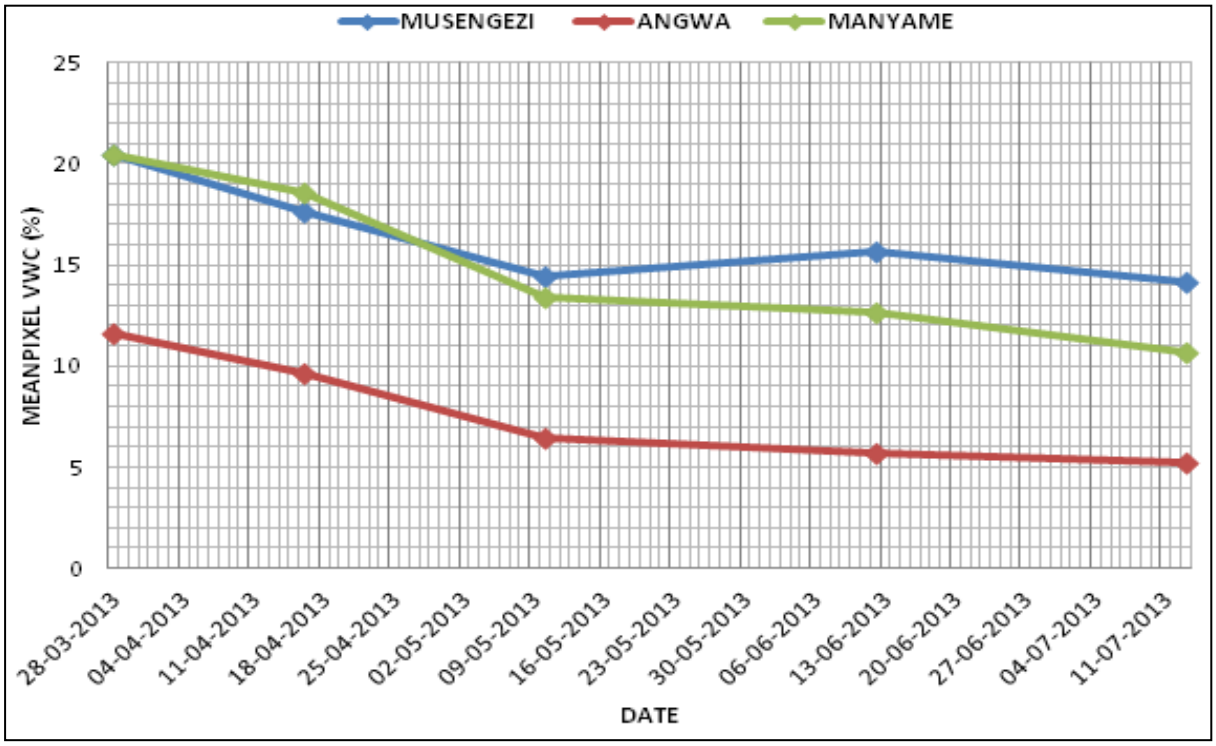

Figure 4.18: Mean pixel upscaled point based soil moisture for all sampling sites

4.3.2. Comparison of soil moisture outputs from SEBS and TOPMODEL to ground based measurements

In this research top soil moisture retrieval was attempted from RS methods developed for estimation of surface turbulent fluxes and TOPMODEL. Fig: 4.19 (a) shows a scatter plot comparing pixel soil moisture values retrieved using remote sensing (SEBS) to direct method

(gravimetric method). As seen from the scatter there is definite relationship in spatial SM variation between the measured soil moisture and the RS derived soil moisture values as explained by high values of the coefficient of determination (R^2) = 0.885 and an average of (R^2) =0.796 for all sampling sites. Although there is good relation in variation of soil moisture there is significant different between SEBS and ground based observations for all sampling sites spatially and temporally (paired t-test; 95% confidence interval; p=0.05) all p values were less than 0.05.

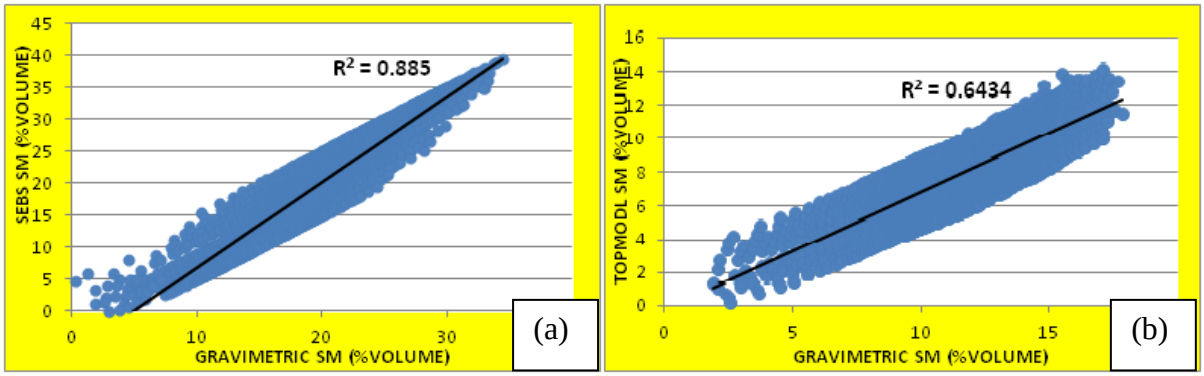

Figure 4.19: Comparison of soil moisture values retrieved using (a)SEBS (b)TOPMODEL to direct method (gravimetric method) at Manyame sampling site for the days 28/03/2013 respectively.

Table 4.4: Correlations of soil moisture values retrieved using SEBS and TOPMODEL methods

		SEBS method	**TOPMODEL method**
Sampling site	Date	CORRELATIONS R^2	CORRELATIONS R^2
MANYAME RIVER	28/03/13	0.885	0.498
	16/04/13	0.716	0.567
	10/05/13	0.768	0.713
	12/06/13	0.813	0.556
	13/07/13	0.755	0.589
ANGWA RIVER	28/03/13	0.667	0.655
	16/04/13	0.823	0.6434
	10/05/13	0.834	0.564
	12/06/13	0.784	0.595
	13/07/13	0.822	0.590
MUSENGEZI RIVER	28/03/13	0.771	-
	16/04/13	0.812	-
	10/05/13	0.824	-
	12/06/13	0.800	-
	13/07/13	0.866	-
Average		**0.796**	**0.597**

SEBS underestimated soil moisture especially at dense vegetation. This mainly due that instantaneous sensible heat flux in SEBS is limited between the dry and the wet limits of the sensible heat flux (Su, 1999). Therefore SEBS can be used to estimate spatial soil moisture variation in grasslands accurately. Figure 4.19 (b) shows a scatter plot comparing soil moisture values simulated by TOPMODEL to ground based measured soil moisture (gravimetric method) As shown by the scatter there is fair relation in spatial variation of SM between the measured soil moisture and the TOPMODEL derived soil moisture values as explained by generally low values (compared to SEBS) of the coefficient of determination (R^2) = 0.6434 and an average of (R^2) =0.597 for Manyame and Angwa sampling sites. Also there is significant different between TOPMODEL SM values and ground based observations for all sampling sites spatially and temporally (paired t-test; 95% confidence interval; p=0.05) all p values were less than 0.05. Hence we reject the reject null hypothesis. The spatial and temporal variation of soil moisture in Mbire district is influenced by high stream flows and floods. TOPMODEL was not able to accurately predict the soil moisture in the flood plain due to the effect of back flows from Zambezi River due high stream flows and Kariba and Cabora Bassa dams operations (Phiri, 2011). May be under-estimation was due to the modeling errors of it could be due to data errors and the spatial distribution of rainfall. This is because four of the five weather stations used in the Thiessen polygon rainfall estimation method was outside the study area thus could have an impact on the simulated discharge

4.4. Results for land evaluation for floodplain agriculture

Fig: 4.20 shows the suitability map provided in this report provide crucial information to farmers in Mbire district as it was derived using several scientific considerations to map optimum land for flood recession farming. In deriving the map environmental implication of river bank cultivation was considered by creating a buffer zone which is critical to soil and water recourses degradation.

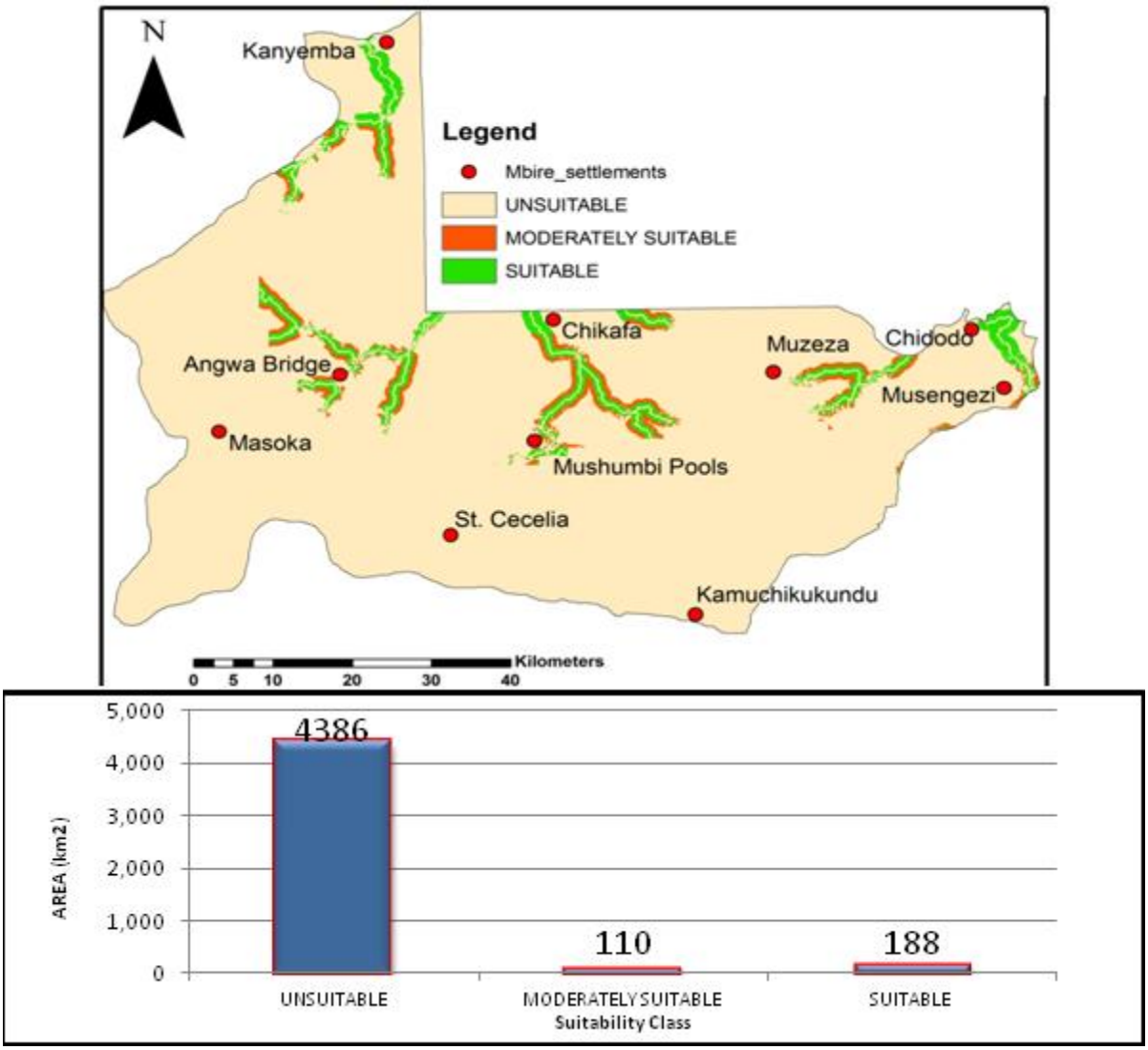

Figure 4.20: Suitability map for flood recession farming and corresponding suitability classes area.

From the results of this study, Mbire district have a total area of about 4684 km^2 and about 6.3% is suitable to moderately suitable for flood recession farming. Most suitable land is located close to the Zambezi River due to the effect of back flows on residual soil moisture accumulation. Vertical height above channel was one of the important factors in deriving the suitability map as it defines areas that are prone to high stream flows and flooding.

Comparing the suitability map to current landcover, 50% percent of the potential suitable to moderately suitable land is being utilised for crop production.

4.5. Conclusions

i. Based on the validation (comparison with ground based measurements) results of this study, the SEBS algorithm gives reasonably good estimates of catchment level top soil moisture and therefore can be used in soil moisture monitoring.

ii. This study demonstrated that the rainfall-runoff model (with calibration results: NS = 0.797, PBIAS = -10.45% and validation results: NS = 0.765, PBIAS= -6.03%). can be extended beyond its original design of using the topographic index for predicting local variations in water Table (Kirkby, 1975) to simulate soil moisture variations in river catchments.

iii. The suitability map for floodplain cultivation in this work provides crucial information to farmers and all stakeholders for proper water resources planning and decision making in Mbire district as it was derived using several scientific considerations to map optimum land for flood recession farming.

4.6. Recommendations

i. There in need to improve the gauging of rivers in the district as to integrate hydrological models and remote sensing methods and ground measurements in soil moisture monitoring and even to validate hydrological models and remote sensing against ground measurements by establishing Automatic Loggers.

ii. Future research should measure hydraulic properties of soils since they play an important role in movement of soil moisture from the land surface to the water table through the unsaturated zone and, hence, affect the runoff and groundwater recharge processes.

iii. Future application of TOPMODEL in the study should incorporate remote sensed meteorological data and move from using the semi-distributed characteristic of the model to distributed model

REFERENCES

Albek, M., U. B. O¨ g˘u¨tveren, et al. (2004). "Hydrological modeling of Seydi Suyu watershed (Turkey) with HSPF." Journal of Hydrology 285 260-271.

Allen, R. G., Pereira, L. S., et al. (1998). Crop evapotranspiration-Guidelines for computing crop water requirements. FAO Irrigation and Drainage Paper 56, FAO, ISBN 92-5-104219-5. Rome, Italy. 56.

Ambroise, B., Beven K., et al. (1996). "Toward a generalization of the TOPMODEL concepts: Topographic indices of hydrological similarity." Water Resources Research 32(7): 2135-2145.

Antonio, C., Klaus, S., Wolfgang, W. and Martinez-Fernandez, J., (2005). 'Validation of ERS scatterometer-derived soil moisture data in the central part of the Duero Basin, Spain'. *Hydrological processes*, 19(8): 1549-1556

Armah, B., Yeo, D., et al. (2013). Assessing Progress in Africa toward the Millennium Development Goals MDG Report 2013.

AWF (2010). Mbire District Draft Natural Resources Management Plan., African Wildlife Foundation.

Band, L. E., Peterson, D. L., et al. (1991). "Forest ecosystem processes at the watershed scale: basis for distributed simulation." Ecol. Modelling 56: 171-196.

Bashour, I.I. and Sayegh, A.H (2007). Methods of Analysis for Soils of Arid and Semi Arid Regions. Food and Agricultural Organisation of the United Nations. Rome.

Ben-asher, J., Matthias, A.D. and Warrick, A.W., (1983). Assessment of evaporation from bare soil by infrared thermometry. *Soil Science Society of American Journal*, 47, pp. 185 191.

Bastiaanssen, W.G.M., and Iwmi, (1998). *Remote sensing in water resources management: the state of the art*. International Water Management Institute (IWMI), Colombo,118 pp

Bastiaanssen, W.G.M., Menenti, M., Feddes, R.A. and Holtslag, A.A.M., (1998). 'A remote sensing surface energy balance algorithm for land (SEBAL). I . Formulation'. *Journal of hydrology*, 212-213: 198-212.

Beven, K. and Kirkby, M.J., 1979. A physically-based variable contributing area model of basin hydrology. Hydrological Sciences Bulletin. 24:43-69.

Beven, K. (1997). ""TOPMODEL: A CRITIQUE"." Hydrological Processes 11: 1069-1085.

Beven, K., 1984. Infiltration into a class of vertically non-uniform soils. Hydrol. Sci. 29 (4), 425–434.

Beven, K., 1997. TOPMODEL: A CRITIQUE. Hydrol. Process. 11, 1069–1085.

Beven, K., Freer, J., 2000. A dynamic TOPMODEL. Hydrol. Process. 15 (10), 1993– 2011.

Beven, K., Lamb, R., Quinn, P., Romanowicz, R., Freer, J., 1995. TOPMODEL. In: Sing,

Beven, K.J., (1997). *TOPMODEL user notes (Windows version)*. Centre for Research on

Environmental Systems and Statistics. Lancaster University, UK.

Beven, K.J., 2001. Rainfall-Runoff Modelling The Primer. John Wiley & Sons, Lancaster, UK.

Beven, K., R. Lamb, et al. (1995). "TOPMODEL. In: Sing VP (Ed), Computer Models of Watershed Hydrology." Water Resources Publications: 627-668, Colorado, USA.

Beven, K. J. and M. J. Kirkby (1979). "A physically based variable contributing area model of basin hydrology." Hydrological Sciences-Bulletin-des Sciences Hydrologiques 24(1): 43-69.

Brutsaert, W., (2005). *Hydrology; an introduction*. Cambridge University Press, Cambridge, 605 pp.

Carlson, T.N., Gillies, R.R., Perry, E.M., (1994). A method to make use of thermal infrared temperature and NDVI measurements to infer surface soil water content and fractional vegetation cover. *Remote Sensing Reviews*, 9, pp. 161-173.

Chen, X., Vierling L., et al. (2004). "Using lidar and effective LAI data to evaluate IKONOS and Landsat 7 ETM+ vegetation cover estimates in a ponderosa pine forest." Remote Sens. Environ 91: 14-26.

Chenje, M. (2000). State of the environment Zambezi Basin 2000. Maseru/Lusaka/Harare, SADC/IUCN/ZRA/SARDC.

CIRAD (2001). The Mankind and the Animal in the Mid Zambezi Valley-Zimbabwe: Boidiversity Conservation and Sustainable Development in the Mid-Zambezi Valley. , Librairie du Cirad, France.

Commission, DG Joint Research Centre, Institute for Environment and Sustainability, Land Management and Natural Hazards Unit, Ispra, Italy, pp.

Cosh, M.H., Jackson, T.J., Bindlish, R. and Prueger, J.H., (2004). 'Water shed scale temporal and spatial stability of soil moisture and its role in validating satellite estimates'. *Remote Sensing of Environment*, 92(4): 427-435

Dahmen E.R., H. M. J. (1989). Screening of Hydrological Data:Tests for Stationarity and Relative Consistency. Wageningen, The Netherlands, International Institute for Land Reclamation and Improvement.

De Lannoy, G. J. M., House, P. R., Verhost, N. E. C., Pauwels, V. R. N., Gish, T. J., (2007). Upscaling of point soil moisturemeasurement field averages at OPE3 test site. *Journal of Hydrology*, 343(1-2):1-11

Dingman, S.L., (2002). Physical hydrology. Prentice Hall, Upper Saddle River, 646pp.

Droughts in the Middle Zambezi: a Case Study of Kanyemba Community, paper submitted for the 12th WaterNet/Warfsa/GWP-SA Symposium to be held in Maputo, Mozambique, 26-28th October 2011

Dorigo, W.A., Wagner, W., Holensin, R., Hahn, S., Paulik, C., Xavier, A., Gruber, A., Drusch, M., Mecklenbury, S., van Oevelen, P., Robock, A., Jackson, T., 2011. The International Soil Moisture Network: a data hosting facility for global in situ soil moisture measurements. Hydrol. Earth Syst. Sci., 15:1675-1698.

Dube, F., 2011. Spatial Erosion Hazard Assessment and Modelling in Mbire District, Zimbabwe: Implications for Catchment Management. MSc Thesis. University of Zimbabwe

Engman, E. T., (1991). 'Application of Microwave Remote Sensing of Soil Moisture for Water Resources and Agriculture'. *Rem. Sens. Environ.*, 35: 213-226.

Evans, R., Carsel, D.K. Sneed, R.E., 2009. Soil, Water and Crop Characteristics important to Irrigation Scheduling. North Carolina Cooperative Extension Service, United States of America. Publication Number AG452-1.

Faculty of Geo-Information and Earth Observation (ITC), Enschede, The Netherlands, 93pp. *Geoprocessing*, 2:315-327. 1985.

FAO (1996). Declaration of World Food Security. World Food Summit. Rome, FAO.

Fritz, H., S. Saïd, et al. (2003). "The effects of agricultural fields and human settlements on the use of rivers by wildlife in the mid-Zambezi valley, Zimbabwe." Landscape Ecology 18: 293–302.

Fullen, A., Catt, J.A., 2004. Soil Management: Problems and Solutions. Arnold Publishers, London.

Garbrecht, J. and L. W. Martz (1999). Digital elevation model issues in water resources modeling. In: Proceedings from invited water resources sessions. ESRI international user conference.

Grayson, R.B. and Western, A.W., (1998).'Towards areal estimation of soil water content from point measurements: time and space stability of mean response'. *Journal of Hydrology*, 207(1-2):68-82.

Gumindoga, W., 2010. Hydrologic Impacts of Landuse Change in the Upper Gilgel Abay River Basin, Ethiopia: TOPMODEL Application., University of Twente

GWP., (2000). Integrated water resources management. *TAC Background Paper No. 4. Global Water Partnership*, Stockolm.

Haggett, P. (Eds.), Processes in Physical and Human Geography. John Wiley, Heinemann, London, pp. 69–90.

Hengl, T., Maathuis, B.H.P., Wang, L., 2007. Terrain parameterization in ILWIS. In: Hengel, Hannes, Reuter (Eds.), 'Geomorphometry' the Textbook. European Commission, DG Joint Research Centre, Institute for Environment and Sustainability, Land Management and Natural Hazards Unit, Ispra, Italy, pp. 29–48 (Chapter 3).

Hornberger, G.M., Beven, K.J., Cosby, B.J. and Sappington, D.E., 1985. 'Shenandoah Watershed Study: Calibration of a Topography-Based, Variable Contributing Area Hydrological Model to a small forested catchment. Water Resour, Res. 21; 1841-1850.

Immerzeel, W.W., Droogers, P. and Gieske, A.S.M., 2006. *Remote sensing and evapotranspiration mapping*: state of the art, FutureWater, Wageningen.

Jia, A., Wang, L., Qu, J. J., Zhang, S., Hao, X., Dasgupta, S., (2007). 'Soil moisture estimation using MODIS and ground measurements in eastern China'. *International Journal of Remote Sensing*, 28(6): 1413-1418

Krause, P., D. P. Boyle, et al. (2005). "Comparison of different efficiency criteria for hydrological model assessment." Advances in Geosciences 5: 89-97.

Kirkby, M.J., Chorley, R.J., 1967. Throughfow, overland flow and erosion. Bull. Int. Assoc. Sci. Hydrol. 12, 5–21.

Kusena, K., 2009. Landcover Change and Impact of Human-Elephant Conflict in The Zimbabwe, Mozambique and Zambia (ZiMoZa) Transboundary Natural Resources Area. MSc. Thesis, CMB, Swedish Biodiversity Centre, Uppsala, Sweden.

LGDA (2009). Mbire District Baseline Survey Report, Lower Guruve Development Association

Lillesand, T. M. and R. W. Kiefer (2000). Remote Sensing and Image Interpretation, John Wiley & Sons, Inc.

Liu, S., Mo, X., Zhao, W., Naemi, V., Dai, D., Shu, C., Mao, L., (2008). 'Temporal Variation of Soil Moisture over the Wuding River Basin assessed with an Eco-Hydrological Model; in-situ observations and remote sensing'. *Hydrology and Earth Systems Sciences Discussions*., 5: 3557-3604.

Lucas, L., F. Janssen, et al. (2002). Principles of Remote Sensing. ITC Educational Textbooks Series; 2, Second Edition.

Ma, Y. , Song, M., Ishikawa, H., Yang, K., Koike, T., Jia, L., Menenti, M., Su, Z. (2007) 'Estimation of the regional evaporative fraction over the Tibetan plateau area by using landsat-7 ETM data and the field observations'. *Journal of the meteorological society of Japan*, 85A, p.p.295-309,

Maathuis, B. H. P. and L. Wang (2006). "Digital Elevation Model based Hydroprocessing." Geocarto International 21(1).

Maathuis, B.H.P., 2007. DEM based Hydro-Processing: Introduction to the Tools Developed, Tutorial with Exercises Version 1. Department of Water Resources, ITC.

Madamombe, E.K., 2004. Zimbabwe: Flood Management Practices-Selected Flood Prone Areas in the Zambezi Basin, WMO/GWP Associated Programme on Flood Management.

Masek, J. G., E. F. Vermote, et al. (2006). "A Landsat surface reflectance data set for North America, 1990-2000." IEEE Geosci. Remote Sens. Lett. 3: 69-72.

Mattikalli, N. M., Engman, E. T., Ahuya, L. R and Jackson, T. J., (1998). 'Microwave remote sensing of soil moisture for estimation soil properties'. *International Journal of Remote sensing* 19(9)1751-1767

Mekonmen, D.F., (2009). Satellite Remote Sensing for Soil Moisture Estimation: Gumara Catchment, Ethiopia. MSc Thesis, International Institute for Geo-Information Science and Earth Observation, Enschede, the Netherlands, Unpublished.

Mlowoka, C., 2008. Relationship between Streambank Cultivation and Soil Erosion in Dedza, Malawi. MSc Thesis. University of Zimbabwe. Zimbabwe, Unpublished.

Monteith, J.L., (1981), 'Evaporation and surface temperature'. *Quarterly Journal of the Royal*

Meteorological Society, 107, pp. 1 27.

Muhammed, A. H. (2012). Satellite based evapotranspiration estimation and runoff simulation: A TOPMODELapplication to the Gilgel Abay catchment, Ethiopia. Geo-Information Science and Earth Observation. Enschede, University of Twente. MSc Geo-Information Science and Earth Observation

Munoz-Caperna, R., Li, Y., Kaplan, D., 2007. Analysis of Soil Moisture and Salinity in the Floodplains of the Loxahatche River Watershed. Agricultural and Biological Engineering Department. University of Florida, United States of America.

Murombedzi, J.C. (1999) Policy Arena Devolution and Stewardship in Zimbabwe's Campfire Programme, *Journal of International Development*, Vol. 11, p287-293.

Nash, J.E., Sutcliffe, J.V., 1970. River flow forecasting through conceptual models. Part I: A discussion of principles. J. Hydrol. 10, 282–290.

Niu, G., Yang, Z., Dickson, R.E., Gulden, L.E., 2005. A simple TOPMODEL-based runoff parameterization (SIMTOP) for use in global climate models. J. Geophys. Res., 110, D21106.

Norman, J.M., (2003). Remote sensing of surface energy fluxes at 10(1)-m pixel resolutions. *Water Resources Research*, 39(8).

Ohio., 2005. Ohio Agronomy Guide 14th Edition, Bulletin 472. The OHIO State University Extension.

Oku, Y., Ishikawa, H., Su, Z. (2007). 'Estimation of land surface heat fluxes over the Tibetan plateau using GMS data'. *J. Appl. Meteorol Clim*, 46(2), p.p.183-195,

Pappenberger et al. (2012), /Report on improved hydrological parameters", Glowasis D30.5, GLOWASIS Global Water Scarcity, Information Service

Philip, G.M., and Watson, D.F., 1982 'A Precise Method for Determining Contoured Surfaces'. *Australian Petroleum Exploration Association Journal* 22: 205-212.

Phiri, M. (2011). An analysis of the Cahora Bassa dam water balance and reservoir operations and their flooding impact on upstream catchments. Civil Engineering. Harare, University of Zimbabwe. MSc: 64.

Quinn, P. F. and K. J. Beven (1993). "Spatial and temporal predictions of soil moisture dynamics, runoff, variable source areas and evapotranspiration for Plynlimon, Mid-Wales." Hydrological Processes 7(4): 425-448.

Quinn, P. F., K. J. Beven, et al. (1995). "The Ln(a/TanB) Index: How to calculate it and how to use it within the Topmodel framework." Hydrological Processes 9: 161-182.

Rientjes, T. H. M. (2007). Modeling in Hydrology. Lecture Notes. Enschede, The Netherlands, ITC.

Robock, A., Vinnikov, K.Y., Srinivasan, G., Entin, J.K., Hollinger, E., Speranskaya, N.A., Liu, S., Namkhai, A., 2000. The Global Soil Moisture Data Bank. B. Am. Meteorol. Soc., 81:1281-1299.

Robson A.J., Whitehead P.G., Johnson R.C., (1993). An application of a physically based

semi -distributed model to the Balqutidder catchments, Journal of Hydrology. 145; 357-370.

Roerink, G.J., Su, Z. and Menenti, M., (2000). 'S-SEBI: A simple remote sensing algorithm to estimate the surface energy balance'. *Physics and Chemistry of the Earth, Part B: Hydrology, Oceans and Atmosphere*, 25(2): 147-157.

Rowell, D.L., (1997). Soil Science Methods and Applications. Longman, England, United Kingdom.

Rwasoka, D. T. (2010). Evapotranspiration in water limited environments: Up-scaling from the crown canopy to the eddy flux footprint. Water Resources. Enschede, University of Twente - ITC. MSc: 89.

Scott, C. A., Bastiaanssen, W. G. M., & Ahmad, M. U. D. (2003). 'Mapping root zone soil moisture using remotely sensed optical imagery'. *Journal of Irrigation and Drainage Engineering-Asce*, 129, 326-335.

Shumba, S., (2012). The Spatial and Temporal Variability of Soil Properties in the Mbire District of Zimbabwe. MSc Thesis, Civil Engineering. University of Zimbabwe. Harare.

Su, Z., (2002).'The Surface Energy Balance System (SEBS) for estimation of turbulent heat fluxes'. *Hydrology. Earth Syst. Sc*, 6, p.p.85-99,

Su, Z., et al., (2003). 'Assessing relative soil moisture with remote sensing data: theory, experimental validation, and application to drought monitoring over the North China Plain'. *Physics and Chemistry of the Earth*, Parts A/B/C, 28(1-3):89-101.

Su, Z., (2002a). *An introduction to the surface energy balance system*.ITC. V.P. (Ed.), Computer Models of Watershed Hydrology, vol. 627–668. Water Resources Publications, Colorado, USA.

Su, Z., (1999). "The Surface Energy Balance System (SEBS) for estimation of turbulent heat fluxes." Hydrol. Earth Syst. Sci. 6(1): 85-100.

Vachaud, G., Passerat De Silans, A., Balabanis, P. and Vauclin, M., (1985). 'Temporal Stability of Spatially Measured Soil Water Probability Density Function'. *Soil Sci Soc Am J*, 49(4):822-828

Van der Lee, J. and Gehrels, J. C., (1990). *Modelling Aquifer Recharge: Introduction to the Lumped Parameter Model EARTH*, Free University of Amsterdam, The Netherlands.

Vicent, S., Pons, F.N., Cuadrat, P., (2004). 'Mapping soil moisture in the central Ebro river valley (Northeast Spain) with Landsat and NOAA satellite imagery: a comparison with meteorological data'. *International Journal of Remote Sensing*., 25: 4325-4350.

Wagner, W., Lemoine, G. and Rott, H., (1999a). 'A Method for Estimating Soil Moisture from ERS Scatterometer and Soil Data'. *Remote Sensing of Environment*, 70(2): 191-207.

Wagner, W., Noll, J., Borgeaud, M. and Rott, H., (1999b). Monitoring soil moisture over the Canadian Prairies with the ERS scatterometer. Ieee Transactions on Geoscience and Remote Sensing, 37(1): 206-216.

Wagner, W., (2003). 'Temporal stability of soil moisture and radar backscatter observed by the

advanced Synthetic Aperture Radar (ASAR)'. *Sensors*, 8(2): 1174-1197

Wang, L., Qu, J. J., Zhang, S., Hao, X., Dasgupta, S., (2007). 'Soil moisture estimation using MODIS and ground measurements in eastern China'. *International Journal of Remote Sensing*, 28(6): 1413-1418

Watson, D.F., Philip G.M., (2000). A Refinement of Inverse Distance Weighted Interpolation.

Wen, J., Su, Z.B. and Ma, Y.M., (2003). 'Determination of land surface temperature and soil moisture from Tropical Rainfall Measuring Mission/Microwave Image remote sensing data'. *Journal of Geophysical Research-Atmospheres*, 108(D2).

Western, A.W., Grayson, R.B., Bloschl, G., (2002). 'Scaling of Moisture: A hydrologic Perspective'. *Annu. Rev. Earth Planet. Sci*., 30:149–80.

Willmott, C. J., S. M. Robeson, et al. (2011). "Short communication - A refined index of model performance." Internationl Journal of Climatology.

Zoratelli, L., Dukes, M., Morgan, K.T., 2010. Interpretation of Soil Moisture Content to determine Soil Field Capacity and avoid over-irrigating sand soils using Soil Moisture Sensors. University of Florida. Institute of Food and Agricultural Science.

ZimStat (2012). Zimbabwe Cencus 2012 : Preliminary Report. Harare, Zimbabwe National Statistics Agency

APPENDICES

Appendix 1. Computed discharge for Angwa and Manyame River sub catchments respectively

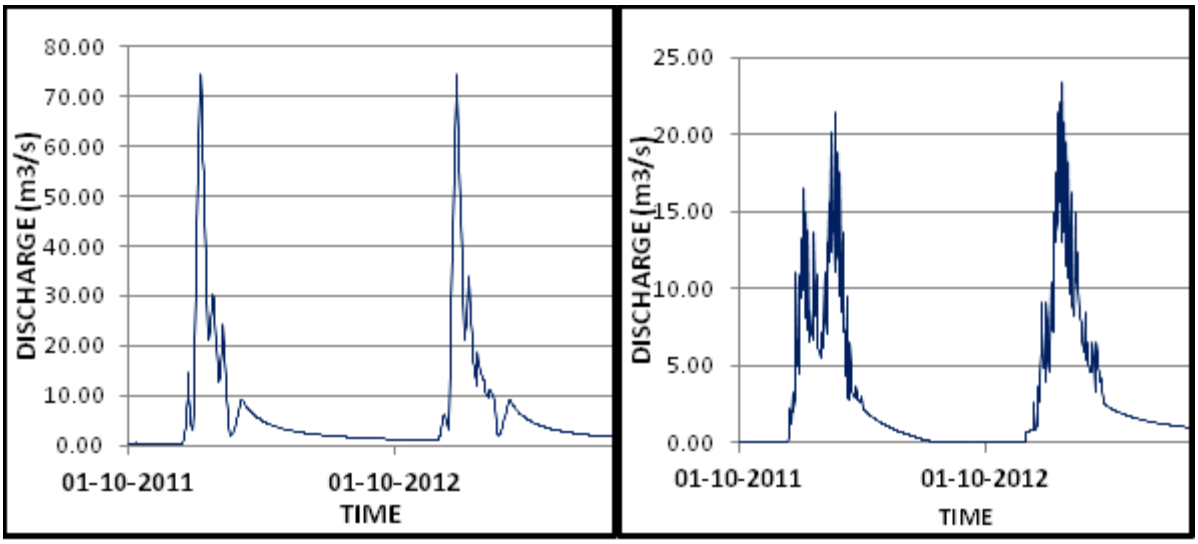

Appendix 2. TOPMODEL parameter file for Manyame River Angwa River sub catchment

12_parameters_for_the MANYAME
SZM (m), lnTo, TD, CHV, RV, SRmax, QO, SRO, INFEX, XKO, HF (psi), DTH (dtheta)
0.0404
3
60
360
1900
0.0750
0.000385618
0.001
0
3
0.135
0.36

12_parameters_for_the ANGWA
SZM (m), lnTo, TD, CHV, RV, SRmax, QO, SRO, INFEX, XKO, HF (psi), DTH (dtheta)
0.0312
3.5
60
200
1900
0.0512
0.000385618
0.001
0
3
0.135
0.36

Appendix 3. Relative evaporation maps for Mbire district

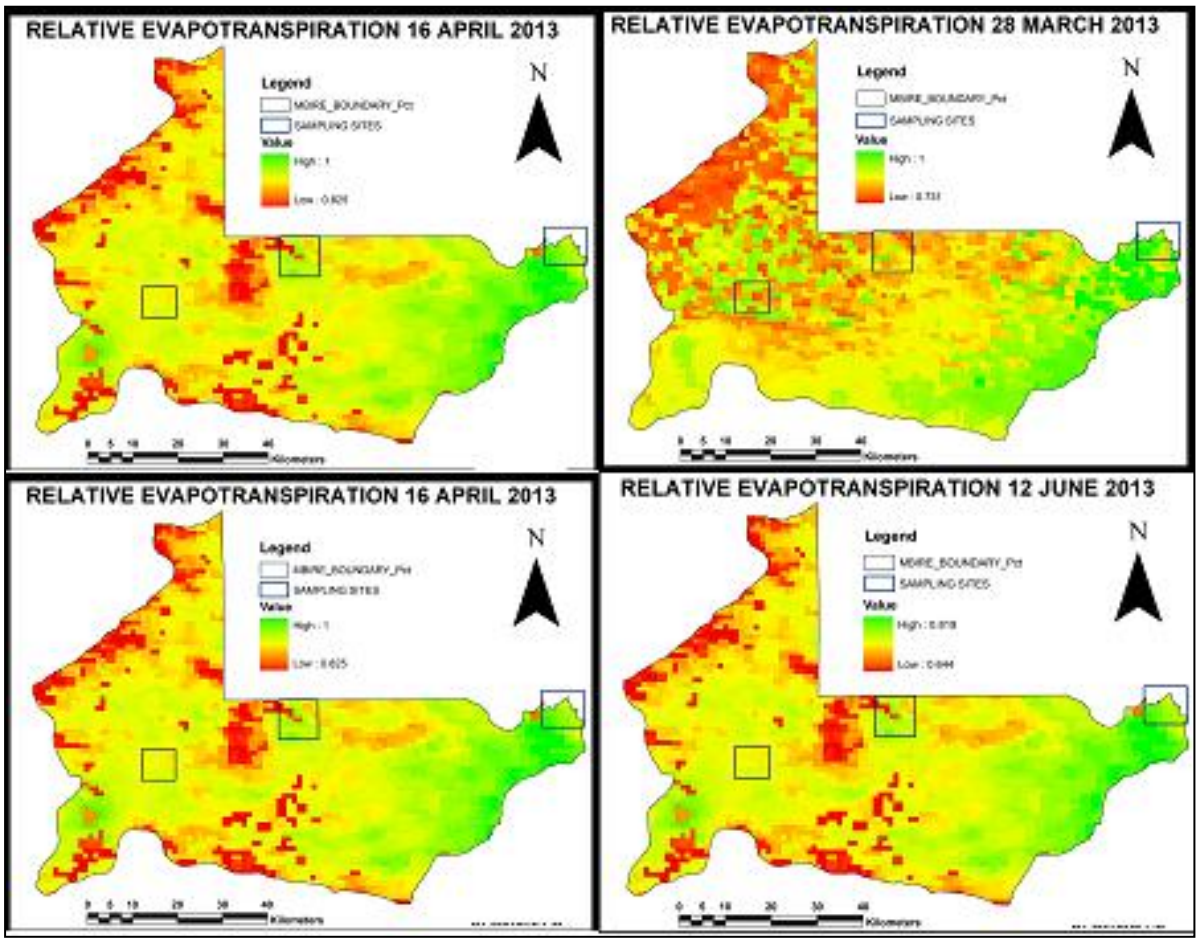

Appendix 4. Angwa River sub catchment TOPMODEL simulated soil moisture maps

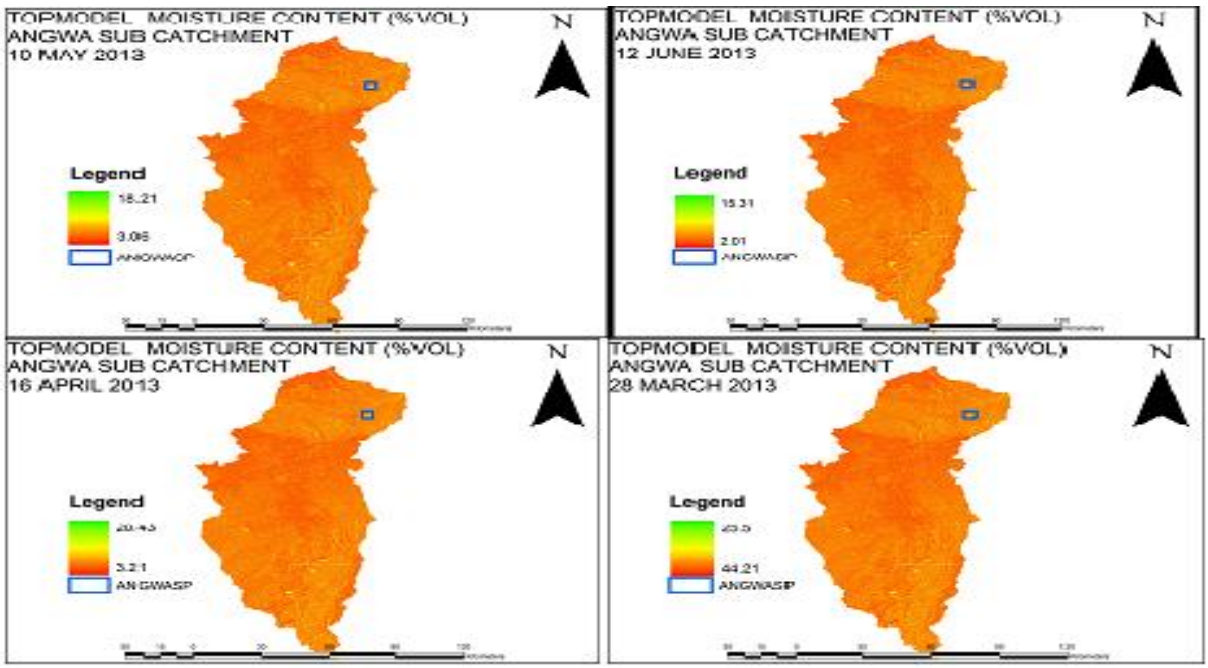

Appendix 5. Angwa River subcatchment area distance map

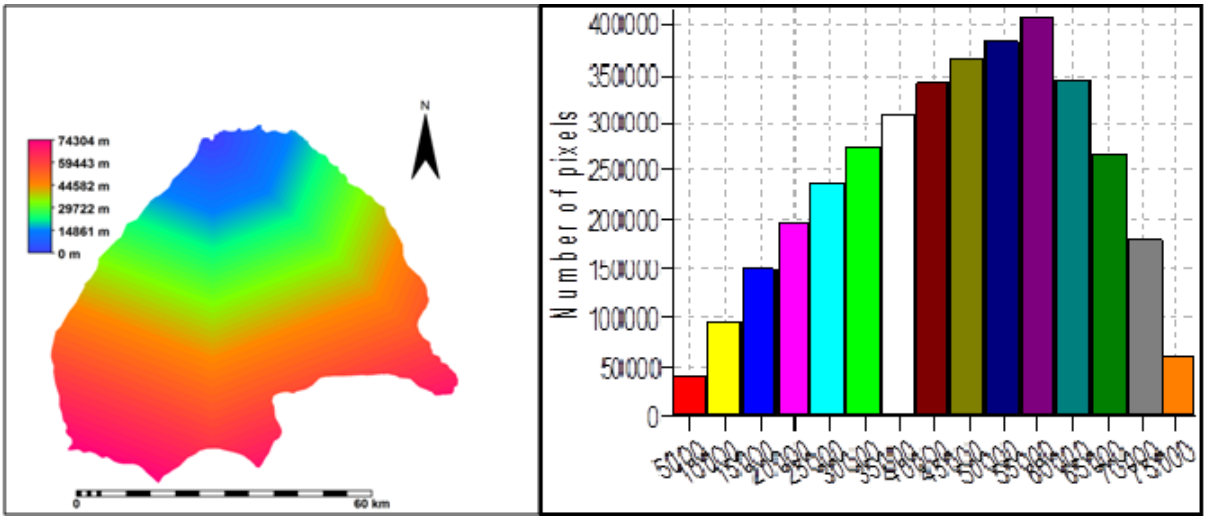

Appendix 6. Manyame River sub-catchment TOPMODEL simulated soil moisture maps

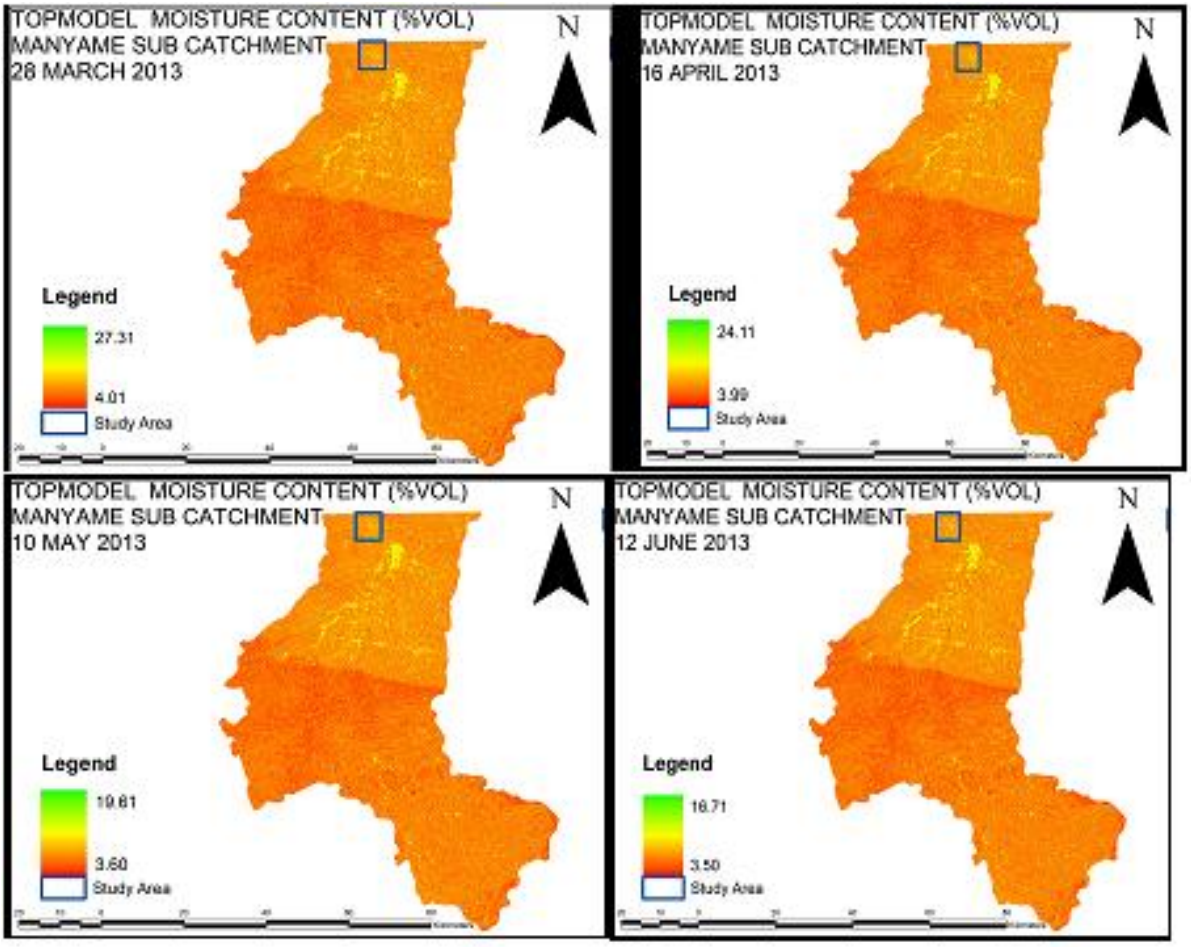

Appendix 7. Mean pixel volumetric soil moisture content for all sampling sites

DATE	SITE	GRAVIMETRIC METHOD	TOPMODEL METHOD	SEBS METHOD
28/03/2013	ANGWA	11.61	8.63	10.81
	MUSENGENGEZI	20.45	-	19.43
	MANYAME	20.98	15.16	17.35
16/04/2013	ANGWA	9.63	7.02	8.34
	MUSENGENGEZI	17.62	-	15.32
	MANYAME	18.61	9.62	16.23
10/05/2013	ANGWA	6.42	5.41	4.12
	MUSENGENGEZI	14.42	-	11.89
	MANYAME	13.42	7.23	11.12
12/06/2013	ANGWA	5.65	5.8	5.54
	MUSENGENGEZI	15.65	-	11.65
	MANYAME	12.66	6.70	8.73
13/07/2013	ANGWA	4.90	4.18	4.11
	MUSENGENGEZI	14.14	-	10.63
	MANYAME	10.68	5.82	6.68

Appendix 8. Summary of comparison of SEBS inferred and TOPMODEL simulated soil moisture to upscaled point based soil moisture in SPSS

			SEBS METHOD		TOPMODEL METHOD	
Sampling site	Date	Confidence interval	CORRELATIONS R^2	P VALUE	CORRELATIONS R^2	P VALUE
MANYAME RIVER	28/03/13	95%	0.885	<0.05	0.498	<0.05
	16/04/13	95%	0.716	<0.05	0.567	<0.05
	10/05/13	95%	0.768	<0.05	0.713	<0.05
	12/06/13	95%	0.813	<0.05	0.556	<0.05
	13/07/13	95%	0.755	<0.05	0.589	<0.05
ANGWA RIVER	28/03/13	95%	0.667	<0.05	0.655	<0.05
	16/04/13	95%	0.823	<0.05	0.6434	<0.05
	10/05/13	95%	0.834	<0.05	0.564	<0.05
	12/06/13	95%	0.784	<0.05	0.595	<0.05
	13/07/13	95%	0.822	<0.05	0.590	<0.05
MUSENGEZI RIVER	28/03/13	95%	0.771	<0.05	-	-
	16/04/13	95%	0.812	<0.05	-	-
	10/05/13	95%	0.824	<0.05	-	-
	12/06/13	95%	0.800	<0.05	-	-
	13/07/13	95%	0.866	<0.05	-	-
Average			**0.796**	**<0.05**	**0.597**	**<0.05**

Appendix 9. Maps: Distance from river networks in Mbire District and from Zambezi River

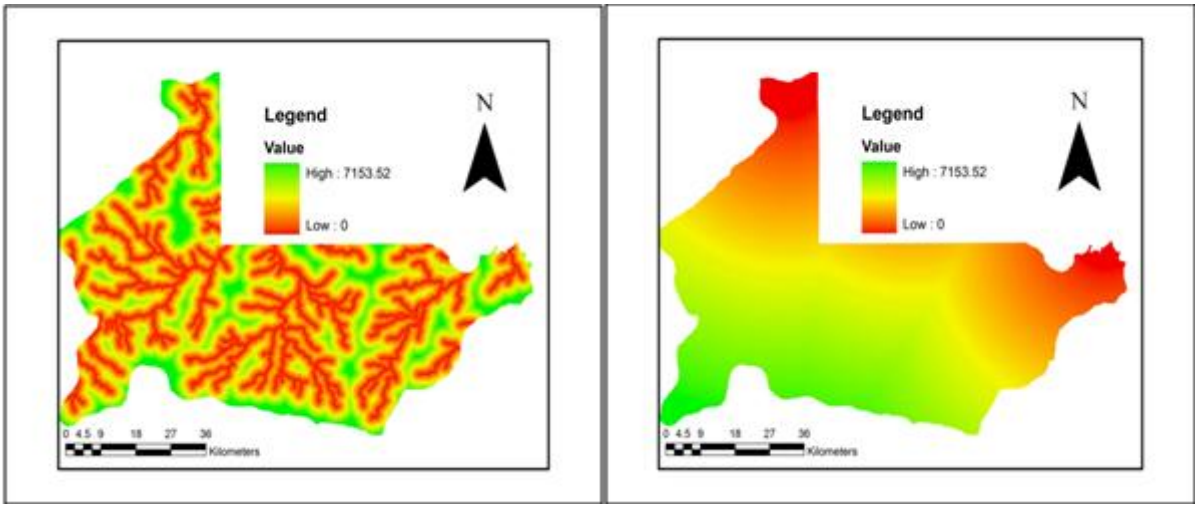

Appendix 10. Map: Slope in Mbire District

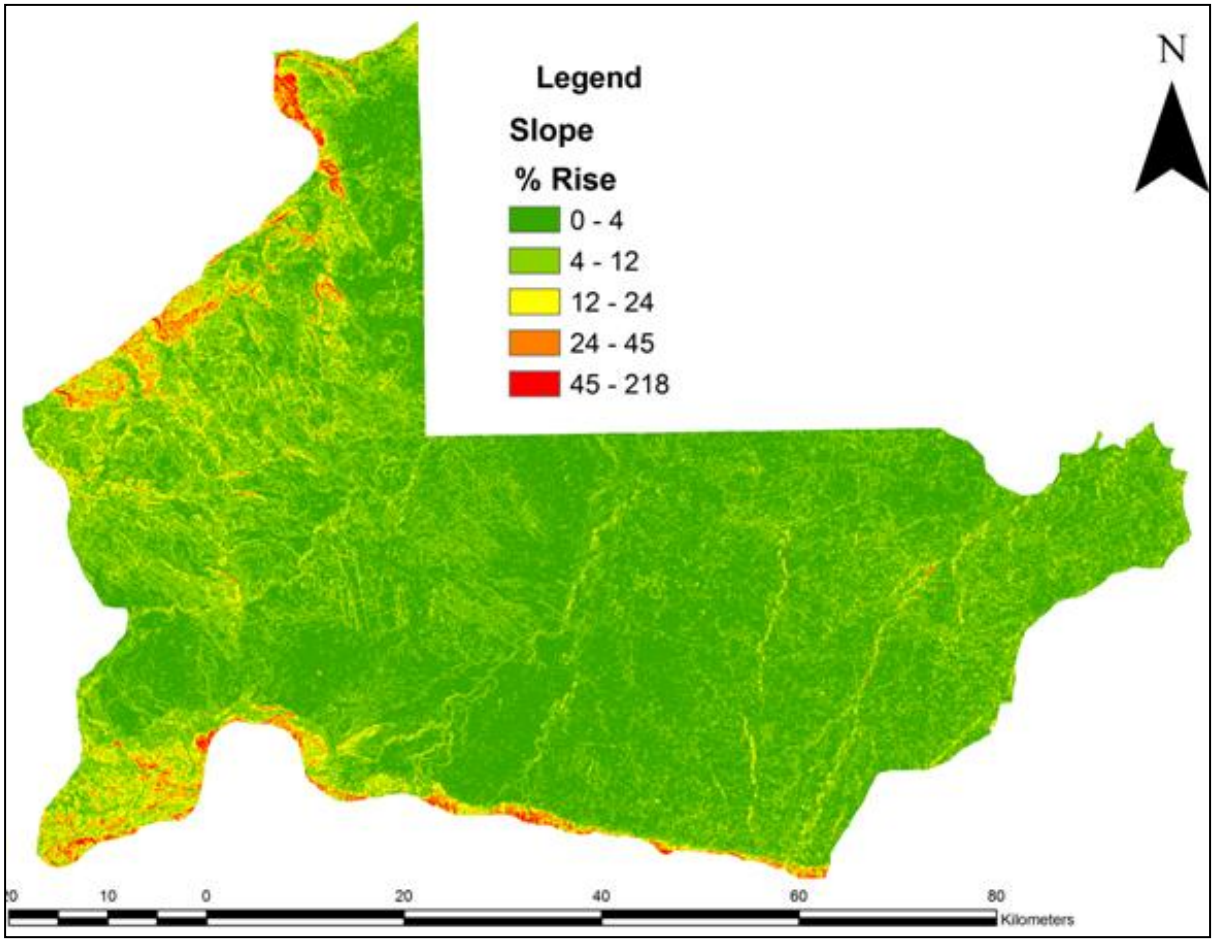

Appendix11. Maps: vertical height above river channels and landcover/use and corresponding area for Mbire district